



National Library  
of Canada

Bibliothèque nationale  
du Canada

Canadian Theses Service    Service des thèses canadiennes

Ottawa, Canada  
K1A 0N4

## NOTICE

The quality of this microform is heavily dependent upon the quality of the original thesis submitted for microfilming. Every effort has been made to ensure the highest quality of reproduction possible.

If pages are missing, contact the university which granted the degree.

Some pages may have indistinct print especially if the original pages were typed with a poor typewriter ribbon or if the university sent us an inferior photocopy.

Reproduction in full or in part of this microform is governed by the Canadian Copyright Act, R.S.C. 1970, c. C-30, and subsequent amendments.

## AVIS

La qualité de cette microforme dépend grandement de la qualité de la thèse soumise au microfilmage. Nous avons tout fait pour assurer une qualité supérieure de reproduction.

S'il manque des pages, veuillez communiquer avec l'université qui a conféré le grade.

La qualité d'impression de certaines pages peut laisser à désirer, surtout si les pages originales ont été dactylographiées à l'aide d'un ruban usé ou si l'université nous a fait parvenir une photocopie de qualité inférieure.

La reproduction, même partielle, de cette microforme est soumise à la Loi canadienne sur le droit d'auteur, SRC 1970, c. C-30, et ses amendements subséquents.

FREE VIBRATION ANALYSIS OF  
RECTANGULAR PLATES  
WITH INTERNAL POINT SUPPORTS

THESIS SUBMITTED  
TO THE SCHOOL OF GRADUATE STUDIES  
AS PARTIAL FULFILLMENT OF THE REQUIREMENTS FOR THE  
DEGREE OF MASTER OF APPLIED SCIENCE

by  
Hans J.L. Öhman

Department of Mechanical Engineering  
UNIVERSITY OF OTTAWA  
OTTAWA, ONTARIO, FEBRUARY, 1991



National Library  
of Canada

Bibliothèque nationale  
du Canada

Canadian Theses Service    Service des thèses canadiennes

Ottawa, Canada  
K1A 0N4

The author has granted an irrevocable non-exclusive licence allowing the National Library of Canada to reproduce, loan, distribute or sell copies of his/her thesis by any means and in any form or format, making this thesis available to interested persons.

The author retains ownership of the copyright in his/her thesis. Neither the thesis nor substantial extracts from it may be printed or otherwise reproduced without his/her permission.

L'auteur a accordé une licence irrévocable et non exclusive permettant à la Bibliothèque nationale du Canada de reproduire, prêter, distribuer ou vendre des copies de sa thèse de quelque manière et sous quelque forme que ce soit pour mettre des exemplaires de cette thèse à la disposition des personnes intéressées.

L'auteur conserve la propriété du droit d'auteur qui protège sa thèse. Ni la thèse ni des extraits substantiels de celle-ci ne doivent être imprimés ou autrement reproduits sans son autorisation.

ISBN 0-315-68073-3

Canada



UNIVERSITÉ D'OTTAWA  
UNIVERSITY OF OTTAWA

*In memory of my mother*

# Abstract

Interest in the free vibration frequencies and associated mode shapes of rectangular plates resting on internal point supports has arisen in connection with the design of electronic circuit boards, solar panels and other industrial problems.

An analytical solution is presented for the free vibration analysis of rectangular plates with multiple internal point supports. The solution is also shown to be easily modified to account for the effects of attached masses. The basic solution for each case consists of the Lévy type solution for a plate with one discrete point support.  $N$  similar solutions for  $N$  discrete point supports are then superimposed to create an eigenvalue matrix from which the plate's natural frequencies and associated mode shapes can be determined. Due to the nature of the Lévy type solution, only plates with two opposite edges simply supported are considered. The remaining edges are either simply supported, clamped or free. There are therefore six possible combinations of plate boundary conditions.

The objective of this thesis is to give a concise and clear description of the mathematical procedure employed and to present the results of some representative frequency and mode shape studies.

# Acknowledgements

First and foremost I would like to express my deep appreciation to Dr. D.J. Gorman for his guidance and supervision which has made this thesis possible.

A sincere thanks to the staff of the Department of Mechanical Engineering, in particular Mr. Don Seaman and Ms. Solange Amyot, for their effort and help that was provided when needed.

I am indebted to my many colleagues and friends at the University of Ottawa, especially Mr. Etienne Bernard, Mr. Mike Tenace, Mr. Luc Mernard, Mr. Rudy Tolkamp and Mr. Amor Jnifene, for their various contributions to this work.

A special thanks to my fiancée, Kelly Grimes, for her kind words of encouragement and moral support.

Last but not least I would like to express my sincerest gratitude to my father, Mr. Lars Öhman, for his invaluable assistance and advice throughout the course of this work.

# Contents

<b>Abstract</b>	<b>i</b>
<b>Acknowledgements</b>	<b>ii</b>
<b>Table of Contents</b>	<b>iii</b>
<b>List of Figures</b>	<b>vi</b>
<b>List of Tables</b>	<b>x</b>
<b>Nomenclature</b>	<b>xii</b>
<b>1 Introduction</b>	<b>1</b>
1.1 The Governing Differential Equation . . . . .	2
1.2 Classical Boundary Conditions . . . . .	4
1.2.1 Simply Supported Edge . . . . .	4
1.2.2 Clamped Edge . . . . .	5
1.2.3 Free Edge . . . . .	5
1.3 Concentrated Force . . . . .	6
1.4 The Lévy Type Solution . . . . .	6

CONTENTS

iv

<b>2 Literature Review</b>	<b>9</b>
2.1 Experimental . . . . .	9
2.2 Finite Element Method . . . . .	11
2.3 The Energy Method . . . . .	11
2.4 Analytical Solution . . . . .	13
<b>3 The Modified Lévy Solution</b>	<b>17</b>
3.1 The Simply Supported Plate with an Internal Point Support . . . . .	17
3.2 The Solution for the Plate Segment with a Clamped Edge . . . . .	23
3.3 The Solution for a Plate Segment with a Free Edge . . . . .	25
3.4 The Six Case Studies . . . . .	27
<b>4 Multiple Point Support Problems</b>	<b>30</b>
4.1 Multiple Internal Point Supports . . . . .	30
4.2 The 'Rigid' Point Support . . . . .	34
4.3 Matrix Modification for Attached Mass . . . . .	36
<b>5 Presentation of Results</b>	<b>38</b>
5.1 Multiple Internal Point Supports . . . . .	38
5.1.1 Comparison of Results . . . . .	41
5.1.2 Eigenvalue Curves . . . . .	44
5.1.3 Associated Mode Shapes . . . . .	56
5.2 Effects of Attached Masses . . . . .	68
5.2.1 Eigenvalue Curves . . . . .	69
5.2.2 Associated Mode Shapes . . . . .	70

<i>CONTENTS</i>	v
<b>6 Discussion of Results</b>	<b>72</b>
6.1 Computed Eigenvalues . . . . .	72
6.2 Eigenvalue Curves . . . . .	74
6.3 Associated Mode Shapes . . . . .	76
<b>7 Conclusions</b>	<b>77</b>
<b>References</b>	<b>79</b>
<b>Appendices</b>	<b>83</b>
<b>A Equations Resulting from Continuity</b>	<b>83</b>
A.1 Case 1, SSSS . . . . .	84
A.2 Case 2, SSSC . . . . .	85
A.3 Case 3, SCSC . . . . .	86
A.4 Case 4, SSSF . . . . .	87
A.5 Case 5, SFSF . . . . .	88
A.6 Case 6, SCSF . . . . .	89
<b>B Computed Eigenvalues</b>	<b>90</b>
B.1 Multiple Internal Point Supports . . . . .	91
B.2 Effects of Attached Masses . . . . .	100
<b>C Illustrative Convergence Test</b>	<b>103</b>
<b>D Computer Program used in Plate Vibration Analysis</b>	<b>105</b>

# List of Figures

1.1	Rectangular plate with conventional and dimensionless coordinate system.	2
1.2	Schematic representation of the Dirac Delta Function modeling a discrete point support along a plate's edge. Point support is at 0.6 units (dimensionless), $k = 32$ .	6
3.1	Rectangular plate with simply supported edges and an internal lateral point support.	17
3.2	Rectangular plate segment with two edges simply supported and a third edge clamped.	22
3.3	Rectangular plate segment with two edges simply supported and a third edge free.	24
3.4	Six possible combinations of rectangular plates with two opposite edges simply supported and the other two simply supported, clamped or free.	28
4.1	Rectangular plate with four discrete point supports.	30
4.2	Four individual point supported plate solutions superimposed to establish the solution for a plate with four internal point supports.	30
4.3	Schematic representation of $4 \times 4$ eigenvalue matrix.	31
4.4	Matrix determinant vs. $\lambda^2$ . Eigenvalue established at $\lambda^2 = 37.65$ (see Appendix B, table B.1, mode 1, $u = v = 0.2$ ).	32

4.5	Rectangular plate with 4 rigid point supports modelled by 16 discrete point supports. . . . .	34
4.6	Rectangular plate with local mass $M$ attached. . . . .	35
5.1	Rectangular plate with four point supports and various boundary conditions. Point supports represented by solid dots (discrete and rigid). . . .	38
5.2	Eigenvalue curves, Case 1, SSSS ( $\phi = 1.0$ , support type: discrete). . . .	43
5.3	Eigenvalue curves, Case 1, SSSS ( $\phi = 1.0$ , support type: rigid). . . . .	43
5.4	Eigenvalue curves, Case 1, SSSS ( $\phi = 1.5$ , support type: discrete). . . .	44
5.5	Eigenvalue curves, Case 1, SSSS ( $\phi = 1.5$ , support type: rigid). . . . .	44
5.6	Eigenvalue curves, Case 2, SSSC ( $\phi = 1.0$ , support type: discrete). . . .	45
5.7	Eigenvalue curves, Case 2, SSSC ( $\phi = 1.0$ , support type: rigid). . . . .	45
5.8	Eigenvalue curves, Case 2, SSSC ( $\phi = 1.5$ , support type: discrete). . . .	46
5.9	Eigenvalue curves, Case 2, SSSC ( $\phi = 1.5$ , support type: rigid). . . . .	46
5.10	Eigenvalue curves, Case 3, SCSC ( $\phi = 1.0$ , support type: discrete). . . .	47
5.11	Eigenvalue curves, Case 3, SCSC ( $\phi = 1.0$ , support type: rigid). . . . .	47
5.12	Eigenvalue curves, Case 3, SCSC ( $\phi = 1.5$ , support type: discrete). . . .	48
5.13	Eigenvalue curves, Case 3, SCSC ( $\phi = 1.5$ , support type: rigid). . . . .	48
5.14	Eigenvalue curves, Case 4, SSSF ( $\phi = 1.0$ , support type: discrete). . . .	49
5.15	Eigenvalue curves, Case 4, SSSF ( $\phi = 1.0$ , support type: rigid). . . . .	49
5.16	Eigenvalue curves, Case 4, SSSF ( $\phi = 1.5$ , support type: discrete). . . .	50
5.17	Eigenvalue curves, Case 4, SSSF ( $\phi = 1.5$ , support type: rigid). . . . .	50
5.18	Eigenvalue curves, Case 5, SFSF ( $\phi = 1.0$ , support type: discrete). . . .	51
5.19	Eigenvalue curves, Case 5, SFSF ( $\phi = 1.0$ , support type: rigid). . . . .	51
5.20	Eigenvalue curves, Case 5, SFSF ( $\phi = 1.5$ , support type: discrete). . . .	52

5.21 Eigenvalue curves, Case 5, SFSF ( $\phi = 1.5$ , support type: rigid). . . . .	52
5.22 Eigenvalue curves, Case 6, SCSF ( $\phi = 1.0$ , support type: discrete). . . . .	53
5.23 Eigenvalue curves, Case 6, SCSF ( $\phi = 1.0$ , support type: rigid). . . . .	53
5.24 Eigenvalue curves, Case 6, SCSF ( $\phi = 1.5$ , support type: discrete). . . . .	54
5.25 Eigenvalue curves, Case 6, SCSF ( $\phi = 1.5$ , support type: rigid). . . . .	54
5.26 First four associated mode shapes for Case 1, SSSS ( $u = v = 0.2$ , $\phi = 1.5$ , support type: discrete). . . . .	55
5.27 First four associated mode shapes for Case 1, SSSS ( $u = v = 0.2$ , $\phi = 1.5$ , support type: rigid). . . . .	56
5.28 First four associated mode shapes for Case 2, SSSC ( $u = v = 0.25$ , $\phi = 1.5$ , support type: discrete). . . . .	57
5.29 First four associated mode shapes for Case 2, SSSC ( $u = v = 0.25$ , $\phi = 1.5$ , support type: rigid). . . . .	58
5.30 First four associated mode shapes for Case 3, SCSC ( $u = v = 0.1$ , $\phi = 1.5$ , support type: discrete). . . . .	59
5.31 First four associated mode shapes for Case 3, SCSC ( $u = v = 0.1$ , $\phi = 1.5$ , support type: rigid). . . . .	60
5.32 First four associated mode shapes for Case 4, SSSF ( $u = v = 0.3$ , $\phi = 1.5$ , support type: discrete). . . . .	61
5.33 First four associated mode shapes for Case 4, SSSF ( $u = v = 0.3$ , $\phi = 1.5$ , support type: rigid). . . . .	62
5.34 First four associated mode shapes for Case 5, SFSF ( $u = v = 0.05$ , $\phi = 1.5$ , support type: discrete). . . . .	63
5.35 First four associated mode shapes for Case 5, SFSF ( $u = v = 0.05$ , $\phi = 1.5$ , support type: rigid). . . . .	64

5.36	First four associated mode shapes for Case 6, SCSF ( $u = v = 0.4$ , $\phi = 1.5$ , support type: discrete). . . . .	65
5.37	First four associated mode shapes for Case 6, SCSF ( $u = v = 0.4$ , $\phi = 1.5$ , support type: rigid). . . . .	66
5.38	Rectangular plate with attached mass and internal point support locations. Attached masses represented by X. . . . .	67
5.39	Fundamental eigenvalue curve, single attached mass, ( $u = v = 0.2$ ). . . . .	68
5.40	Fundamental eigenvalue curves, varying mass location, ( $u = v = 0.25$ ). . . . .	68
5.41	Fundamental mode shapes for varying mass ratio. $M_r$ at $u = v = 0.5$ (solid arrow), four point supports at $u = v = 0.15$ (solid dots), $\phi = 1.5$ . . . . .	69
5.42	Fundamental mode shapes for two varying mass locations on line $u = 0.5$ and $v = 0.1, 0.9$ $0.2, 0.8$ $0.3, 0.7$ $0.4, 0.6$ (solid arrow). Four point supports at $u = v = 0.25$ (solid dots). $\phi = 1.5$ . . . . .	70

# List of Tables

5.1	Comparison of first three computed eigenvalues $\lambda^2$ , Case 1, SSSS, from present analysis and Bapat's( ) for plate with one discrete point support.	41
5.2	Comparison of first three computed eigenvalues $\lambda^2$ , Case 1, SSSS, from present analysis and Bapat's( ) for plate with two discrete point supports.	41
5.3	Comparison of first three computed eigenvalues $\lambda^2$ , Case 3, SCSC, from present analysis and Bapat's( ) for plate with one discrete point support.	42
5.4	Comparison of first three computed eigenvalues $\lambda^2$ , Case 3, SCSC, from present analysis and Bapat's( ) for plate with two discrete point supports. * Eigenvalues are suspect. . . . .	42
5.5	Comparison of first three computed eigenvalues $\lambda^2$ , Case 5, SFSS, from present analysis and Bapat's( ) for plate with one discrete point support.	43
5.6	Comparison of first three computed eigenvalues $\lambda^2$ , Case 5, SFSS, from present analysis and Bapat's( ) for plate with two discrete point supports. * Eigenvalues are suspect. . . . .	43
B.1	Computed Eigenvalues $\lambda^2$ , Case 1, SSSS ( $\phi = 1.0$ , support type: discrete).	92
B.2	Computed Eigenvalues $\lambda^2$ , Case 1, SSSS ( $\phi = 1.0$ , support type: rigid).	92
B.3	Computed Eigenvalues $\lambda^2$ , Case 1, SSSS ( $\phi = 1.5$ , support type: discrete).	92
B.4	Computed Eigenvalues $\lambda^2$ , Case 1, SSSS ( $\phi = 1.5$ , support type: rigid).	93
B.5	Computed Eigenvalues $\lambda^2$ , Case 2, SSSC ( $\phi = 1.0$ , support type: discrete).	93

B.6	Computed Eigenvalues $\lambda^2$ , Case 2, SSSC ( $\phi = 1.0$ , support type: rigid).	93
B.7	Computed Eigenvalues $\lambda^2$ , Case 2, SSSC ( $\phi = 1.5$ , support type: discrete).	94
B.8	Computed Eigenvalues $\lambda^2$ , Case 2, SSSC ( $\phi = 1.5$ , support type: rigid).	94
B.9	Computed Eigenvalues $\lambda^2$ , Case 3, SCSC ( $\phi = 1.0$ , support type: discrete).	94
B.10	Computed Eigenvalues $\lambda^2$ , Case 3, SCSC ( $\phi = 1.0$ , support type: rigid).	95
B.11	Computed Eigenvalues $\lambda^2$ , Case 3, SCSC ( $\phi = 1.5$ , support type: discrete).	95
B.12	Computed Eigenvalues $\lambda^2$ , Case 3, SCSC ( $\phi = 1.5$ , support type: rigid).	95
B.13	Computed Eigenvalues $\lambda^2$ , Case 4, SSSF ( $\phi = 1.0$ , support type: discrete).	96
B.14	Computed Eigenvalues $\lambda^2$ , Case 4, SSSF ( $\phi = 1.0$ , support type: rigid).	96
B.15	Computed Eigenvalues $\lambda^2$ , Case 4, SSSF ( $\phi = 1.5$ , support type: discrete).	96
B.16	Computed Eigenvalues $\lambda^2$ , Case 4, SSSF ( $\phi = 1.5$ , support type: rigid).	97
B.17	Computed eigenvalues $\lambda^2$ , Case 5, SFSF ( $\phi = 1.0$ , support type: discrete).	97
B.18	Computed eigenvalues $\lambda^2$ , Case 5, SFSF ( $\phi = 1.0$ , support type: rigid).	97
B.19	Computed eigenvalues $\lambda^2$ , Case 5, SFSF ( $\phi = 1.5$ , support type: discrete).	98
B.20	Computed eigenvalues $\lambda^2$ , Case 5, SFSF ( $\phi = 1.5$ , support type: rigid).	98
B.21	Computed eigenvalues $\lambda^2$ , Case 6, SCSF ( $\phi = 1.0$ , support type: discrete).	98
B.22	Computed eigenvalues $\lambda^2$ , Case 6, SCSF ( $\phi = 1.0$ , support type: rigid).	99
B.23	Computed eigenvalues $\lambda^2$ , Case 6, SCSF ( $\phi = 1.5$ , support type: discrete).	99
B.24	Computed eigenvalues $\lambda^2$ , Case 6, SCSF ( $\phi = 1.5$ , support type: rigid).	99
B.25	Computed eigenvalues $\lambda^2$ , varying mass ratios ( $\phi = 1.0$ ).	101
B.26	Computed eigenvalues $\lambda^2$ , varying mass ratios ( $\phi = 1.5$ ).	101
B.27	Computed eigenvalues $\lambda^2$ , varying mass locations ( $M_r = 0.4$ , $\phi = 1.0$ ).	102
B.28	Computed eigenvalues $\lambda^2$ , varying mass locations ( $M_r = 0.4$ , $\phi = 1.5$ ).	102

# Nomenclature

$a$	plate lateral dimension
$b$	plate lateral dimension
$D$	$= Eh^3/\{12(1 - \nu^2)\}$ , plate flexural rigidity
$E$	Young's modulus of the plate material
$f$	plate vibration frequency (hertz)
$h$	plate thickness
$k$	number of terms in series solution
$k^*$	upper limit for number of terms in summation series
$m$	summation parameter in series solution
$M$	attached local mass
$M_r$	ratio of attached mass to mass of plate
$P$	harmonic concentrated driving force
$P^*$	$= -2Pb^3/Da^2$ , dimensionless concentrated driving force
$q(x, y)$	lateral loading on the plate surface
$t$	time (seconds)
$T$	maximum kinetic energy
$U$	maximum strain energy
$u$	dimensionless coordinate of driving force
$u^*$	$= 1 - u$
$v$	dimensionless coordinate of driving force
$v^*$	$= 1 - v$

$W(\xi, \eta)$	amplitude of plate lateral displacement
$x, y$	plate spatial coordinates
$\lambda^2$	$= \omega a^2 \sqrt{\rho/D}$ , plate eigenvalue
$\rho$	mass of plate per unit area
$\omega$	circular frequency of vibration (radians/second)
$\phi$	$= b/a$ , plate aspect ratio
$\nu$	Poisson's ratio for the plate material
$\nu^*$	$= 2 - \nu$
$\delta$	net displacement of plate at driven point location
$\xi$	$= x/a$ , dimensionless plate spatial coordinate
$\eta$	$= y/b$ , dimensionless plate spatial coordinate
$\alpha_m$	plate solution parameter defined in text
$\beta_m$	plate solution parameter defined in text
$\gamma_m$	plate solution parameter defined in text
$\sigma_m$	plate solution parameter defined in text

# Chapter 1

## Introduction

The free vibration analysis of thin rectangular plates with various edge conditions and resting on internal point supports has gained considerable attention over the recent years, most notably in connection with prolonging the fatigue life of electronic circuit boards and the delicate components mounted on them [1],[2]. The electronic circuit board is being continually employed in new and increasingly demanding environments (i.e. aerospace, marine, automotive, etc.) where the board and the mounted components can be exposed to greater mechanical and thermal stresses. Designing the circuit board to only withstand the static stress may prove to be inadequate. The designer must now be concerned with the possibility that large cyclic displacements and stresses could be induced by periodic or random time varying forces acting on the board's supports. He/She must therefore insure, if possible, that the board's natural frequencies are out of the range of the frequencies where harmonic excitation is anticipated. By considering these factors during the design process, the fatigue life of the board and the mounted components can be lengthened. Failure to do this can result in highly undesirable vibrations of the electronic components and may severely shorten their working life.

Rectangular plates with a specified set of boundary conditions (i.e. clamped, simply supported or free edge) will exhibit large amplitude displacements at certain discrete frequencies which are defined as the natural frequencies of the plate. Each natural fre-

quency has an associated mode shape; the displacement shape the plate exhibits during vibration at a specific natural frequency. Modifying the plate's boundary conditions and/or support positions will alter these frequencies and the associated mode shapes. By pre-determining the plates natural frequencies the designer can position the supports and attached masses to insure that the plates natural frequency is out of range of the driving frequency. The optimal positioning of the electronic components can also be determined by use of the mode shape data. The components should be mounted where the plate experiences minimum displacement during vibration. If the components are located where the plate undergoes high displacement, they will also experience high acceleration thus increasing the dynamic stress on the electronic board and components.

## 1.1 The Governing Differential Equation

The rectangular plates discussed in this report are assumed to be thin plates with small deflection and the following assumptions [3]:

- There is no deformation in the mid-plane of the plate. This plane remains neutral during bending.
- Points of the plate lying initially on a normal-to-the-mid-plane of the plate remain on the normal-to-the-mid-plane after bending.
- The normal stresses in the direction transverse to the plate can be disregarded.

The differential equation governing the pure bending of plates subjected to lateral static loading can be obtained from numerous books dealing with the theory of plates. It's development is presented in detail by Timoshenko [3] and the final equation is written here for convenience.

$$\frac{\partial^4 W(x, y)}{\partial x^4} + 2 \frac{\partial^4 W(x, y)}{\partial x^2 \partial y^2} + \frac{\partial^4 W(x, y)}{\partial y^4} = \frac{q(x, y)}{D} \quad (1.1)$$

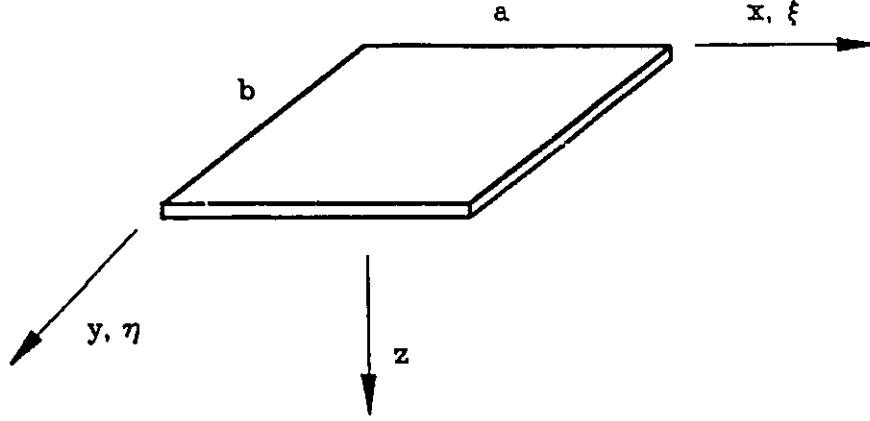


Figure 1.1: Rectangular plate with conventional and dimensionless coordinate system.

where  $q(x, y)$  is the applied static load.

In the free vibration analysis of rectangular plates, the static load acting on a differential element is replaced by an inertia force  $\rho dA \frac{\partial^2 W}{\partial t^2}$  due to the oscillatory motion of the plate and this inertia force opposes acceleration of the plate. The full development of the free vibration equation is presented in detail by Gorman [4]. The final form in the  $x, y$  - coordinate frame is given here.

$$\frac{\partial^4 W(x, y)}{\partial x^4} + 2 \frac{\partial^4 W(x, y)}{\partial x^2 \partial y^2} + \frac{\partial^4 W(x, y)}{\partial y^4} - \frac{\omega^2 \rho}{D} W(x, y) = 0 \quad (1.2)$$

Gorman emphasizes the importance of Eq.(1.2), as it governs the free vibration of all thin plates undergoing small amplitude vibration. To further simplify the analysis the dimensionless space variables  $\xi$  and  $\eta$  are introduced, where  $\xi = x/a$ ,  $\eta = y/b$  and  $a$  and  $b$  are the plate dimensions, as shown in Fig.(1.1).

With further development the fully dimensionless governing differential equation is given as [4]

$$\frac{\partial^4 W(\xi, \eta)}{\partial \eta^4} + 2\phi^2 \frac{\partial^4 W(\xi, \eta)}{\partial \eta^2 \partial \xi^2} + \phi^4 \frac{\partial^4 W(\xi, \eta)}{\partial \xi^4} - \phi^4 \lambda^4 W(\xi, \eta) = 0 \quad (1.3)$$

where  $\lambda^2 = \omega a^2 \sqrt{\rho/D}$  is defined as the eigenvalue and  $\phi = b/a$  is the plate aspect ratio.

It is the solution to Eq.(1.3) that is desired for a particular set of boundary conditions. The solution process consists of determining the eigenvalue  $\lambda^2$  (dimensionless frequency), from which a specific plate's natural frequency  $\omega$  (rad/s) can be found. Having determined the eigenvalue, the associated displacement  $W(\xi, \eta)$  can be calculated as a function  $\xi$  and  $\eta$ . By calculating the displacements for an evenly distributed set of coordinates (a grid) on the plates surface the mode shape for a particular eigenvalue  $\lambda^2$  can then be plotted.

## 1.2 Classical Boundary Conditions

Before proceeding further to obtain solutions for Eq.(1.3) for various case studies, a full description of the classical boundary conditions is given here for convenient reference. A detailed description of the development of the boundary conditions in dimensionless coordinates is found in Ref.[4].

### 1.2.1 Simply Supported Edge

$$\begin{aligned} (W(\xi, \eta))_{\xi=1} &= 0 \\ \left( \frac{\partial^2 W(\xi, \eta)}{\partial \xi^2} \right)_{\xi=1} &= 0 \end{aligned} \quad (1.4)$$

Eq.(1.4) states that along the simply supported edge  $\xi = 1$ , all lateral displacements and all bending moments must be equal to zero.

### 1.2.2 Clamped Edge

$$\begin{aligned} (W(\xi, \eta))_{\xi=1} &= 0 \\ \left( \frac{\partial W(\xi, \eta)}{\partial \xi} \right)_{\xi=1} &= 0 \end{aligned} \quad (1.5)$$

Eq.(1.5) states that along the clamped edge  $\xi = 1$  there must be zero lateral displacement and zero slope normal to the boundary.

### 1.2.3 Free Edge

The boundary conditions for the completely free edge are of a more complicated nature than those for the simply supported or clamped edge. A detailed description of the theoretical development of the boundary conditions for the free edge is given by Timoshenko [3]. In terms of dimensionless coordinates according to Ref.[4] for the free edge

edge  $\xi = 1$

$$\begin{aligned} \left( \frac{\partial^2 W(\xi, \eta)}{\partial \xi^2} + \frac{\nu}{\phi^2} \frac{\partial^2 W(\xi, \eta)}{\partial \eta^2} \right)_{\xi=1} &= 0 \\ \left( \frac{\partial^3 W(\xi, \eta)}{\partial \xi^3} + \frac{\nu}{\phi^2} \frac{\partial^3 W(\xi, \eta)}{\partial \xi \partial \eta^2} \right)_{\xi=1} &= 0 \end{aligned} \quad (1.6)$$

edge  $\eta = 1$

$$\begin{aligned} \left( \frac{\partial^2 W(\xi, \eta)}{\partial \eta^2} + \nu \phi^2 \frac{\partial^2 W(\xi, \eta)}{\partial \xi^2} \right)_{\eta=1} &= 0 \\ \left( \frac{\partial^3 W(\xi, \eta)}{\partial \eta^3} + \nu \phi^2 \frac{\partial^3 W(\xi, \eta)}{\partial \eta \partial \xi^2} \right)_{\eta=1} &= 0 \end{aligned} \quad (1.7)$$

The first boundary condition of Eqs. (1.6) and (1.7) states that the bending moments along the edges equal zero. The second boundary condition states that the vertical edge reaction along the edges are zero.

### 1.3 Concentrated Force

In the analysis of rectangular plates (dynamic or static) with internal point supports, the mathematical solution must be able to incorporate the effects of a concentrated force created by the point support. A Fourier sine series expansion of the Dirac Delta function has been used with considerable success in representing the concentrated forces of a point support or attached mass, [2], [4], [5], [6], [7]. A detailed description of the Dirac Delta function is given in Ref.[7] where the final form is given as

$$q(\xi) = 2P \sum_{m=1}^{\infty} \sin m\pi u \sin m\pi\xi \quad (1.8)$$

Eq.(1.8) is a series representation of a concentrated force which is applied to the lateral surface of the plate by either a point support or attached mass and has the units of force/unit length. The distributed force along the plate edge is highly peaked at a dimensionless distance  $u$  from the origin and exerts virtually no net force or moment elsewhere along the edge. It will be shown that this same function can be used to depict accurately an internal point support, and, with slight modification, represent the inertia force due to a concentrated mass (see Fig. 1.2).

### 1.4 The Lévy Type Solution

In the analysis of the free vibrating plate with two opposite edges simply supported, the solution to Eq.(1.3) can be taken in a series form attributed to M. Lévy and further developed by Gorman [4].

$$W(\xi, \eta) = \lim_{k \rightarrow \infty} \sum_{m=1}^k Y_m(\eta) \sin m\pi\xi \quad (1.9)$$

Each term of Eq.(1.9) fully satisfies the boundary conditions at  $\xi = 0$  and  $\xi = 1$  (zero displacement, zero bending moment). Substitution of Eq.(1.9) into the governing equation, Eq.(1.3), yields

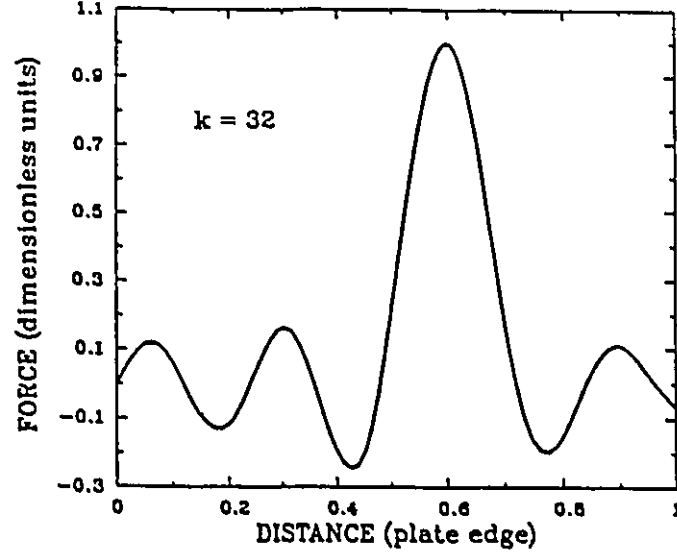


Figure 1.2: Schematic representation of the Dirac Delta Function modeling a discrete point support along a plate's edge. Point support is at 0.6 units (dimensionless),  $k = 32$ .

$$\frac{d^4 Y_m(\eta)}{d\eta^4} - 2\phi^2(m\pi)^2 \frac{d^2 Y_m \eta}{d\eta^2} + \phi^4 \{(m\pi)^4 - \lambda^4\} Y_m(\eta) = 0 \quad (1.10)$$

for each value of  $m$ .

Eq.(1.9) is an ordinary fourth-order homogeneous differential equation with constant coefficients. The solution is,

for  $\lambda^2 > (m\pi)^2$

$$Y_m(\eta) = A_m \cosh \beta_m \eta + B_m \sinh \beta_m \eta + C_m \sin \gamma_m \eta + D_m \cos \gamma_m \eta \quad (1.11)$$

and, for  $\lambda^2 < (m\pi)^2$

$$Y_m(\eta) = A_m \cosh \beta_m \eta + B_m \sinh \beta_m \eta + C_m \sinh \gamma_m \eta + D_m \cosh \gamma_m \eta \quad (1.12)$$

where

$$\beta_m = \sqrt{\lambda^2 + (m\pi)^2}$$

and

$$\gamma_m = \phi \sqrt{\lambda^2 - (m\pi)^2} \quad \text{or} \quad \gamma_m = \phi \sqrt{(m\pi)^2 - \lambda^2}$$

whichever is real.

Eq.(1.9), and Eqs.(1.11) and (1.12), represent the full solution for the free vibrating rectangular plate with two opposite edges simply supported. The final step in the solution consists of determining  $A_m, B_m, C_m$  and  $D_m$  subject to the appropriate constraints of the boundary conditions on the remaining two opposite edges and the internal concentrated forces (internal point supports).

# Chapter 2

## Literature Review

A review of the literature indicates that the free vibration analysis of rectangular plates with interior point supports has received very little attention until the 1980's, with exception of the lone study in 1953 by Nowacki [8] where he presented an analytical solution for the rectangular plate simply supported on all four sides and having an internal point support.

After 1980 considerable effort has been expended in the study of rectangular plates using various approaches including experimental, the finite element method, the energy method and analytical solutions. The emphasis has been directed towards plates with completely free edges with only a limited amount of studies on the rectangular plate with at least two opposite edges simply supported. A discussion will be presented here on the numerous studies on rectangular plates with internal supports and various boundary conditions.

### 2.1 Experimental

Fenech and Tran [9] presented results on an experimental program to determine the natural frequencies and associated mode shapes for a rectangular plate clamped in the middle of its four sides (bolt attachments) and also for the case when one of the four

bolts has failed (i.e. a plate bolted on only three of its four sides). The experimental program was connected with determining the response of structural components excited by turbulent flow. The test was performed on a thin aluminum plate which was excited by an electromagnetic exciter and the resonance frequencies were detected using a piezoelectric accelerometer. The first 49 natural frequencies were determined as well as some of the associated mode shapes. Fenech notes “the absence of an explicit analytical solution for the plate natural modes of vibration”<sup>1</sup>.

Kunz [1] discusses the importance of minimizing the vibration levels of electronic circuit boards in order to lengthen the fatigue life of both the delicate electronic components and circuit boards. Using a typical circuit board, the natural frequencies and associated mode shapes were found for various point support locations (screw attachments) by means of a random vibration testing technique. The goal was to optimize the support locations of the circuit board by determining the natural frequencies for various support positions. The experimental data were plotted and curve fitted. The highest natural frequency on the curve was then defined to be the optimal support location.

Gorman and Singal [2] conducted an investigation on the comparison of experimental and analytical results on the free vibration analysis of rectangular plates with various point supports. The experimental program consisted of testing a thin aluminum rectangular plate with internal bolt supports. The natural frequencies and associated mode shapes were determined for various support locations and plate aspect ratios. The testing was performed using an impact hammer and a fixed accelerometer. The experimental results showed very close agreement with the analytical results.

The experimental work reviewed here indicates that studies have been limited to plates with free edges with internal supports or clamped supports in the middle of the free edge. The rectangular plate with clamped or simply supported edge conditions does not appear to have been investigated. This is most probably due to the difficulty in creating a true clamped or simply supported edge.

---

<sup>1</sup>Ref.[9], page 210

## 2.2 Finite Element Method

Venkateswara [10] used the finite element method to fully analyse the rectangular plate with free edge conditions and internal supports positioned along the diagonal. High precision conforming triangular plate bending elements are used with uniform and nonuniform division. The nonuniform division was used as the point supports approached the center of the plate. Values were presented for the natural frequencies of a square plate, symmetrically supported at four points along the diagonal and comparison with analytical results were also presented showing good agreement.

Raju and Ambo-Rao [11] also studied a similar problem using the finite element method. The triangular bending element with eighteen degrees of freedom (six degrees of freedom at each vertice) was used. The accuracy of the analysis was first checked with known values for the simply supported plate and then results were compared with published data for a similar problem. The solution technique was restricted to using uniform mesh sizes.

The finite element method has been shown to give very good results for the point supported plate problem, but in order to study various support positions, the boundary conditions must be changed a number of times. Each point support must also be located at the node of an element mesh and this can have a restriction on the locations of the point supports. These factors can complicate the analysis considerably and lead to an inefficient method for investigating the vibration of rectangular plates with various support positions.

## 2.3 The Energy Method

Narita [12], [13], [14] has solved numerous plate vibration problems by the classical Ritz method. The method is based on the equations for the maximum strain and maximum kinetic energy which are expressed by

$$U = \frac{1}{2} \int \int_A \left\{ D_x \left( \frac{\partial^2 w}{\partial x^2} \right)^2 + 2D_{xy} \frac{\partial^2 w}{\partial x^2} \frac{\partial^2 w}{\partial y^2} + D_y \left( \frac{\partial^2 w}{\partial y^2} \right)^2 + 4D_k \left( \frac{\partial^2 w}{\partial x \partial y} \right)^2 \right\} dA \quad (2.1)$$

$$T = \frac{1}{2} \rho h \omega^2 \int \int_A w^2 dA \quad (2.2)$$

These are the equations for a thin orthotropic plate and can easily be simplified for the isotropic case. Applying the Ritz method, the trial function denoting the deflection of the plate is expressed by the polynomial form

$$W_{mn}(\xi, \eta) = \sum_{m=0}^M \sum_{n=0}^N A_{mn} \xi^m \eta^n \quad (2.3)$$

The deflection is constrained at the point support location and Eq.(2.3) must therefore satisfy the constraint conditions

$$W_{mn}(\xi_i, \eta_i) = 0 \quad (2.4)$$

Lagrange's undetermined multipliers are introduced into the constraint equations and then added to the total potential energy equation, where the resulting function is minimized with respect to the coefficients  $A_{mn}$ . Narita has used this method for plates with internal supports along the diagonals [12], point supports on cantilever plates [13], corner point supported shells [14], and orthotropic elliptical plates [15]. Narita notes that for the case of a rectangular plate with point supports along the diagonal "it is evident that the point support locations have significant effects on the natural frequencies, in particular when the support locations are not at the plate edges"<sup>2</sup>.

A similar approach has been used by Laura [16], [17], [18] to analyse rectangular plates with corner supports, attached mass and internal supports. The approach is by a polynomial co-ordinate function coupled with the Rayleigh-Schmidt approach. Again the basis of this solution technique is to require that the maximum strain energy of the

---

<sup>2</sup>Ref.[12], page 596

vibrating system is to be equal to the maximum kinetic energy. Laura considered the rectangular plate with two adjacent sides clamped, the other two free except for a corner point support. He also analyzed a similar plate but replaced the clamped edge with a simply supported edge [16]. Both plates carried an internal concentrated mass. Laura has analyzed plates with elastic constraints on the edges and an internal mass [17] and plates with internal masses and internal elastic supports [18]. Laura writes that “in spite of its technical importance the problem of vibrating elastic plates carrying concentrated masses with internal [elastic] supports has been the subject of a very limited number of investigations”<sup>3</sup>.

## 2.4 Analytical Solution

The most comprehensive approach to date in the free vibration analysis of rectangular plates with internal point supports has been by analytical solutions to the governing plate equation, Eq.(1.3). It is through this approach that the present problem will be discussed and solved. A brief review of similar problems and solutions will be given here.

Kersten [19], has considered the free vibrating plate problem with a corner point support by means of the modal constraint method . The analysis is concerned with a rectangular plate with two adjacent sides free with one point support on the corner. The method of solution utilizes the beam eigenfunction. The results are compared with results from the Ritz method. He notes that there were discrepancies in his numerical values and that there is room for additional research.

Bapat [20], [21], [22], [23], [24], has done considerable analytical work on the free vibration problem of rectangular plates. The method of solution consists of solving the governing differential equation subject to the constraint of the appropriate boundary conditions and the lateral loadings. The work done by Bapat most relevant to this thesis

---

<sup>3</sup>Ref.[18], page 135

is found in Ref.[24], where he considers the rectangular plate with two opposite edges simply supported and the remaining edges simply supported, clamped or free. The rectangular plate can have single or multiple internal point supports. The analysis by Bapat can incorporate any number of point supports at any arbitrary location provided that the supports are positioned on a single line perpendicular to the simply supported edges (the supports can not be located along separate perpendicular lines). The method of solution is similar to the solution in this thesis in that the plate is separated into two segments at the point support location and conditions of continuity are enforced across the partition of the two segments. Bapat has chosen to model the point support by a 'flexibility function', Ref.[21], that represents the distribution of a fictitious elastic restraint over the boundary, which is such that it has a zero value at the point support location but assumes large values resulting in negligible restraint over the rest of the partition line. Results from Ref.[24] are compared with results from the present analysis. Certain discrepancies are found and discussed.

Gorman has researched the area of rectangular plates with internal supports or edge point supports with considerable success. He is also credited for his pioneering technique with the method of superposition in the free vibration analysis of rectangular plates. In Ref.[25] Gorman solves the problem of a rectangular plate resting on symmetrical internal point supports by means of the Lévy type solution and the method of superposition. Gorman uses 'building blocks' to break the original problem into a number of smaller problems. Once each building block is solved, the solutions are superimposed. Constants are then adjusted such that the superimposed set of building blocks satisfy the constraints of the boundary conditions. Superposition requires the following to be true,

$$W(\xi, \eta) = W_1(\xi, \eta) + W_2(\xi, \eta) + W_3(\xi, \eta) \quad (2.5)$$

Gorman considers only one quadrant of the plate due to the symmetry of the support position and mode shapes.  $W_1(\xi, \eta)$  and  $W_2(\xi, \eta)$  are the solution for the completely

free plate.  $W_3(\xi, \eta)$  is solved using the representation of a harmonic force of amplitude  $P$  and frequency  $\omega$  applied at the point support location. An eigenvalue matrix is then formed from the solutions of the building blocks and any value of the eigenvalue  $\lambda^2$  that results in a zero determinant of the matrix is the natural frequency of the plate.

Saliba [26] developed a method of analyzing rectangular cantilever plates with symmetrically distributed point supports along the free edges. Through exploitation of the method of superposition and techniques developed by Gorman [4], a solution for the point supported cantilever plate was obtained by superimposed solutions that were readily obtained by classical methods. Saliba writes that “unlike numerical and other approximate solutions, the analytical solution satisfies exactly the differential equation throughout the plate. It also satisfies all boundary conditions to any desired degree of accuracy”<sup>4</sup>.

In Ref.[2] Gorman develops a solution for arbitrary located point supports. The analysis is similar to that in Ref.[25] except there are no restrictions with respect to symmetry. The solution is developed for the completely free plate by superimposing solutions from four separate building blocks. This solution is then superimposed with a building block driven by a harmonic point force. Here no restriction is imposed on the number of point supports, since the solution for each support is superimposed with the solution for the completely free plate. An eigenvalue matrix is then established using the solution for the completely free plate and the solutions for each point support. Eigenvalues  $\lambda^2$ , are then determined that cause the determinant to equal zero. Having a solution that is not restricted in terms of number and/or locations of point supports Gorman was able to devise a ‘rigid’ point support that prohibits the rotation of the plate element at the support location as well as the lateral displacement. Experimental results indicated that the rigid support accurately depicts a screw or bolt attachment. It was also shown that the point support solution could be easily modified to account for the effects of an attached mass.

---

<sup>4</sup>Ref.[26], page 381

Gorman's comprehensive book "Free Vibration Analysis of Rectangular Plates", Ref.[4], presents a detailed description of the solution for the point supported plate with simply supported edges. It is this solution that is further developed in this thesis to incorporate the effects of various boundary conditions and multiple internal point supports.

# Chapter 3

## The Modified Lévy Solution

The free vibration analysis of rectangular plates with two opposite edges simply supported can be achieved by means of a modified Lévy type solution. The rectangular plate with various boundary conditions on the remaining edges and internal supports can be fully analyzed provided the following conditions are satisfied.

- The plate's free vibration must be controlled by the governing equation Eq.(1.3).
- The lateral loadings (points supports, attached masses) and imposed boundary conditions do not introduce any nonlinearities into the problem.

These two conditions ensure that Lévy type solutions can be obtained and that the method of superposition is applicable.

### 3.1 The Simply Supported Plate with an Internal Point Support

Before attending to the problem of a rectangular plate with multiple internal point supports and various edge conditions, the solution for the steady state vibration of a simply supported rectangular plate driven by a concentrated harmonic force on it's

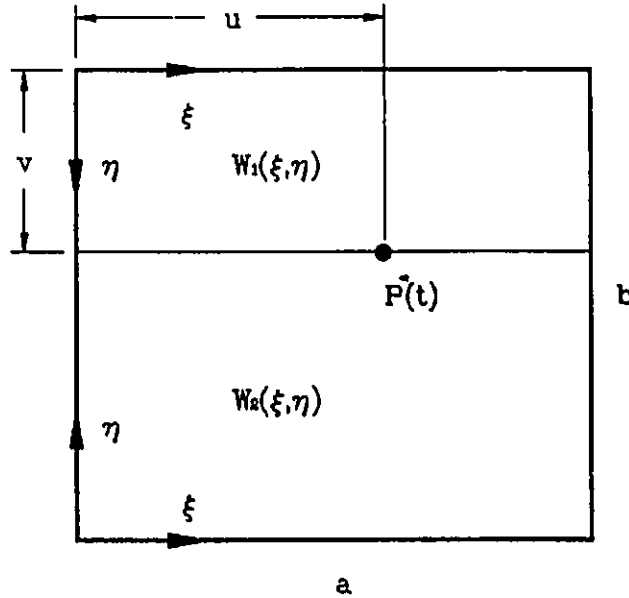


Figure 3.1: Rectangular plate with simply supported edges and an internal lateral point support.

lateral surface will be described. Here reference will be made to the solution presented in Ref.[4].

Consider the simply supported rectangular plate with an internal point support, Fig.(3.1). The point support is at coordinates  $\xi = u$ ,  $\eta = v$  and prohibits all lateral displacement of the plate at the support location. The support is represented by a time varying force  $P \sin \omega t$ , where  $P$  is the amplitude of the harmonic force.

The plate is divided into two segments, segment I and segment II, and the partition line of the two segments is drawn through the point support, parallel to the  $\xi$  axis at  $\eta = v$ .

Due to the simply supported conditions at  $\xi = 0$  and  $\xi = 1$  the Lévy-type solution is applicable. Therefore for segment I the solution appears in the form

$$W_1(\xi, \eta) = \sum_{m=1}^{\infty} Y_m(\eta) \sin m\pi\xi \quad (3.1)$$

where the subscript 1 refers to solutions applicable to segment I. Due to the simply

supported conditions at  $\eta = 0$ , the number of unknown constants can be reduced from four to two by enforcement of the boundary conditions.

for  $\lambda^2 > (m\pi)^2$

$$\begin{aligned}
Y_m(\eta)|_{\eta=0} &= A_m \cosh \beta_m(0) + B_m \sinh \beta_m(0) + C_m \sin \gamma_m(0) \\
&+ D_m \cos \gamma_m(0) = 0 \\
\frac{d^2 Y_m(\eta)}{d\eta^2} \Big|_{\eta=0} &= A_m \beta_m^2 \cosh \beta_m(0) + B_m \beta_m^2 \sinh \beta_m(0) - C_m \gamma_m^2 \sin \gamma_m(0) \\
&- D_m \cos \gamma_m(0) = 0
\end{aligned} \tag{3.2}$$

and, for  $\lambda^2 < (m\pi)^2$

$$\begin{aligned}
Y_m(\eta)|_{\eta=0} &= A_m \cosh \beta_m(0) + B_m \sinh \beta_m(0) + C_m \sinh \gamma_m(0) \\
&+ D_m \cosh \gamma_m(0) = 0 \\
\frac{d^2 Y_m(\eta)}{d\eta^2} \Big|_{\eta=0} &= A_m \beta_m^2 \cosh \beta_m(0) + B_m \beta_m^2 \sinh \beta_m(0) + C_m \gamma_m^2 \sinh \gamma_m(0) \\
&+ D_m \gamma_m^2 \cosh \gamma_m(0) = 0
\end{aligned} \tag{3.3}$$

Therefore, eliminating two of the unknowns and substituting into Eq.(3.1) we obtain

$$\begin{aligned}
W_1(\xi, \eta) &= \sum_{m=1,2}^{k^*} (A_m \sinh \beta_m \eta + B_m \sin \gamma_m \eta) \sin m\pi \xi \\
&+ \sum_{m=k^*+1}^{\infty} (A_m \sinh \beta_m \eta + B_m \sinh \gamma_m \eta) \sin m\pi \xi
\end{aligned} \tag{3.4}$$

similarly for segment II

$$\begin{aligned}
W_2(\xi, \eta) &= \sum_{m=1,2}^{k^*} (C_m \sinh \beta_m \eta + D_m \sin \gamma_m \eta) \sin m\pi \xi \\
&+ \sum_{m=k^*+1}^{\infty} (C_m \sinh \beta_m \eta + D_m \sinh \gamma_m \eta) \sin m\pi \xi
\end{aligned} \tag{3.5}$$

where

$$\beta_m = \phi\sqrt{\lambda^2 + (m\pi)^2}$$

$$\gamma_m = \phi\sqrt{\lambda^2 - (m\pi)^2} \quad \text{or} \quad \gamma_m = \phi\sqrt{(m\pi)^2 - \lambda^2}$$

which ever is real, and the first summation refers to terms for which  $\lambda^2 > (m\pi)^2$ .

It remains to establish the four unknowns  $A_m, B_m, C_m, D_m$  (two unknowns for each plate segment) which can be determined by enforcement of the four continuity conditions across the partition of the plate segments. The conditions of continuity are:

1. The plate's displacement must be continuous across the partition of the two segments.

$$Y_1(\eta)|_{\eta=v} = Y_2(\eta)|_{\eta=v} \quad (3.6)$$

2. The slope of the plate taken in a direction normal to the partition must be continuous.

$$\left. \frac{dY_1(\eta)}{d\eta} \right|_{\eta=v} = - \left. \frac{dY_2(\eta)}{d\eta} \right|_{\eta=v} \quad (3.7)$$

3. The bending moments across the partition must be continuous.

$$\left. \frac{d^2Y_1(\eta)}{d\eta^2} \right|_{\eta=v} = \left. \frac{d^2Y_2(\eta)}{d\eta^2} \right|_{\eta=v} \quad (3.8)$$

4. There must be an equilibrium force balance between the applied force  $P^* \sin \omega t$  and the vertical edge reactions taken along the edges of the plate segments across the partition line.

$$\left. \frac{d^3Y_1(\eta)}{d\eta^3} \right|_{\eta=v} + \left. \frac{d^3Y_2(\eta)}{d\eta^3} \right|_{\eta=v} = P^* \sin m\pi u \quad (3.9)$$

where  $P^* = -2Pb^3/Da^2$

A detailed description of the development of the fourth continuity condition can be found in Ref.[4]. Here the applied force is provided by the point support and is represented by the series expansion of the Dirac Delta function,

$$q(\xi) = \sum_{m=1}^{\infty} 2 \sin m\pi u \sin m\pi \xi \quad (3.10)$$

The term  $\sin m\pi \xi$  is common to both sides of Eq.(3.9) and is therefore eliminated from the equation.

Enforcement of the four continuity conditions leads to the following set of equations, for  $\lambda^2 > (m\pi)^2$

$$\begin{aligned} A_m \sinh \beta_m v + B_m \sin \gamma_m v - C_m \sinh \beta_m v^* - D_m \sin \gamma_m v^* &= 0 \\ A_m \beta_m \cosh \beta_m v + B_m \gamma_m \cos \gamma_m v + C_m \beta_m \cosh \beta_m v^* + D_m \gamma_m \cos \gamma_m v^* &= 0 \\ A_m \beta_m^2 \sinh \beta_m v - B_m \gamma_m^2 \sin \gamma_m v - C_m \beta_m^2 \sinh \beta_m v^* + D_m \gamma_m^2 \sin \gamma_m v^* &= 0 \\ A_m \beta_m^3 \cosh \beta_m v - B_m \gamma_m^3 \cos \gamma_m v + C_m \beta_m^3 \cosh \beta_m v^* - D_m \gamma_m^3 \cos \gamma_m v^* &= P^* \sin m\pi u \end{aligned} \quad (3.11)$$

and, for  $\lambda^2 < (m\pi)^2$

$$\begin{aligned} A_m \sinh \beta_m v + B_m \sinh \gamma_m v - C_m \sinh \beta_m v^* - D_m \sinh \gamma_m v^* &= 0 \\ A_m \beta_m \cosh \beta_m v + B_m \gamma_m \cosh \gamma_m v + C_m \beta_m \cosh \beta_m v^* + D_m \gamma_m \cosh \gamma_m v^* &= 0 \\ A_m \beta_m^2 \sinh \beta_m v + B_m \gamma_m^2 \sinh \gamma_m v - C_m \beta_m^2 \sinh \beta_m v^* - D_m \gamma_m^2 \sinh \gamma_m v^* &= 0 \\ A_m \beta_m^3 \cosh \beta_m v + B_m \gamma_m^3 \cosh \gamma_m v + C_m \beta_m^3 \cosh \beta_m v^* + D_m \gamma_m^3 \cosh \gamma_m v^* &= P^* \sin m\pi u \end{aligned} \quad (3.12)$$

where  $v^* = 1 - v$

The above set of algebraic simultaneous equations can be solved in a straight forward manner utilizing well known trigonometric identities. Solving Eqs.(3.11) and Eqs.(3.12) for the unknowns we obtain,

$$\begin{array}{ll} \lambda^2 > (m\pi^2) & \lambda^2 < (m\pi^2) \\ A_m = \frac{P^* \sin m\pi u \sinh \beta_m v^*}{(\beta_m^2 + \gamma_m^2) \beta_m \sinh \beta_m} & A_m = \frac{P^* \sin m\pi u \sinh \beta_m v^*}{(\beta_m^2 - \gamma_m^2) \beta_m \sinh \beta_m} \\ B_m = \frac{P^* \sin m\pi u \sin \gamma_m v^*}{(\beta_m^2 + \gamma_m^2) \gamma_m \sin \gamma_m} & B_m = -\frac{P^* \sin m\pi u \sinh \gamma_m v^*}{(\beta_m^2 - \gamma_m^2) \gamma_m \sinh \gamma_m} \\ C_m = \frac{P^* \sin m\pi u \sinh \beta_m v}{(\beta_m^2 + \gamma_m^2) \beta_m \sinh \beta_m} & C_m = \frac{P^* \sin m\pi u \sinh \beta_m v}{(\beta_m^2 - \gamma_m^2) \beta_m \sinh \beta_m} \\ D_m = \frac{P^* \sin m\pi u \sin \gamma_m v}{(\beta_m^2 + \gamma_m^2) \gamma_m \sin \gamma_m} & D_m = -\frac{P^* \sin m\pi u \sinh \gamma_m v}{(\beta_m^2 - \gamma_m^2) \gamma_m \sinh \gamma_m} \end{array} \quad (3.13)$$

With the unknowns evaluated the solution for the steady-state response of an undamped simply supported plate subjected to a harmonic force acting on the plate lateral surface is complete. Substitution of the constants  $A_m, B_m$  and  $C_m, D_m$  into Eq.(3.4) and Eq.(3.5) yields

$$\begin{aligned}
W_1(\xi, \eta) &= P^* \sum_{m=1,2}^{k^*} \frac{\sin m\pi u}{\beta_m^2 + \gamma_m^2} \left( \frac{\sinh \beta_m v^* \sinh \beta_m \eta}{\beta_m \sinh \beta_m} - \frac{\sin \gamma_m v^* \sin \gamma_m \eta}{\gamma_m \sin \gamma_m} \right) \\
&\quad \times \sin m\pi \xi \\
&+ P^* \sum_{m=k^*+1}^{\infty} \frac{\sin m\pi u}{\beta_m^2 - \gamma_m^2} \left( \frac{\sinh \beta_m v^* \sinh \beta_m \eta}{\beta_m \sinh \beta_m} - \frac{\sinh \gamma_m v^* \sinh \gamma_m \eta}{\gamma_m \sinh \gamma_m} \right) \\
&\quad \times \sin m\pi \xi
\end{aligned} \tag{3.14}$$

$$\begin{aligned}
W_2(\xi, \eta) &= P^* \sum_{m=1,2}^{k^*} \frac{\sin m\pi u}{\beta_m^2 + \gamma_m^2} \left( \frac{\sinh \beta_m v \sinh \beta_m \eta}{\beta_m \sinh \beta_m} - \frac{\sin \gamma_m v \sin \gamma_m \eta}{\gamma_m \sin \gamma_m} \right) \\
&\quad \times \sin m\pi \xi \\
&+ P^* \sum_{m=k^*+1}^{\infty} \frac{\sin m\pi u}{\beta_m^2 - \gamma_m^2} \left( \frac{\sinh \beta_m v \sinh \beta_m \eta}{\beta_m \sinh \beta_m} - \frac{\sinh \gamma_m v \sinh \gamma_m \eta}{\gamma_m \sinh \gamma_m} \right) \\
&\quad \times \sin m\pi \xi
\end{aligned} \tag{3.15}$$

To establish the eigenvalue  $\lambda^2$ , from Eq.(3.14) the condition of zero lateral displacement is enforced at the point support location ( $\xi = u$  and  $\eta = v$ ). To obtain the associated mode shapes,  $\lambda^2$  is substituted into Eq.(3.14) and Eq.(3.15) and the displacements  $W_1(\xi, \eta), W_2(\xi, \eta)$  are calculated.

This solution process is the basis to every problem covered in this thesis. All solutions for the remaining types of plates, with multiple supports and attached masses will be developed and obtained in a similar manner.

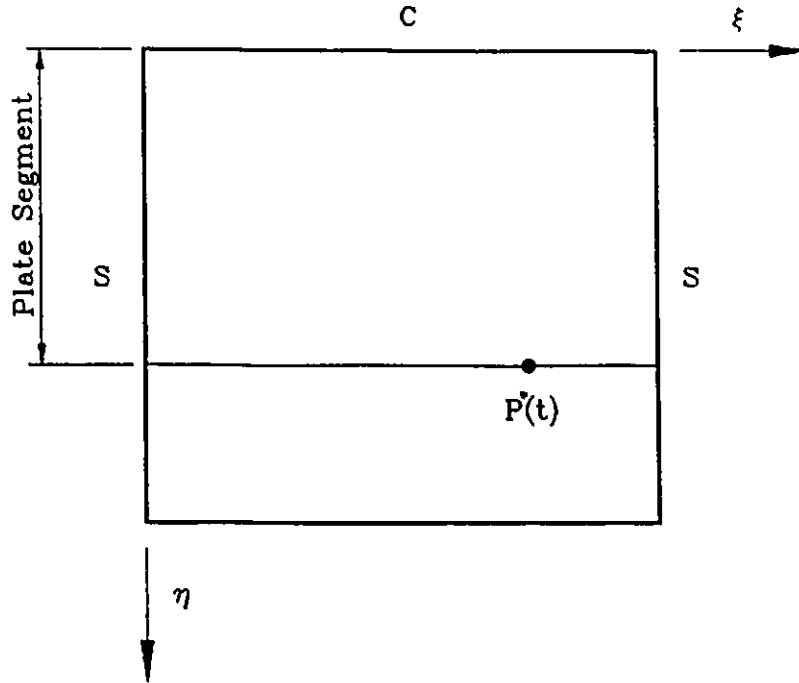


Figure 3.2: Rectangular plate segment with two edges simply supported and a third edge clamped.

### 3.2 The Solution for the Plate Segment with a Clamped Edge

Following the same procedure as that for the simply supported edge, the Lévy solution can be modified to incorporate the effects of a clamped edge.

In Fig.(3.2) there is drawn a segment of a plate with two opposite edges simply supported and a third edge clamped. In view of the clamped edge boundary condition we can write,

for  $\lambda^2 > (m\pi)^2$

$$\begin{aligned} Y_m|_{\eta=0} &= A_m \cosh \beta_m(0) + B_m \sinh \beta_m(0) + C_m \sin \gamma_m(0) + D_m \cos \gamma_m(0) \\ &= 0 \end{aligned}$$

$$\begin{aligned} \left. \frac{dY_m(\eta)}{d\eta} \right|_{\eta=0} &= A_m \beta_m \sinh \beta_m(0) + B_m \beta_m \cosh \beta_m(0) + C_m \gamma_m \cos \gamma_m(0) - D_m \gamma_m \sin \gamma_m(0) \\ &= 0 \end{aligned} \quad (3.16)$$

and, for  $\lambda^2 < (m\pi^2)$

$$\begin{aligned} Y_m(\eta)|_{\eta=0} &= A_m \cosh \beta_m(0) + B_m \sinh \beta_m(0) + C_m \sinh \gamma_m(0) + D_m \cosh \gamma_m(0) \\ &= 0 \\ \left. \frac{dY_m(\eta)}{d\eta} \right|_{\eta=0} &= A_m \beta_m \sinh \beta_m(0) + B_m \beta_m \cosh \beta_m(0) + C_m \gamma_m \sinh \gamma_m(0) + D_m \gamma_m \cosh \gamma_m(0) \\ &= 0 \end{aligned} \quad (3.17)$$

The four unknowns can be reduced to two unknowns and the Lévy solution can be written as

$$\begin{aligned} W(\xi, \eta) &= P^* \sum_{m=1,2}^{k^*} \left( A_m (\sinh \beta_m \eta - \frac{\beta_m}{\gamma_m} \sin \gamma_m \eta) + B_m (\cosh \beta_m \eta - \cos \gamma_m \eta) \right) \\ &\quad \times \sin m\pi\xi \\ &+ P^* \sum_{m=k^*+1}^{\infty} \left( A_m (\sinh \beta_m \eta - \frac{\beta_m}{\gamma_m} \sinh \gamma_m \eta) + B_m (\cosh \beta_m \eta - \cosh \gamma_m \eta) \right) \\ &\quad \times \sin m\pi\xi \end{aligned} \quad (3.18)$$

where  $\beta_m, \gamma_m$  and  $k^*$  take on their usual meanings and the constants  $A_m$  and  $B_m$  remain to be evaluated.

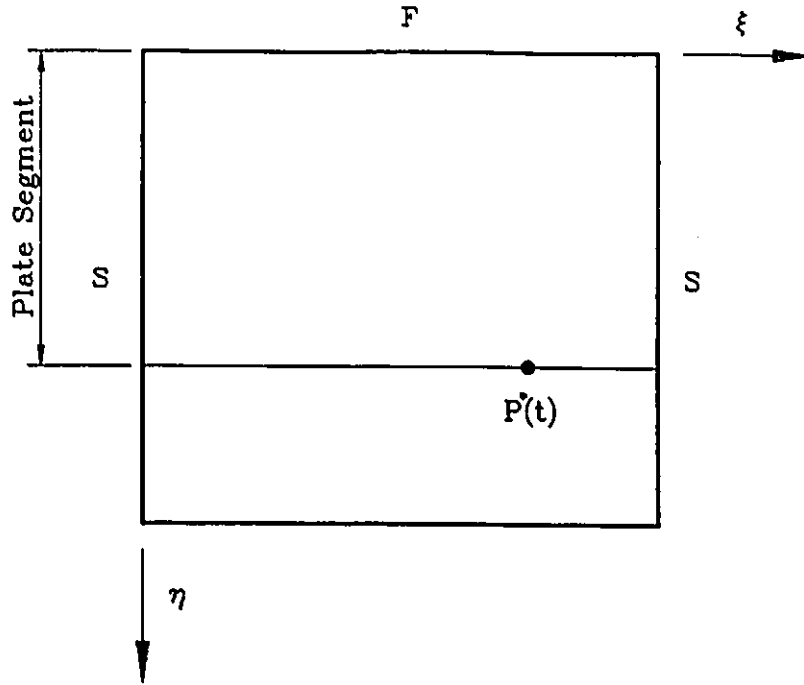


Figure 3.3: Rectangular plate segment with two edges simply supported and a third edge free.

### 3.3 The Solution for a Plate Segment with a Free Edge

Although the boundary conditions for the free edge are of a more complicated nature than those for the simply supported or clamped edge, the determination of the Lévy solution for the free edge segment is obtained in a similar manner.

Enforcing the boundary conditions for the free edge yields

for  $\lambda^2 > (m\pi)^2$

$$\begin{aligned}
 \left. \frac{\partial^2 W(\xi, \eta)}{\partial \eta^2} + \nu \phi^2 \frac{\partial^2 W(\xi, \eta)}{\partial \xi^2} \right|_{\eta=0} &= A_m \beta_m^2 \cosh \beta_m(0) + B_m \beta_m^2 \sinh \beta_m(0) \\
 - C_m \gamma_m^2 \sin \gamma_m(0) - D_m \gamma_m^2 \cos \gamma_m(0) - \nu \phi^2 (m\pi)^2 (A_m \cosh \beta_m(0) \\
 + B_m \sinh \beta_m(0) + C_m \sin \gamma_m(0) + D_m \cos \gamma_m(0)) &= 0
 \end{aligned} \tag{3.19}$$

$$\begin{aligned}
\left. \frac{\partial^3 W(\xi, \eta)}{\partial \eta^3} + \nu^* \phi^2 \frac{\partial^3 W(\xi, \eta)}{\partial \eta \partial \xi^2} \right|_{\eta=0} &= A_m \beta^3 \sinh \beta_m(0) + B_m \beta^3 \cosh \beta_m(0) \\
&- C_m \gamma^3 \cos \gamma_m(0) + D_m \gamma^3 \sin \gamma_m(0) - \nu^* \phi^2 (m\pi)^2 (A_m \beta_m \sinh \beta_m(0) \\
&+ B_m \beta_m \cosh \beta_m(0) + C_m \gamma_m \cos \gamma_m(0) - D_m \gamma_m \sin \gamma_m(0)) = 0
\end{aligned} \tag{3.20}$$

and, for  $\lambda^2 < (m\pi)^2$

$$\begin{aligned}
\left. \frac{\partial^2 W(\xi, \eta)}{\partial \eta^2} + \nu \phi^2 \frac{\partial^2 W(\xi, \eta)}{\partial \xi^2} \right|_{\eta=0} &= A_m \beta_m^2 \cosh \beta_m(0) + B_m \beta_m^2 \sinh \beta_m(0) \\
&+ C_m \gamma_m^2 \sinh \gamma_m(0) + D_m \gamma_m^2 \cosh \gamma_m(0) - \nu \phi^2 (m\pi)^2 (A_m \cosh \beta_m(0) \\
&+ B_m \sinh \beta_m(0) + C_m \sinh \gamma_m(0) + D_m \cosh \gamma_m(0)) = 0
\end{aligned} \tag{3.21}$$

$$\begin{aligned}
\left. \frac{\partial^3 W(\xi, \eta)}{\partial \eta^3} + \nu^* \phi^2 \frac{\partial^3 W(\xi, \eta)}{\partial \eta \partial \xi^2} \right|_{\eta=0} &= A_m \beta^3 \sinh \beta_m(0) + B_m \beta^3 \cosh \beta_m(0) \\
&+ C_m \gamma^3 \cosh \gamma_m(0) + D_m \gamma^3 \sinh \gamma_m(0) - \nu^* \phi^2 (m\pi)^2 (A_m \beta_m \sinh \beta_m(0) \\
&+ B_m \beta_m \cosh \beta_m(0) + C_m \gamma_m \cosh \gamma_m(0) + D_m \gamma_m \sinh \gamma_m(0)) = 0
\end{aligned} \tag{3.22}$$

Therefore, by eliminating two of the unknowns, the Lévy type solution for the free edge segment can be written as

$$\begin{aligned}
W(\xi, \eta) &= P^* \sum_{m=1,2}^{k^*} (A_m \{ \cosh \beta_m \eta + \frac{\beta_m^2 - \nu \phi^2 (m\pi)^2}{\gamma_m^2 + \nu \phi^2 (m\pi)^2} \cos \gamma_m \eta \} \\
&+ B \{ \sinh \beta_m \eta + \frac{\beta^3 + \beta \nu^* \phi^2 (m\pi)^2}{\gamma_m^2 - \gamma_m \nu^* \phi^2 (m\pi)^2} \sin \gamma_m \eta \}) \sin m\pi \xi \\
&+ P^* \sum_{m=k^*+1}^{\infty} (A_m \{ \cosh \beta_m \eta - \frac{\beta_m^2 - \nu \phi^2 (m\pi)^2}{\gamma_m^2 - \nu \phi^2 (m\pi)^2} \cosh \gamma_m \eta \} \\
&+ B_m \{ \sinh \beta_m \eta - \frac{\beta^3 - \beta \nu^* \phi^2 (m\pi)^2}{\gamma^3 - \gamma_m \nu^* \phi^2 (m\pi)^2} \sinh \gamma_m \eta \}) \sin m\pi \xi
\end{aligned} \tag{3.23}$$

### 3.4 The Six Case Studies

On account of using the Lévy type solution the analysis is restricted to rectangular plates with at least two opposite edges simply supported. However, the two remaining edges can be any combination of simply supported, clamped or free. There are therefore six possible combinations of plate boundary conditions. Each set or combination of boundary conditions is identified by a case number and a four letter code. For simplicity, the following abbreviations shall be used.

S – simply supported

C – clamped

F – free

For example, consider Case 2, SSSC (simple-simple-simple-clamped) where the plate edge conditions are counted from the far left edge in a counter-clockwise manner (see Fig.(3.4)). The full solution for Case 2, SSSC with an internal point support is obtained in the same manner as that for the simply supported plate, Case 1, SSSS (see Sec.(3.1)). The solution for the top clamped edge is given by Eq.(3.18) and shall be referred to as  $W_1(\xi, \eta)$ . The solution for the bottom simply supported edge is given by Eq.(3.4) and shall be referred to as  $W_2(\xi, \eta)$ . Enforcing the four continuity conditions across the partition line of the plate segments yields a nonhomogeneous set of four equations with four unknowns  $A_m, B_m, C_m, D_m$  (two unknowns per solution). It was shown that for Case 1, SSSS, the four unknowns were determined with relative ease. For the remaining case studies the resulting equations from enforcement of the continuity conditions are not as easily solved. Instead a computer code is implemented to solve for the unknowns. The fully developed sets of equations resulting from the enforcement of the continuity conditions for each case study is available in Appendix A.

Returning to Case 2, SSSC, after the numerical values of the unknown constants are calculated they are substituted into the appropriate solution  $W_1(\xi, \eta), W_2(\xi, \eta)$  and eigenvalues are determined by setting the solutions equal to zero at the point support

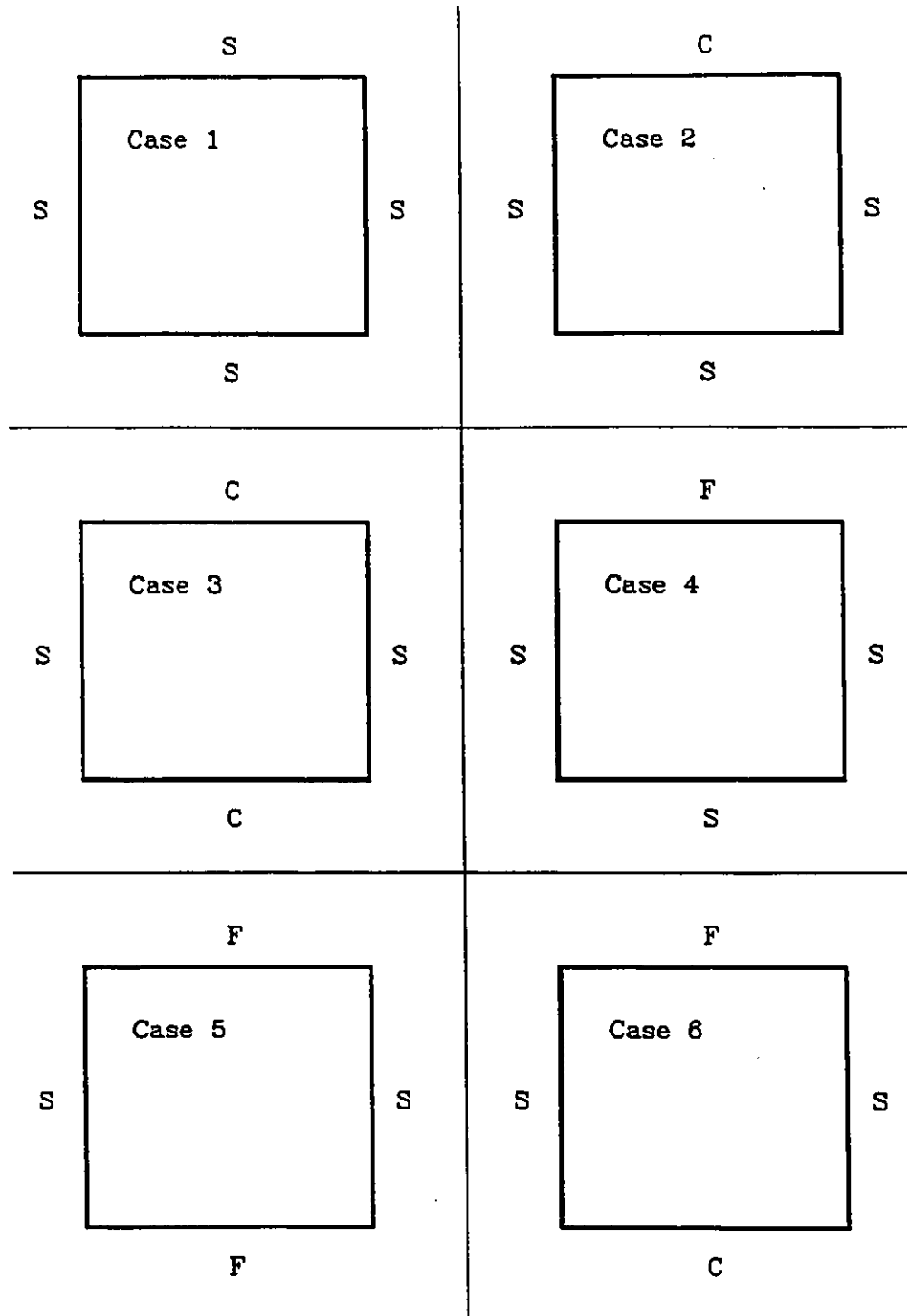


Figure 3.4: Six possible combinations of rectangular plates with two opposite edges simply supported and the other two simply supported, clamped or free.

location.

$$W_1(u, v) = W_2(u, v^*) = 0 \quad (3.24)$$

Having determined the eigenvalues it is a straight forward procedure to substitute the values back into the solutions to obtain the associated mode shapes.

This solution procedure is employed for all the case studies covered in this thesis and, by the method of superposition, is further developed to take into account the effects of multiple internal supports and/or attached masses.

# Chapter 4

## Multiple Point Support Problems

### 4.1 Multiple Internal Point Supports

With the solution available for the rectangular plate with a single discrete point support, the analysis can now be extended to incorporate a rectangular plate with  $N$  discrete point supports, each of which prohibits lateral displacement of the plate at the point of application but imparts no bending moments to the plate.

Consider the rectangular plate in Fig.(4.1) with four symmetrically distributed internal point supports. To determine the complete solution, a full individual solution is required, of the type discussed in Chapter 3, for each discrete point support (Fig. 4.2). By the method of superposition each individual solution is superimposed, one-on-top-of-the-other, generating an eigenvalue matrix, shown schematically in Fig(4.3). The eigenvalue matrix establishes a mathematical relationship between the driving forces of the point supports, the individual plate solutions and the total displacement of the plate at each of the discrete point support locations. The free vibration eigenvalues  $\lambda^2$  of the plate are then determined by establishing those values of the parameter  $\lambda^2$  which permits a nontrivial solution for the eigenvalue matrix equations.

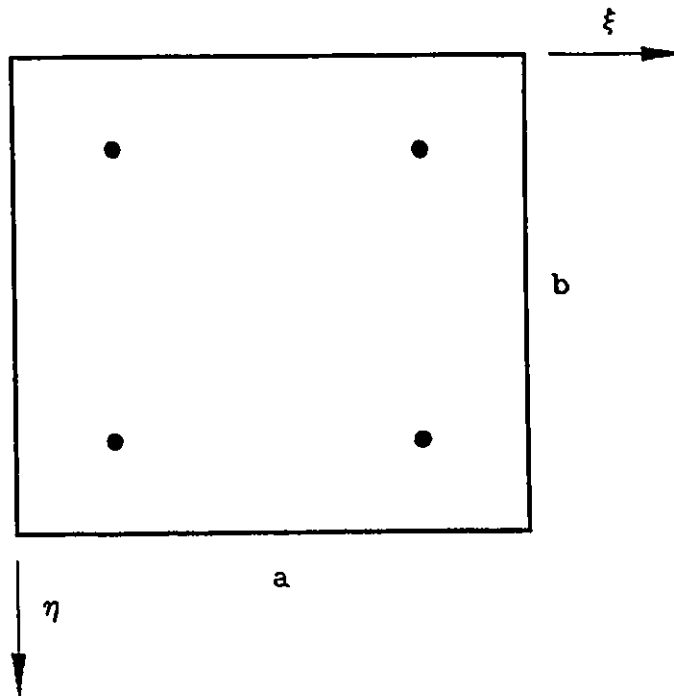


Figure 4.1: Rectangular plate with four discrete point supports.

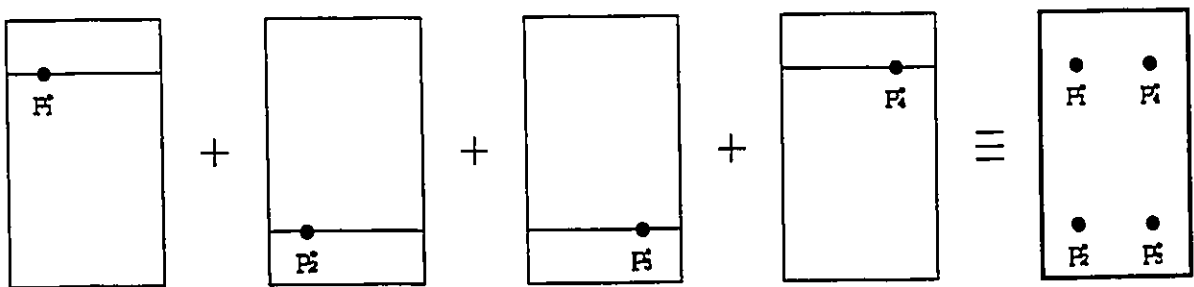


Figure 4.2: Four individual point supported plate solutions superimposed to establish the solution for a plate with four internal point supports.

$$\begin{array}{cccccc}
 P_1^* & P_2^* & P_3^* & P_4^* & & \\
 - & - & - & - & \delta_1 & \\
 - & - & - & - & \delta_2 & \\
 - & - & - & - & \delta_3 & \\
 - & - & - & - & \delta_4 & 
 \end{array}$$

Figure 4.3: Schematic representation of  $4 \times 4$  eigenvalue matrix.

$P_1^*, P_2^*, P_3^*, P_4^*$  are the driving force amplitudes. The symbols  $\delta_1, \delta_2, \delta_3, \delta_4$  represent the net displacement of the plate at each point supported location. Each element in the first row of the matrix, when multiplied by the force amplitude  $P_i^*$  immediately above it, represents the contribution of each individual plate solution to the net plate displacement at the driven point location  $\delta_i$ . In fact, the  $i, j$  element of the matrix represents the contribution of the solution driven at point  $j$  to the displacement at driven point  $i$ . Enforcing the condition that there must be zero displacement at the driving force locations (i.e.  $\delta_1 = \delta_2 = \delta_3 = \delta_4 = 0$ ) the  $4 \times 4$  matrix represents a homogeneous set of algebraic equations relating the driving force amplitudes  $P_1^*, P_2^*, P_3^*, P_4^*$ .

Eigenvalues for the rectangular plate with specified boundary conditions and internal point supports are then determined by the following procedure.

1. A trial value is selected for the parameter  $\lambda^2$ , well below the first mode eigenvalue.
2. The matrix associated with this trial value is generated.
3. The determinant of the homogeneous matrix is computed and stored.
4. The value of  $\lambda^2$  is increased by a specified increment, and the procedure is repeated until the determinant undergoes a sign change.
5. The eigenvalue is then obtained by reducing the increment and determining the value of  $\lambda^2$  for which the determinant vanishes (see Fig.(4.4)).
6. Upon establishing the first (fundamental) eigenvalue the procedure is repeated in order to obtain the desired higher eigenvalues.

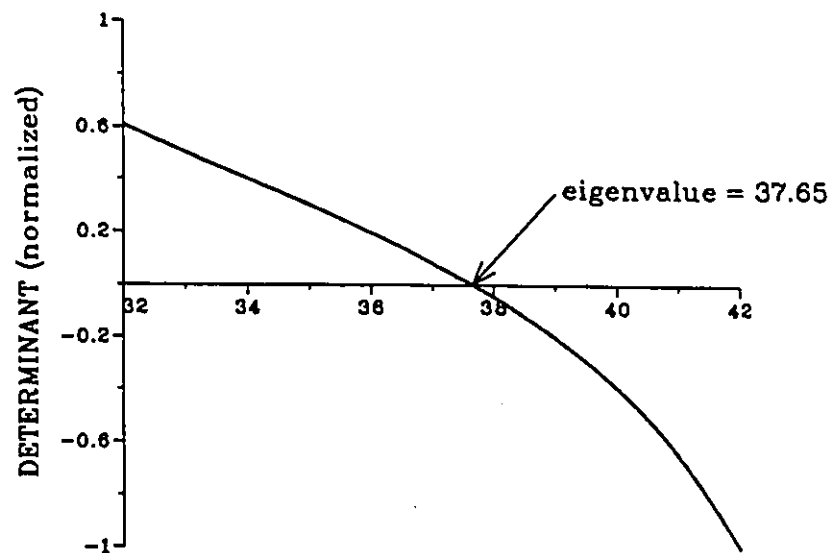


Figure 4.4: Matrix determinant vs.  $\lambda^2$ . Eigenvalue established at  $\lambda^2 = 37.65$  (see Appendix B, Table B.1, mode 1,  $u = v = 0.2$ ).

To determine the associated mode shape, one of the driving force amplitudes,  $P_1^*$ , is set equal to unity. A solution for the remaining force amplitudes is then obtained from the set of simultaneous nonhomogeneous algebraic equations. With this information available, the mode shape comprising the sum of all the force driven solutions can be obtained and plotted.

The eigenvalue matrix of this type can be easily generated using a computer code once the coordinates of the driving points are described. The values  $u, v, u^*, v^*$  will be different for each force-driven solution. They will be determined once the driving points are specified. There is no restriction on the size of the eigenvalue matrix and therefore no limit on the number of point supports. The addition of each point support only increases the matrix size by one column and one row.

## 4.2 The 'Rigid' Point Support

The term 'rigid' point support refers to a support at a point that prohibits both lateral displacement and rotation of the plate at the support location. This type of support is usually provided by screw type fasteners or local welds. In Ref.[2] the rigid point support has been modelled mathematically by a cluster of four discrete closely spaced point supports. Each discrete point support forbids plate lateral motion at its point of application. It does not itself, however, oppose rotation of the plate and imparts no moment to it. To achieve a rigid point support four discrete point supports are utilized, one at each end of mutually perpendicular lines, intersecting in the middle of the rigid support location and parallel to the edges of the plate. While each discrete point support prohibits plate lateral displacement, only, the combination of the two pairs of supports prohibits rotation of the plate in either of the above mentioned two directions.

It was found that increasing the number of discrete point supports from 4 to 5 (adding a discrete point support to the middle of the rigid point support area to increase

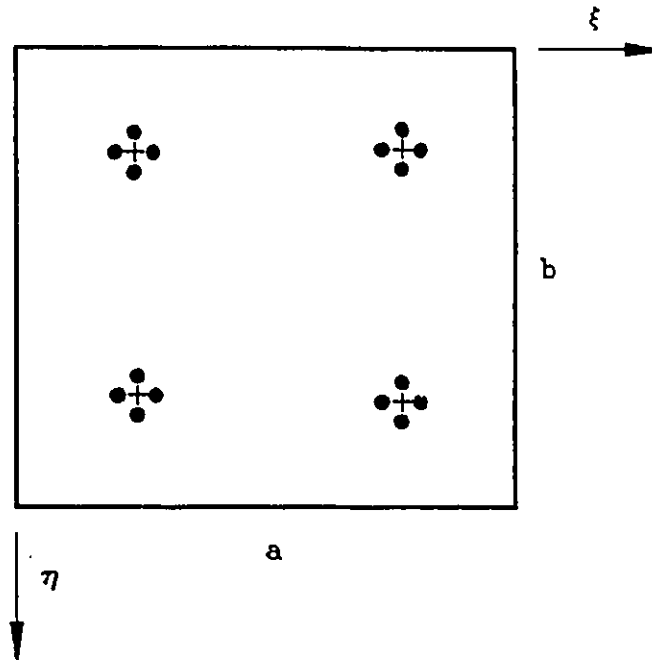


Figure 4.5: Rectangular plate with 4 rigid point supports modelled by 16 discrete point supports.

the rigid effect of the support) had only a minimal effect on the computed eigenvalue. Thus it was felt that the corresponding increase in computer time could not be justified and that the more computer efficient '4 point' solution provided sufficiently accurate simulation of a rigid point support. To model a plate with four rigid point supports (Fig. 4.5), each discrete point support location must be fully defined. This results in a  $16 \times 16$  eigenvalue matrix. The same procedure as that described in Sec.(4.1) in determining the eigenvalue is then applied.

In ref.[2], Gorman modelled four  $\frac{5''}{8}$  diameter bolts on a  $10'' \times 15''$  aluminum plate ( $\phi = 1.5$ ) by four rigid point supports. Each rigid point support was modelled by four discrete point supports. The discrete point support locations were determined by the bolt radius,  $\frac{5''}{16}$ . Converting the bolt radius into dimensionless units, the discrete point supports were located at  $\frac{5}{16} \times \frac{1}{10} = .03125$  units from the center of the support, parallel to the  $\xi$  axis and  $\frac{5}{16} \times \frac{1}{15} = .02083$  units from the support, parallel to the  $\eta$  axis. These

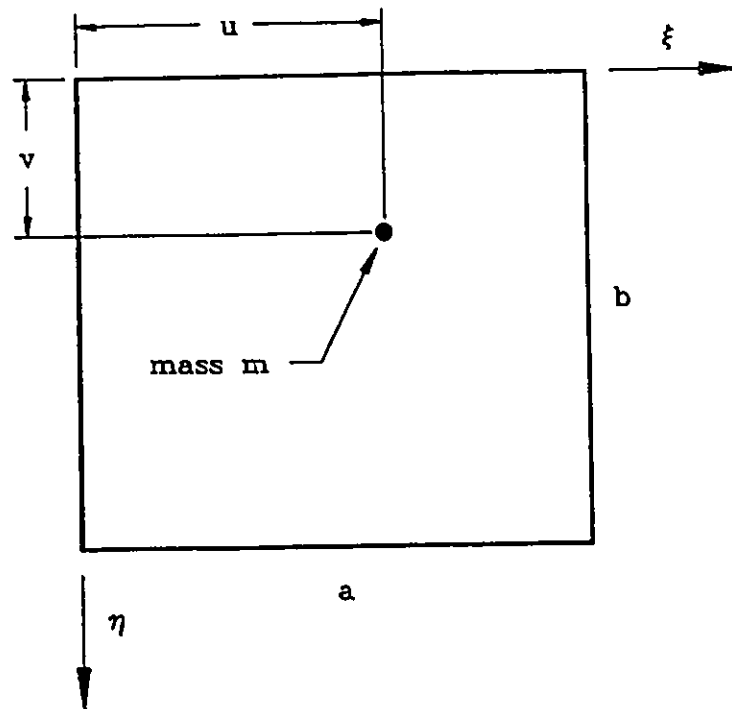


Figure 4.6: Rectangular plate with local mass  $M$  attached.

same dimensions are utilized in this thesis for plates with aspect ratio  $\phi = 1.5$ . For plates with aspect ratio  $\phi = 1.0$ , the discrete point supports are located at  $\frac{5}{16} \times \frac{1}{10} = .03125$  units from the center of the support, parallel to the  $\xi$  axis and as well as  $\frac{5}{16} \times \frac{1}{10} = .03125$  units from the center of the support, parallel to the  $\eta$  axis.

### 4.3 Matrix Modification for Attached Mass

Consider the rectangular plate of Fig.(4.6) with a localized mass  $M$  attached at the dimensionless co-ordinates  $u$  and  $v$ . The mass exerts a harmonic inertia force on the plate which opposes motion and whose amplitude equals  $M\omega^2 aW(u, v)$ , where  $W(u, v)$  is the net dimensionless displacement at the co-ordinates  $u$  and  $v$ . It is easily shown that as far as the plate is concerned it experiences a local harmonic force acting in the direction of displacement of the plate and with dimensionless amplitude

$$P^* = -2\phi^4 M_r \lambda^4 W(u, v) \quad (4.1)$$

Denoting the contributions to displacement at the point  $u, v$  due to the driving forces  $P_1^*, P_2^*$  etc., associated with the discrete points supports as  $P_1^* W_1(u, v), P_2^* W_2(u, v)$ , etc., it follows from Eq.(4.1) that

$$P^* Q = P_1^* W_1(u, v) + P_2^* W_2(u, v) + \dots + P^* W_M(u, v) \quad (4.2)$$

where the last term relates to displacement due to the inertia force associated with the added mass only and

$$Q = \frac{-1}{2\phi^4 M_r \lambda^4} \quad (4.3)$$

Eq.(4.2) may be written as

$$P_1^* W_1(u, v) + P_2^* W_2(u, v) + \dots + P^* \{W_M(u, v) - Q\} = 0 \quad (4.4)$$

Eq.(4.4) describes how the eigenvalue matrix can be modified when, in addition to discrete point supports, there is an attached mass. Initially, all locations of discrete point supports and attached masses are considered to be locations of discrete point supports. Suppose at the  $N$ 'th location there is an attached mass. One only needs to return to the element  $N, N$  of the matrix and modify it as indicated in Eq.(4.4), i.e. the appropriate quantity  $Q$  should be subtracted from this element. It can be seen here that the eigenvalue matrix can be easily modified for a single attached mass or multiple attached masses and will only marginally effect the complexity of the computer analysis.

# Chapter 5

## Presentation of Results

The results for the free vibration analysis of rectangular plates with two opposite edges simply supported are presented here for a) multiple internal point supports and b) multiple internal point supports and attached masses. Eigenvalue curves are generated (eigenvalue vs. point support position) and plotted along with some associated mode shapes. Computed eigenvalues (four digit accuracy) from the eigenvalue curves are presented in Appendix B.

### 5.1 Multiple Internal Point Supports

For Case 1: SSSS, Case 3: SCSC, and Case 5: SFSE results of the present method are first compared with results presented by Bapat [24]. Bapat's analysis was able to incorporate the effects of multiple point supports but restricted the location of the point supports to a single line perpendicular to the simply supported edges,  $\xi = 0$  and  $\xi = 1$ . In general good agreement is obtained between the present solution method and Bapat's solution method except certain discrepancies are found. These will be discussed later.

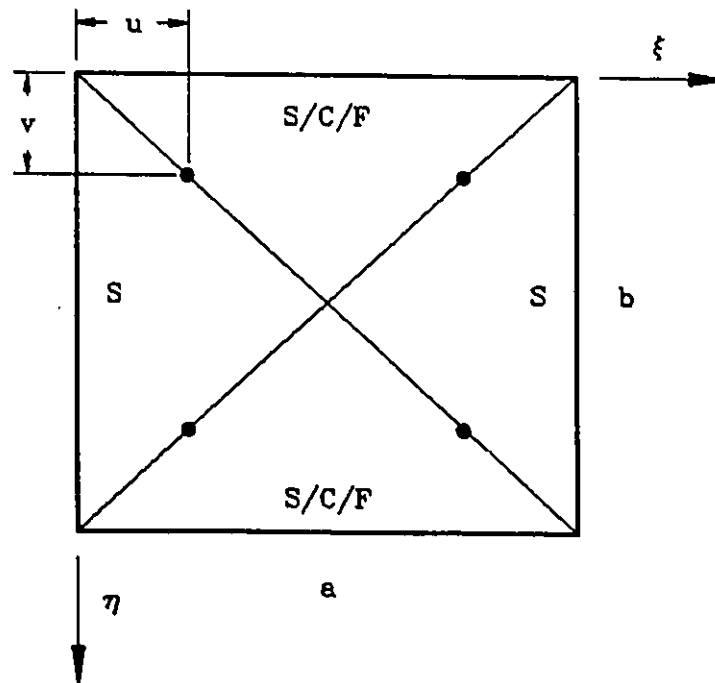


Figure 5.1: Rectangular plate with four point supports and various boundary conditions. Point supports represented by solid dots (discrete and rigid).

For each case study the eigenvalue curves are determined for the following point support types and plate aspect ratio combinations.

- aspect ratio  $\phi = 1.0$ , point support type: discrete
- aspect ratio  $\phi = 1.0$ , point support type: rigid
- aspect ratio  $\phi = 1.5$ , point support type: discrete
- aspect ratio  $\phi = 1.5$ , point support type: rigid

The discrete point supports and rigid point supports are the same as those discussed in Chapter 4.

For each combination, the plate is given a point support at four symmetrically distributed locations lying on the plate's diagonals at dimensionless distance  $u$  and  $v$  from the ends of the plate (see Fig. 5.1). Unless otherwise stated the parameters  $u$  and  $v$  will always refer the point support location. Eigenvalues are determined for various

values of  $u = v$  and plotted. Using a small increment of the point support locations eigenvalue curves can then be generated. The eigenvalue curves are presented for the first four eigenvalues.

The first four associated mode shapes are also presented for specific point support locations (both discrete and rigid point supports are compared).

### 5.1.1 Comparison of Results

Table 5.1: Comparison of first three computed eigenvalues  $\lambda^2$ , Case 1, SSSS, from present analysis and Bapat's( ) for plate with one discrete point support.

$u$	$v$	plate aspect ratio $\phi$			
		0.5		1.0	
0.6	0.6	69.86	(69.855)	36.73	(36.728)
		106.8	(106.79)	70.58	(70.574)
		144.8	(144.78)	83.29	(83.292)
0.7	0.6	62.04	(62.036)	31.46	(31.458)
		121.9	(119.46)	71.19	(71.186)
		143.4	(143.37)	90.60	(90.593)

Table 5.2: Comparison of first three computed eigenvalues  $\lambda^2$ , Case 1, SSSS, from present analysis and Bapat's( ) for plate with two discrete point supports.

$u$	$v$	plate aspect ratio $\phi$			
		0.5		1.0	
0.6	0.6	103.7	(103.66)	41.57	(41.571)
		113.3	(113.27)	65.22	(65.220)
		176.4	(176.40)	77.90	(77.890)
0.6	0.75	86.51	(86.502)	31.20	(31.197)
		98.01	(98.006)	57.13	(57.128)
		150.7	(150.69)	82.89	(82.882)

Table 5.3: Comparison of first three computed eigenvalues  $\lambda^2$ , Case 3, SCSC, from present analysis and Bapat's( ) for plate with one discrete point support.

$u$	$v$	plate aspect ratio $\phi$			
		0.5		1.0	
0.6	0.6	109.1	(109.10)	45.28	(45.257)
		139.8	(139.65)	61.83	(61.809)
		178.7	(178.39)	85.62	(85.551)
0.7	0.6	103.5	(103.53)	39.35	(39.330)
		152.1	(152.03)	65.41	(65.402)
		181.7	(181.24)	85.11	(85.056)

Table 5.4: Comparison of first three computed eigenvalues  $\lambda^2$ , Case 3, SCSC, from present analysis and Bapat's( ) for plate with two discrete point supports. \* Eigenvalues are suspect.

$u$	$v$	plate aspect ratio $\phi$			
		0.5		1.0	
0.6	0.6	135.9	(135.87)	55.84	(55.835)
		149.8	(149.79)	72.40	(72.398)
		236.9	(236.90)	97.21	(97.208)
0.6	0.75	122.0	(127.59)	40.17	(54.743)*
		130.6	(133.97)	62.41	(69.327)*
		183.6	(187.77)	98.48	(94.585)*

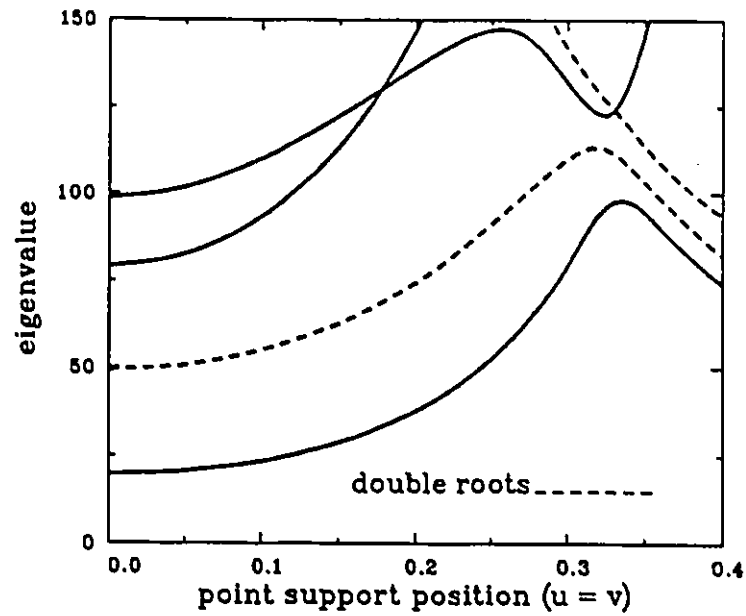
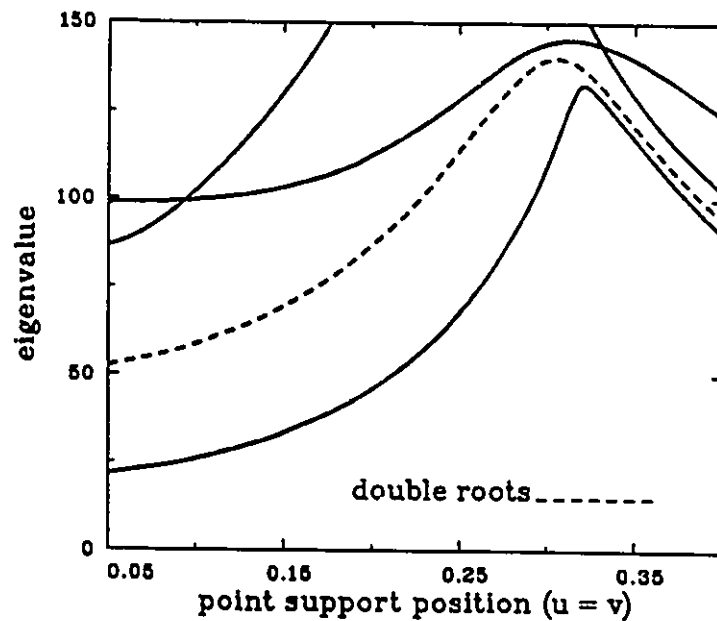
Table 5.5: Comparison of first three computed eigenvalues  $\lambda^2$ , Case 5, SFSF, from present analysis and Bapat's( ) for plate with one discrete point support.

		plate aspect ratio $\phi$			
		0.5		1.0	
$u$	$v$				
0.6	0.6	24.74	(24.738)	15.00	(14.999)
		33.01	(33.025)	22.69	(22.692)
		58.70	(58.694)	38.28	(38.283)
0.7	0.6	22.49	(22.480)	14.80	(14.803)
		28.86	(28.858)	20.20	(20.195)
		60.20	(60.201)	37.59	(37.588)

Table 5.6: Comparison of first three computed eigenvalues  $\lambda^2$ , Case 5, SFSF, from present analysis and Bapat's( ) for plate with two discrete point supports. \* Eigenvalues are suspect.

		plate aspect ratio $\phi$			
		0.5		1.0	
$u$	$v$				
0.6	0.6	25.38	(25.381)	15.08	(15.080)
0.2	0.6	56.55	(42.632)*	24.57	(23.469)*
		62.71	(56.548)	44.50	(24.565)
0.6	0.75	21.01	(21.010)	13.37	(13.369)
0.2	0.75	50.82	(43.321)*	35.67	(25.552)*
		75.49	(51.629)	42.58	(35.677)

## 5.1.2 Eigenvalue Curves

Figure 5.2: Eigenvalue curves, Case 1, SSSS ( $\phi = 1.0$ , support type: discrete).Figure 5.3: Eigenvalue curves, Case 1, SSSS ( $\phi = 1.0$ , support type: rigid).

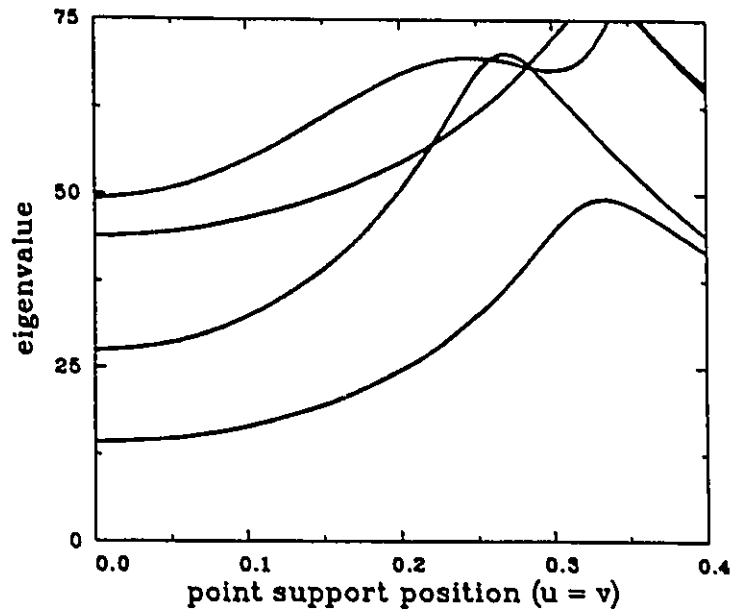


Figure 5.4: Eigenvalue curves, Case 1, SSSS ( $\phi = 1.5$ , support type: discrete).

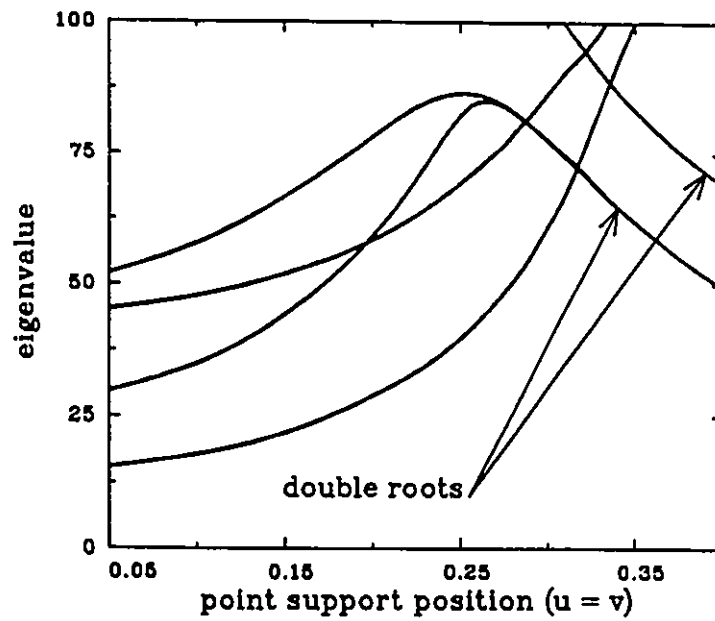


Figure 5.5: Eigenvalue curves, Case 1, SSSS ( $\phi = 1.5$ , support type: rigid).

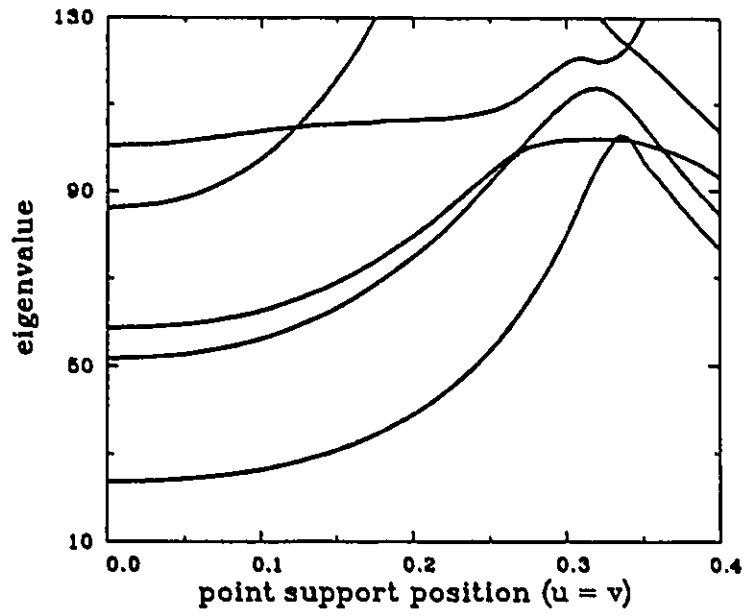


Figure 5.6: Eigenvalue curves, Case 2, SSSC ( $\phi = 1.0$ , support type: discrete).

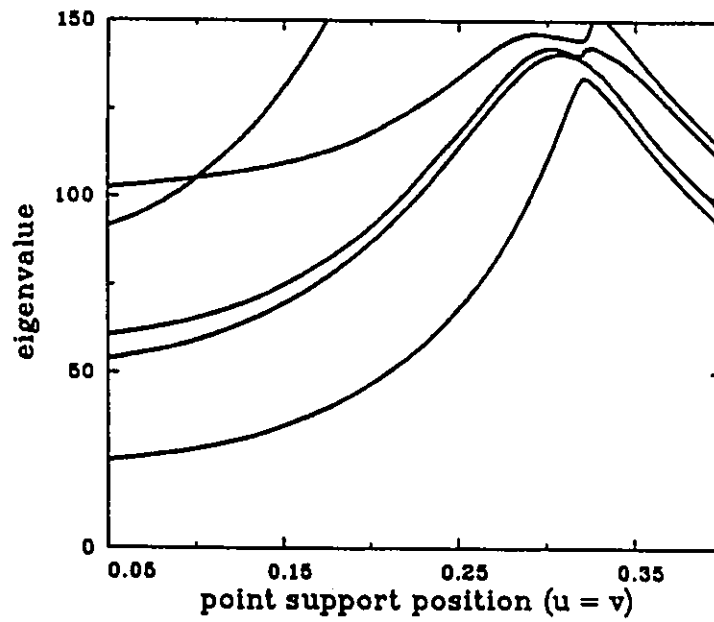


Figure 5.7: Eigenvalue curves, Case 2, SSSC ( $\phi = 1.0$ , support type: rigid).

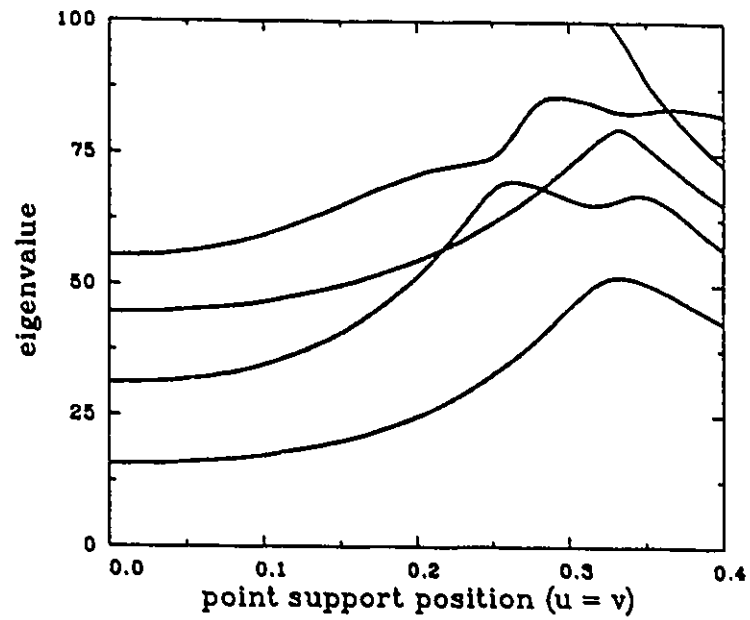


Figure 5.8: Eigenvalue curves, Case 2, SSSC ( $\phi = 1.5$ , support type: discrete).

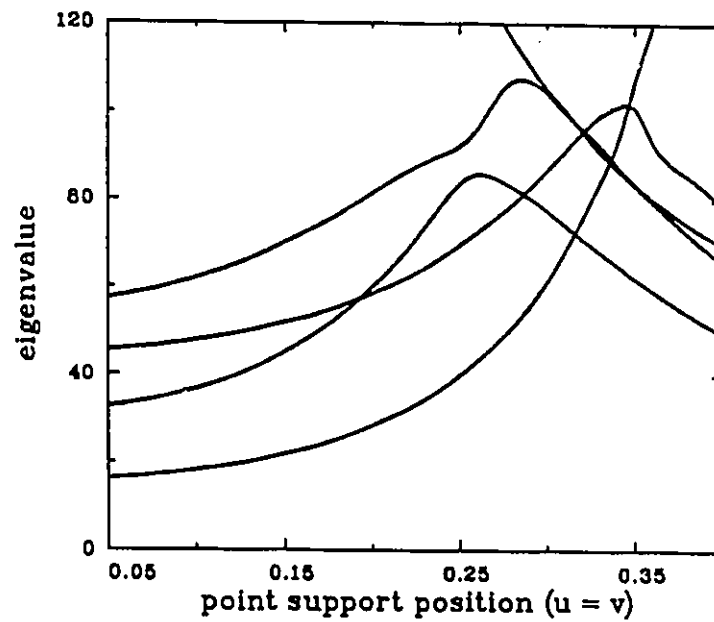


Figure 5.9: Eigenvalue curves, Case 2, SSSC ( $\phi = 1.5$ , support type: rigid).

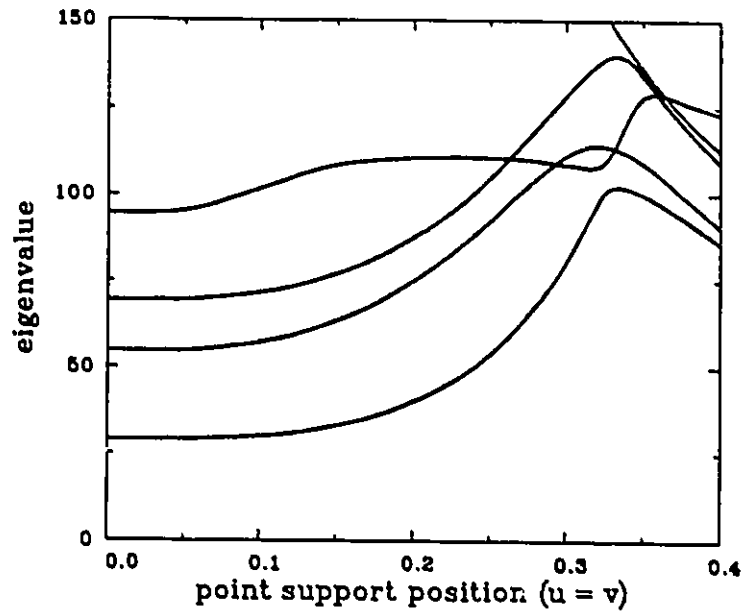


Figure 5.10: Eigenvalue curves, Case 3, SCSC ( $\phi = 1.0$ , support type: discrete).

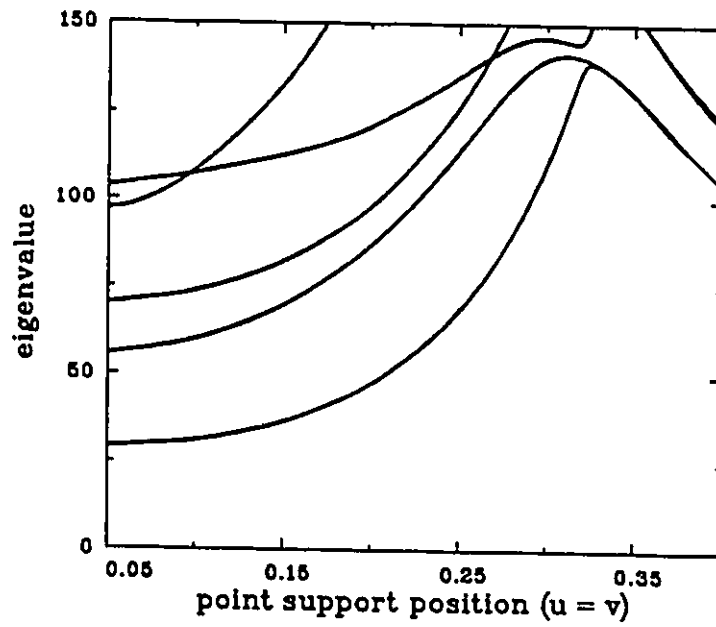


Figure 5.11: Eigenvalue curves, Case 3, SCSC ( $\phi = 1.0$ , support type: rigid).

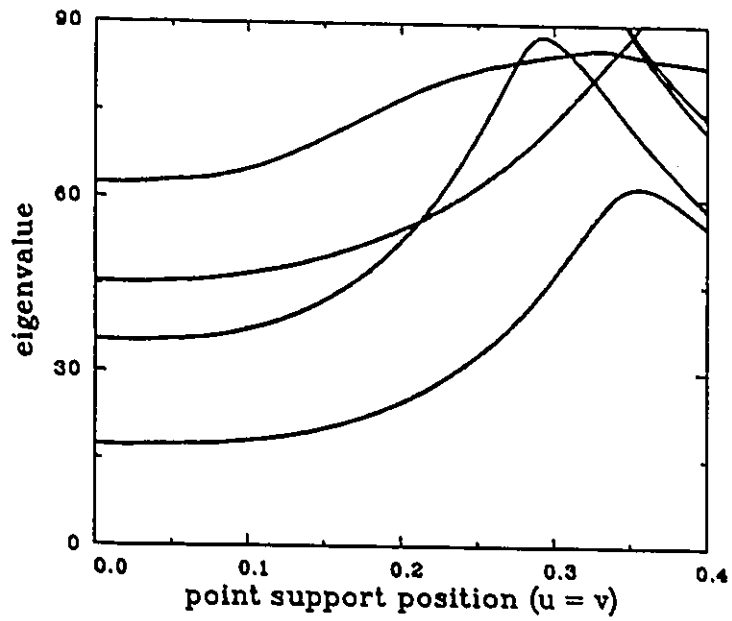


Figure 5.12: Eigenvalue curves, Case 3, SCSC ( $\phi = 1.5$ , support type: discrete).

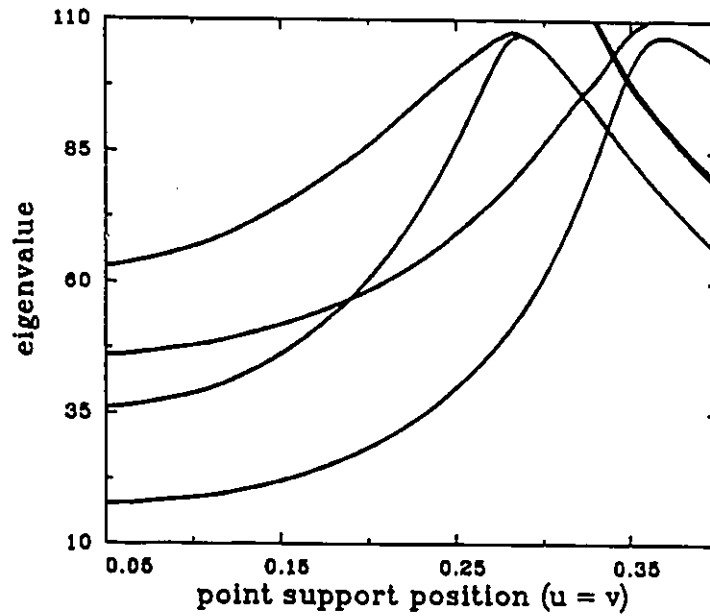


Figure 5.13: Eigenvalue curves, Case 3, SCSC ( $\phi = 1.5$ , support type: rigid).

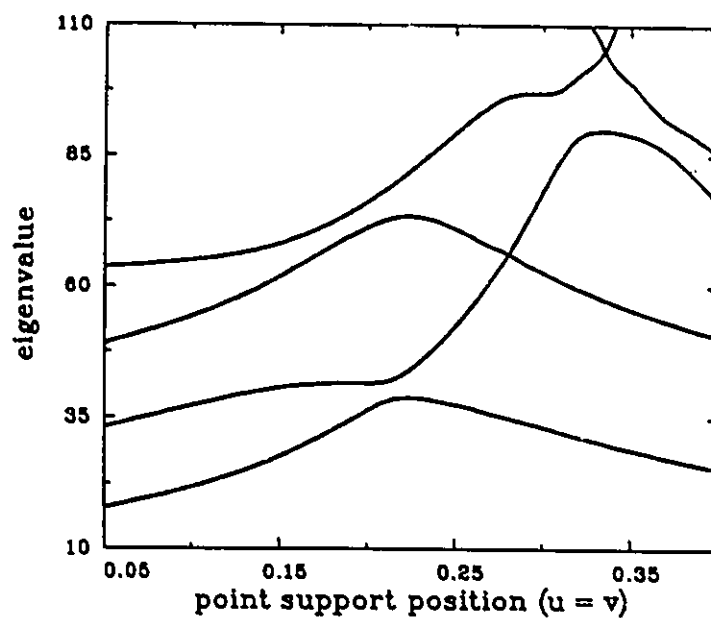


Figure 5.14: Eigenvalue curves, Case 4, SSSF ( $\phi = 1.0$ , support type: discrete).

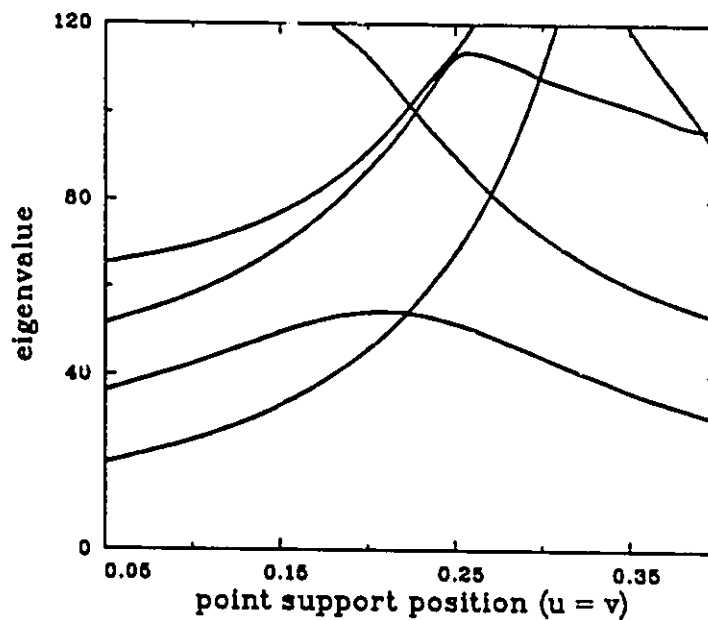


Figure 5.15: Eigenvalue curves, Case 4, SSSF ( $\phi = 1.0$ , support type: rigid).

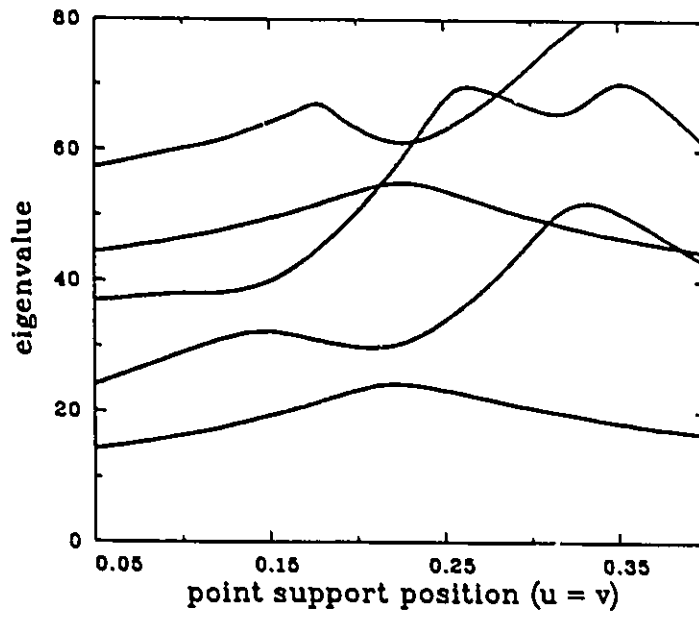


Figure 5.16: Eigenvalue curves, Case 4, SSSF ( $\phi = 1.5$ , support type: discrete).

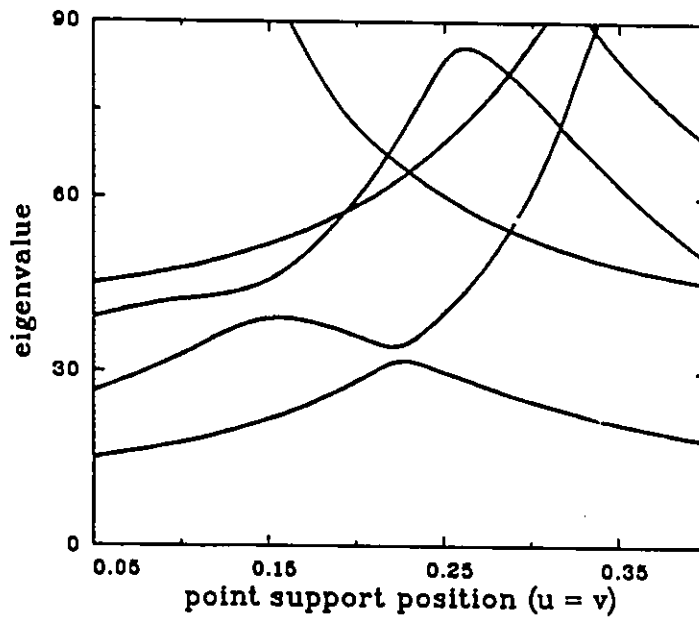


Figure 5.17: Eigenvalue curves, Case 4, SSSF ( $\phi = 1.5$ , support type: rigid).

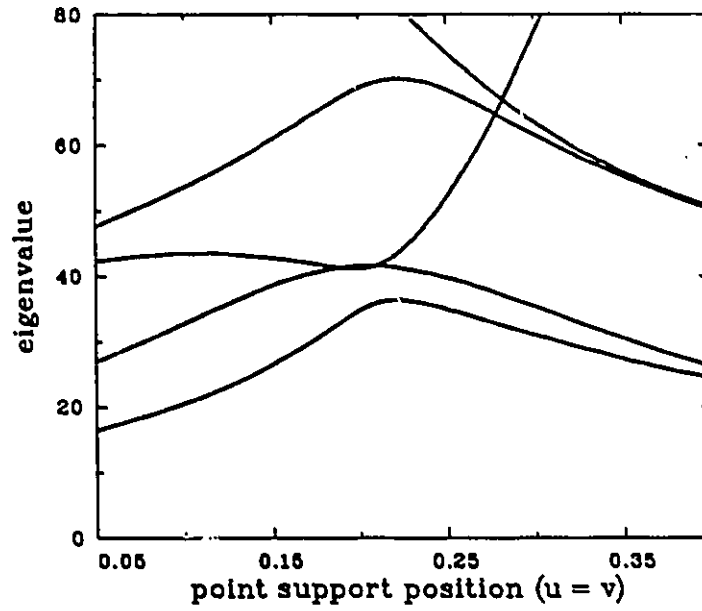


Figure 5.18: Eigenvalue curves, Case 5, SFSF ( $\phi = 1.0$ , support type: discrete).

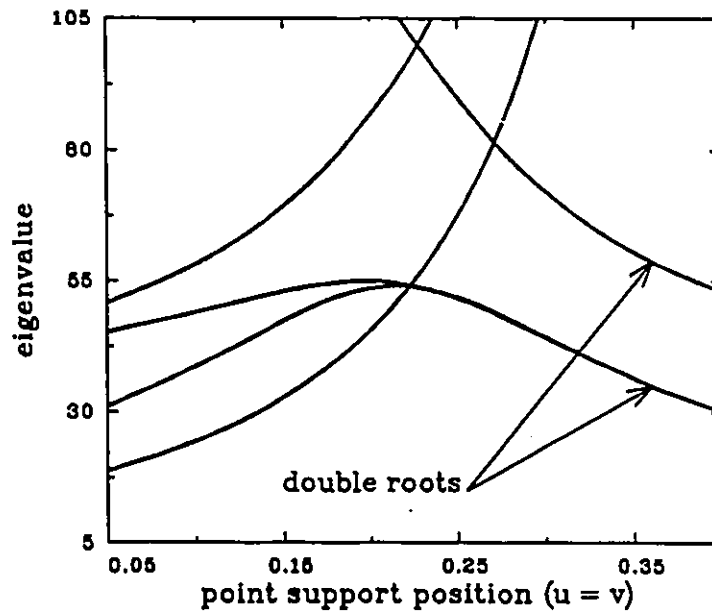


Figure 5.19: Eigenvalue curves, Case 5, SFSF ( $\phi = 1.0$ , support type: rigid).

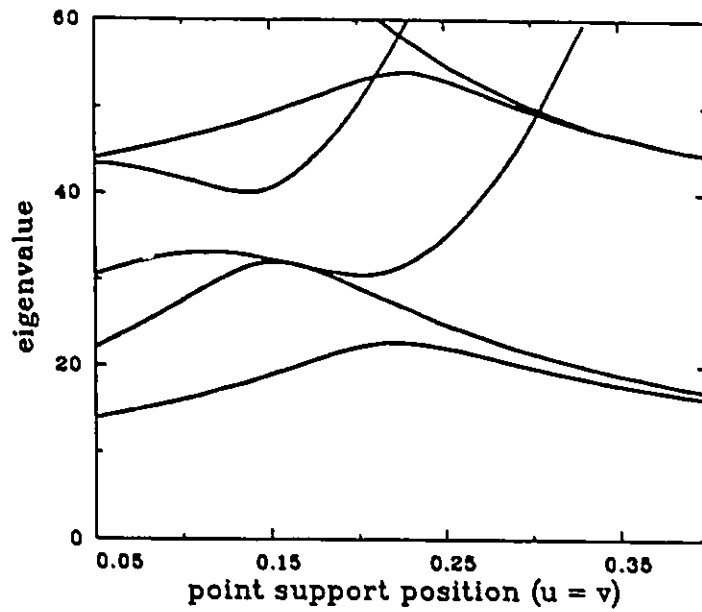


Figure 5.20: Eigenvalue curves, Case 5, SFSF ( $\phi = 1.5$ , support type: discrete).

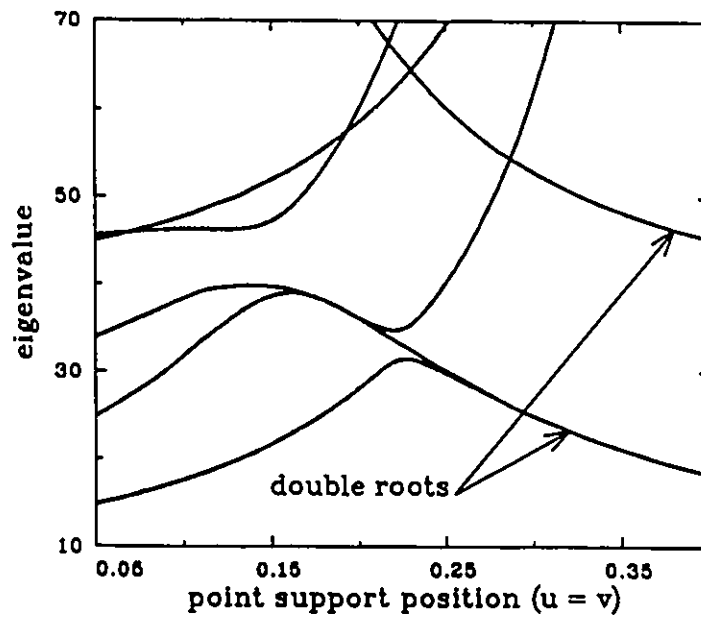


Figure 5.21: Eigenvalue curves, Case 5, SFSF ( $\phi = 1.5$ , support type: rigid).

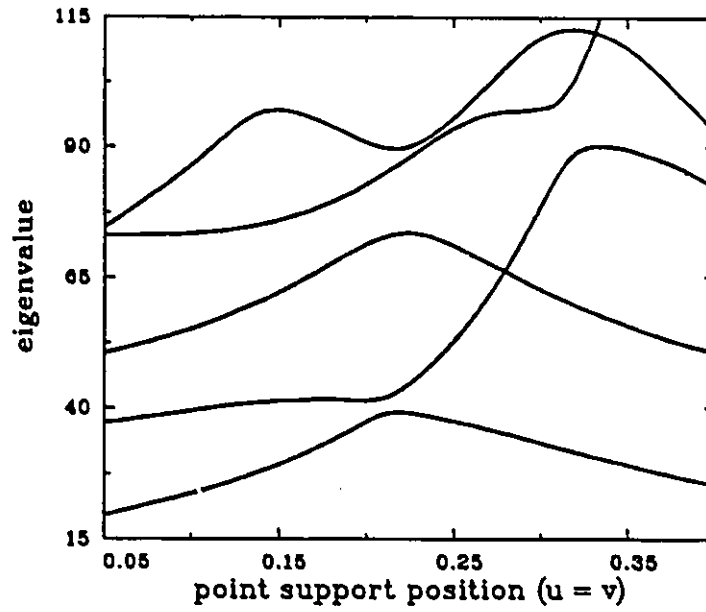


Figure 5.22: Eigenvalue curves, Case 6, SCSF ( $\phi = 1.0$ , support type: discrete).

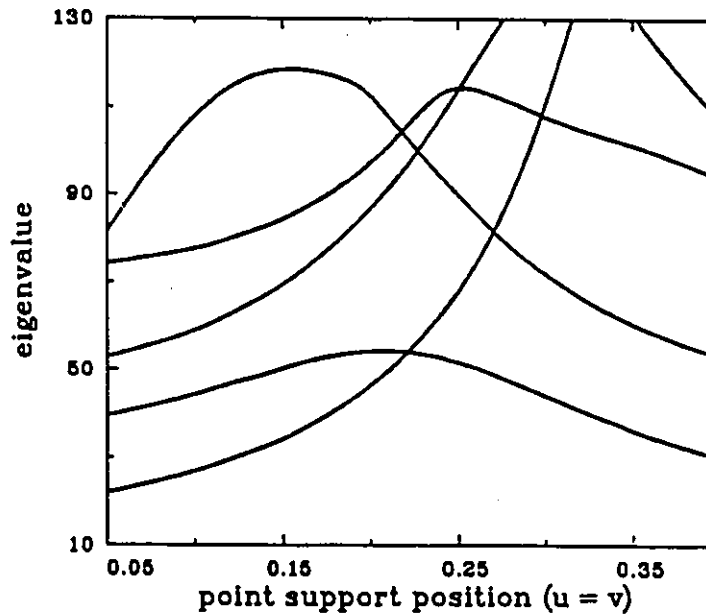


Figure 5.23: Eigenvalue curves, Case 6, SCSF ( $\phi = 1.0$ , support type: rigid).

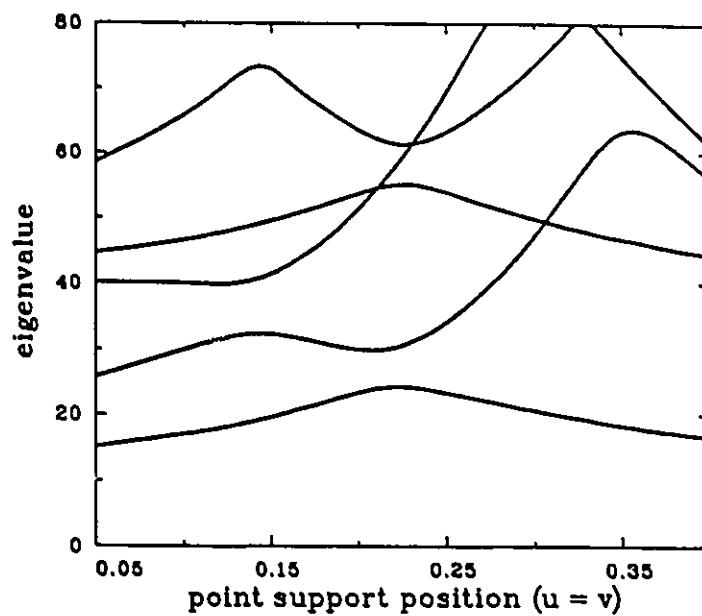


Figure 5.24: Eigenvalue curves, Case 6, SCSF ( $\phi = 1.5$ , support type: discrete).

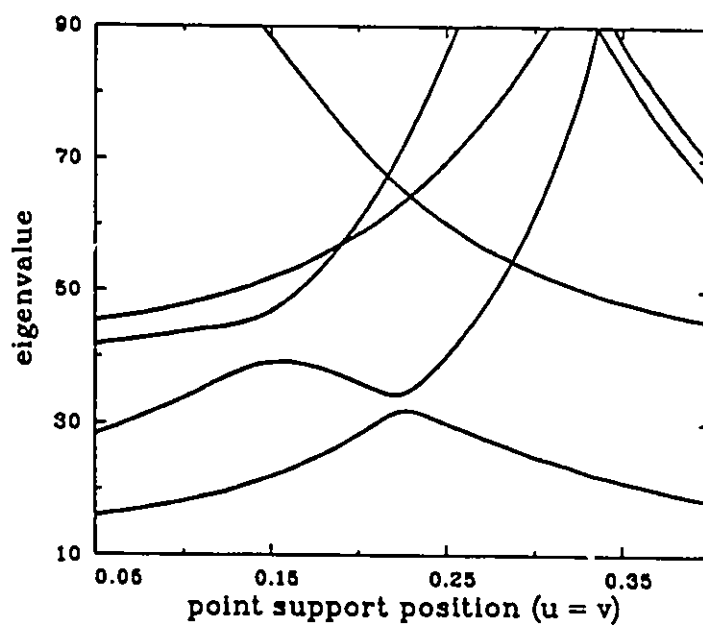


Figure 5.25: Eigenvalue curves, Case 6, SCSF ( $\phi = 1.5$ , support type: rigid).

## 5.1.3 Associated Mode Shapes

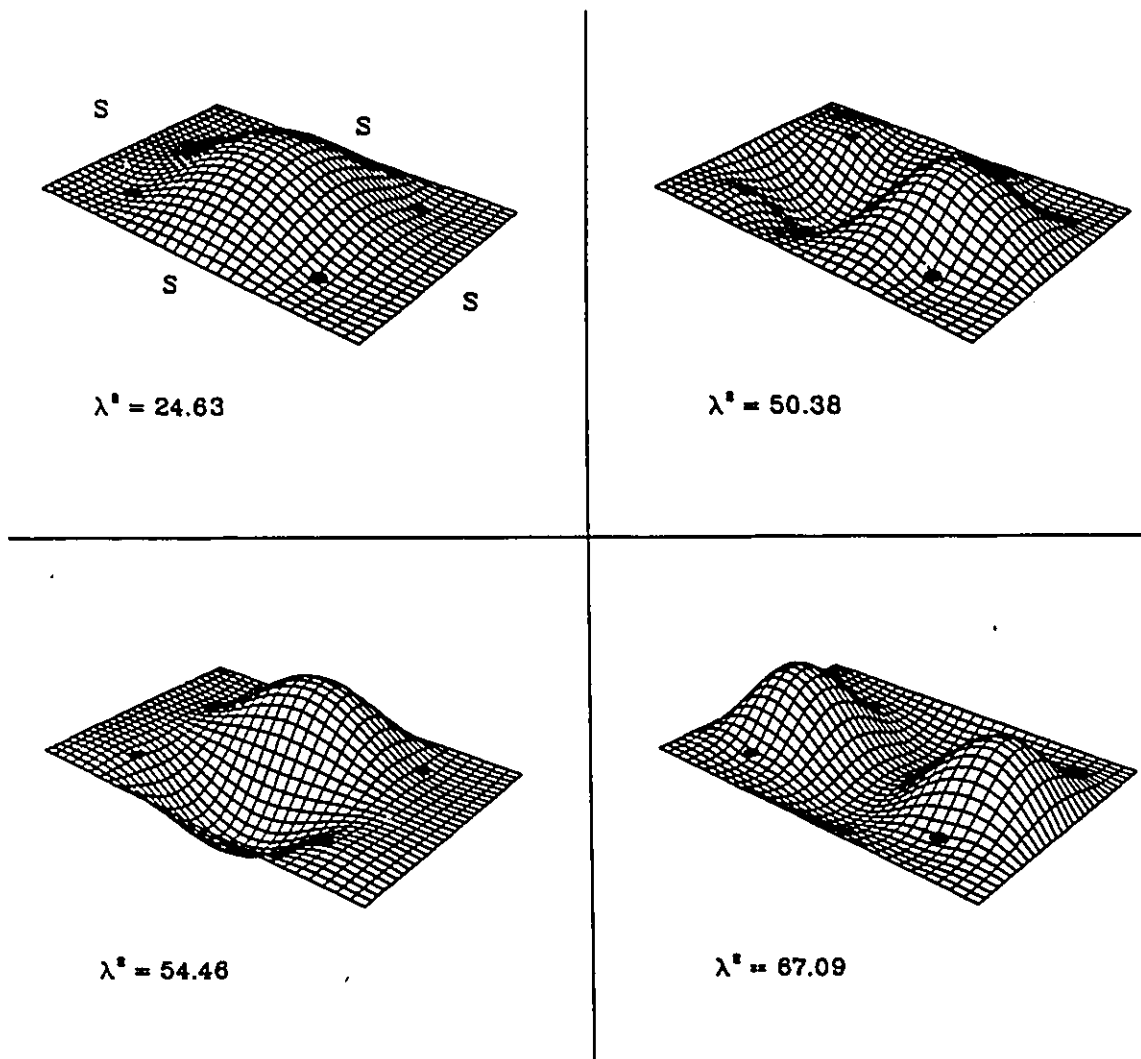


Figure 5.26: First four associated mode shapes for Case 1, SSSS ( $u = v = 0.2$ ,  $\phi = 1.5$ , support type: discrete).

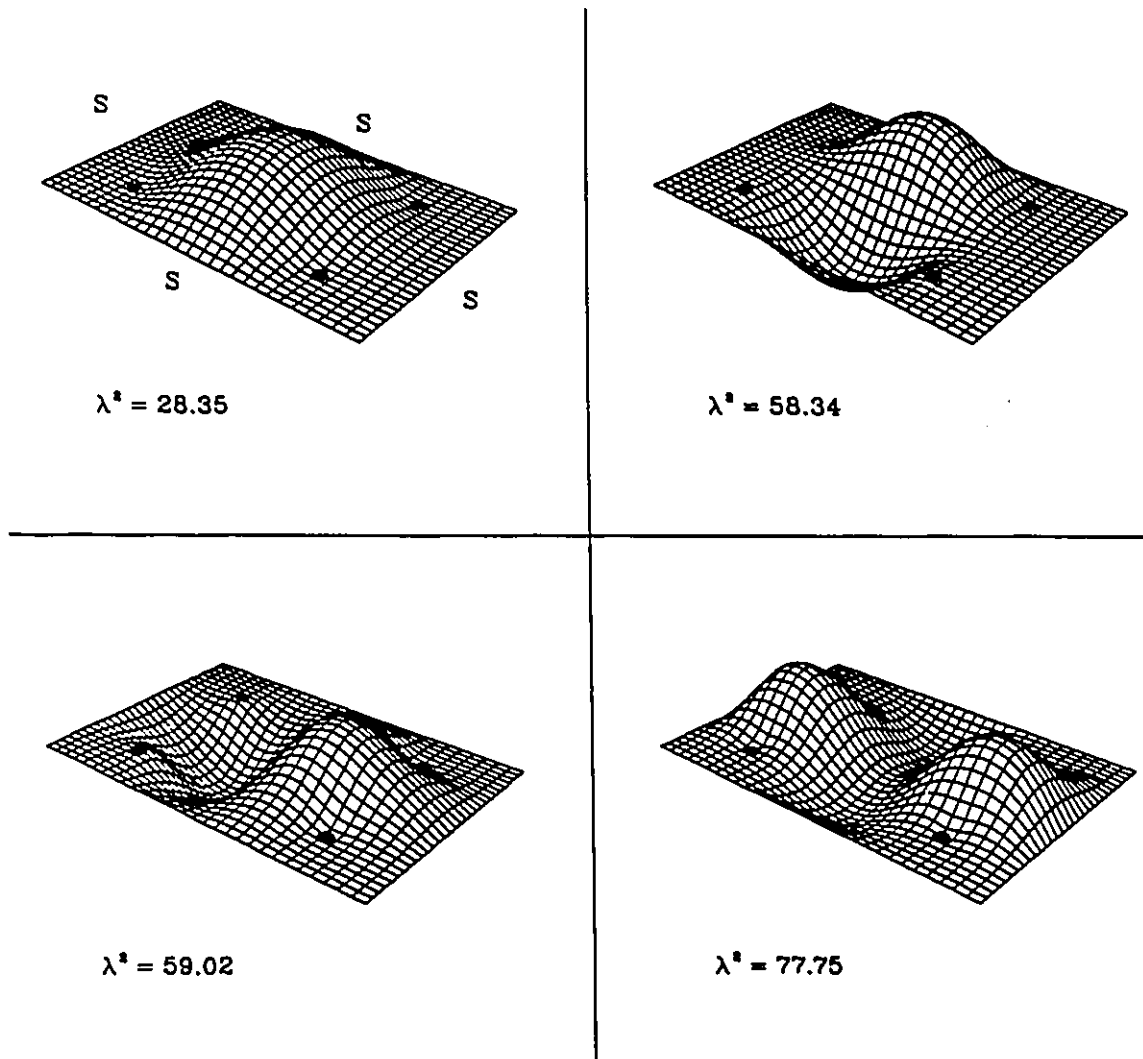


Figure 5.27: First four associated mode shapes for Case 1, SSSS ( $u = v = 0.2$ ,  $\phi = 1.5$ , support type: rigid).

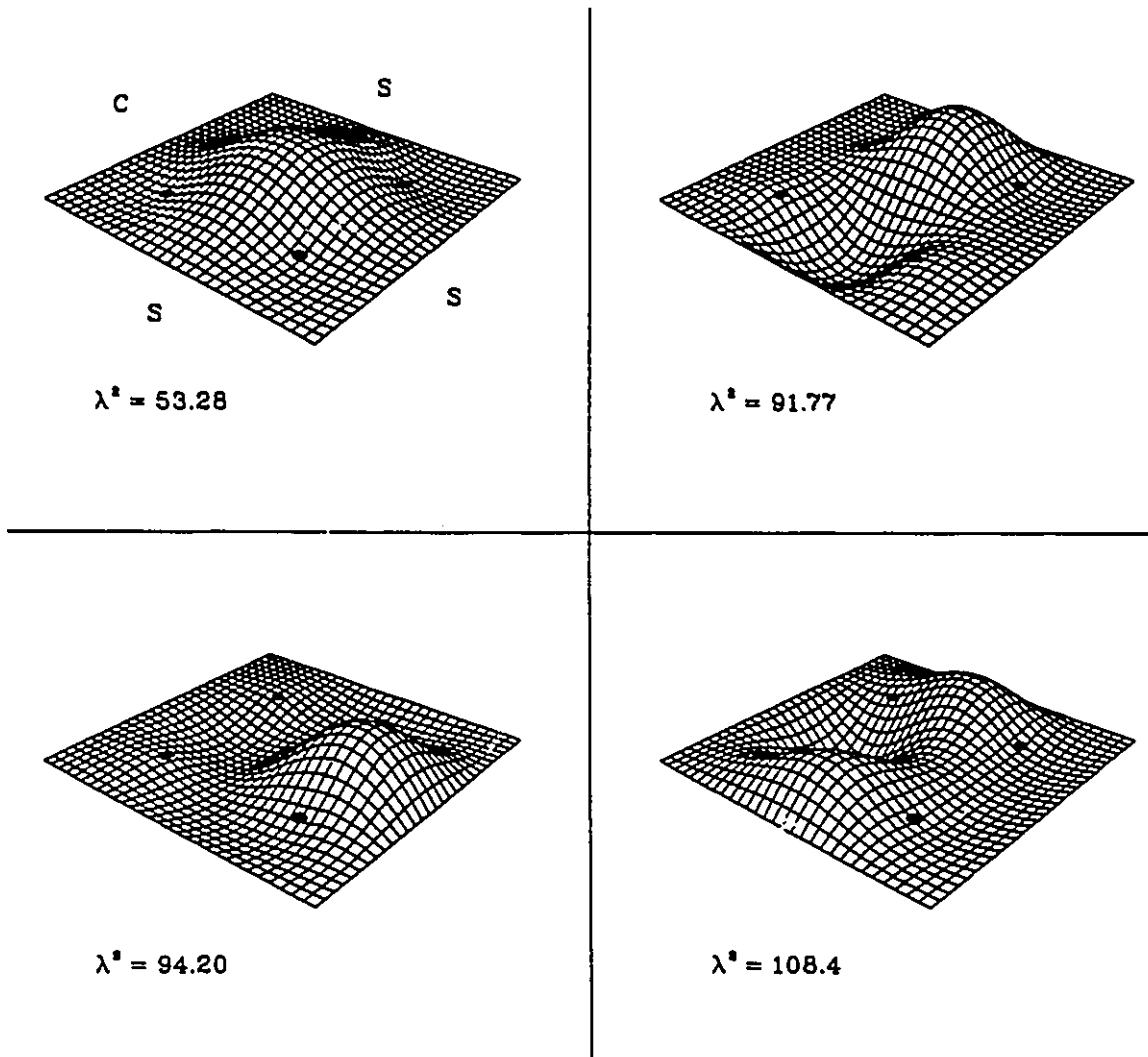


Figure 5.28: First four associated mode shapes for Case 2, SSSC ( $u = v = 0.25$ ,  $\phi = 1.5$ , support type: discrete).

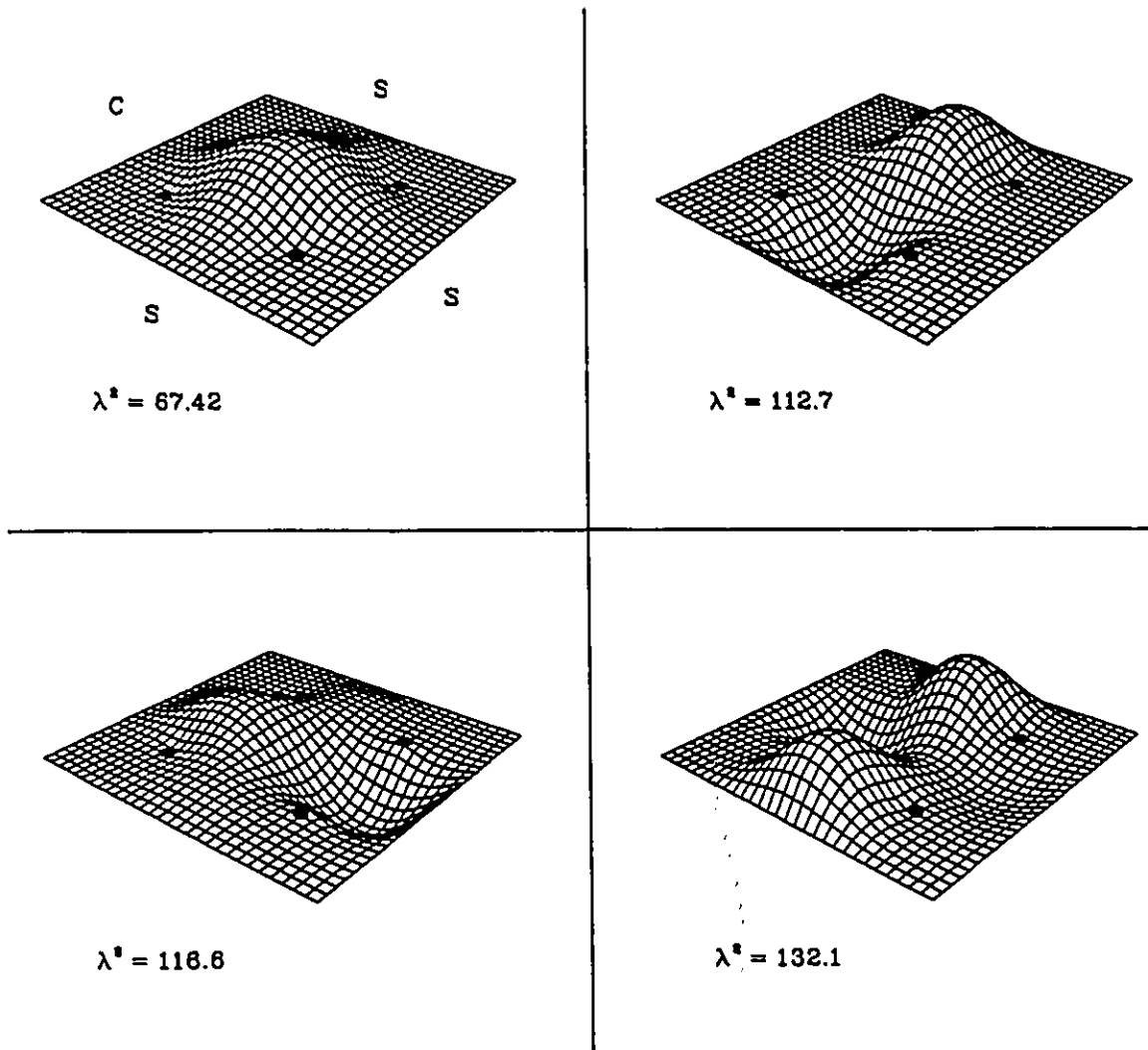


Figure 5.29: First four associated mode shapes for Case 2, SSSC ( $u = v = 0.25$ ,  $\phi = 1.5$ , support type: rigid).

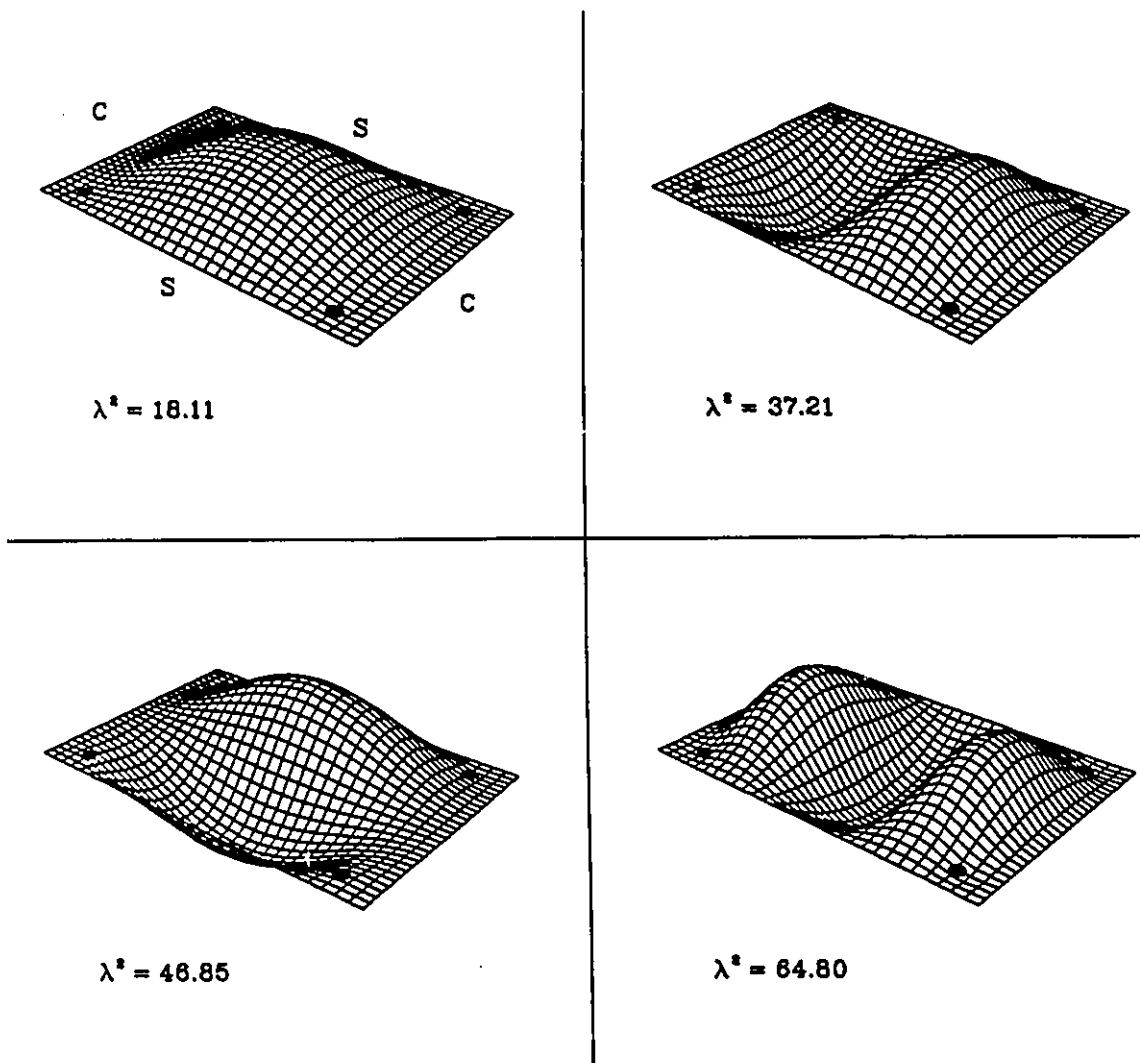


Figure 5.30: First four associated mode shapes for Case 3, SCSC ( $u = v = 0.1$ ,  $\phi = 1.5$ , support type: discrete).

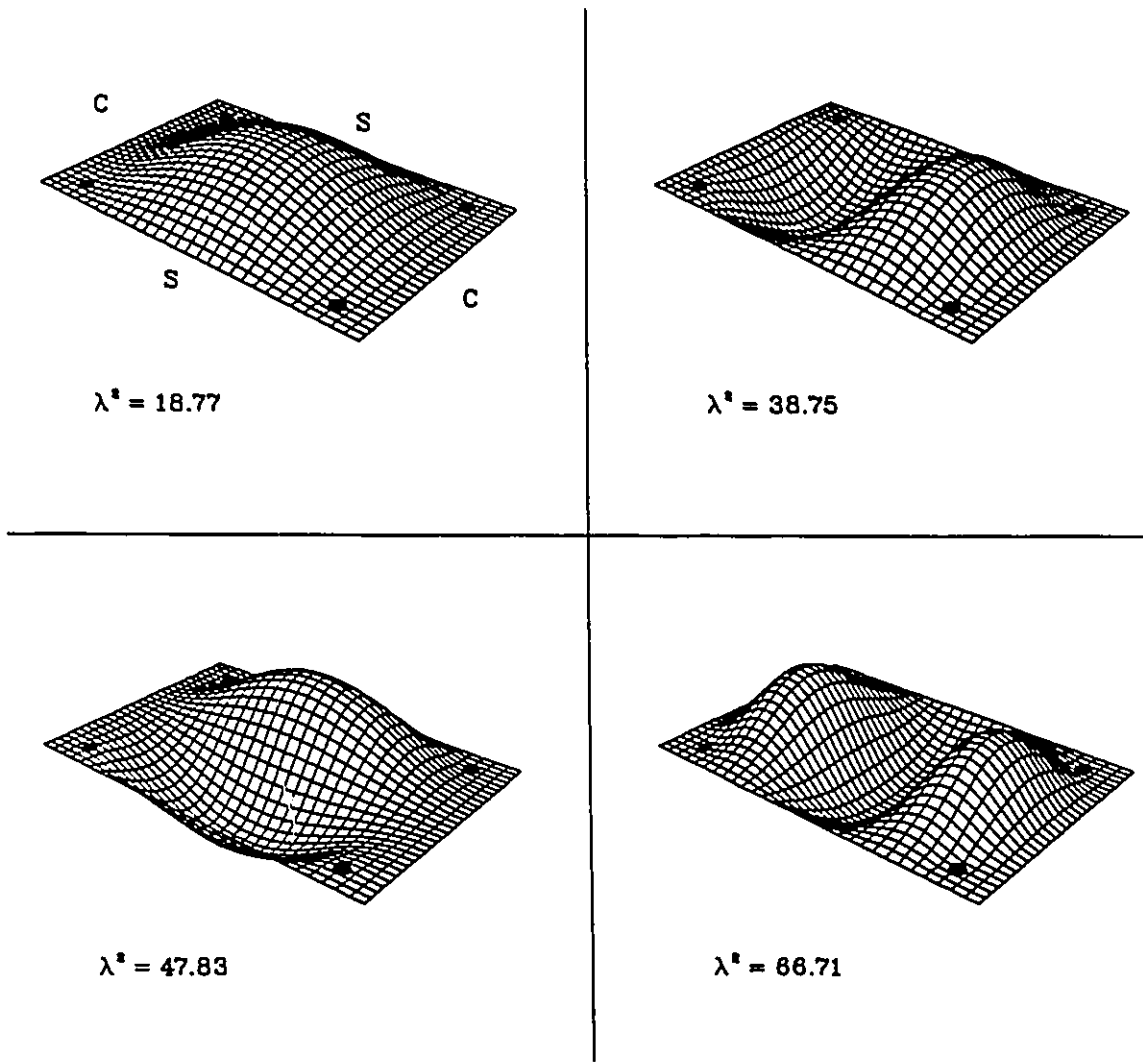


Figure 5.31: First four associated mode shapes for Case 3, SCSC ( $u = v = 0.1$ ,  $\phi = 1.5$ , support type: rigid).

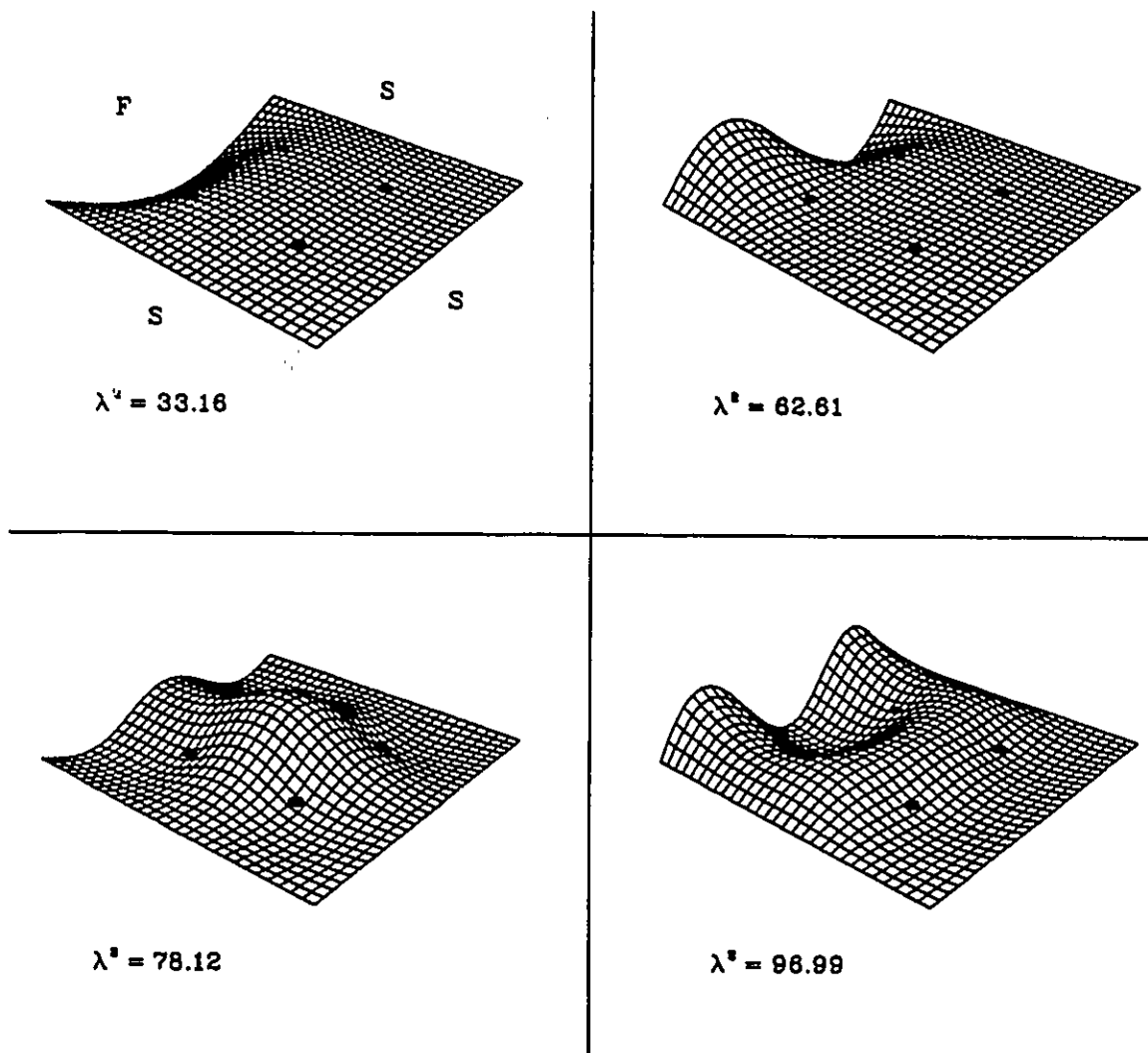


Figure 5.32: First four associated mode shapes for Case 4, SSSF ( $u = v = 0.3$ ,  $\phi = 1.5$ , support type: discrete).

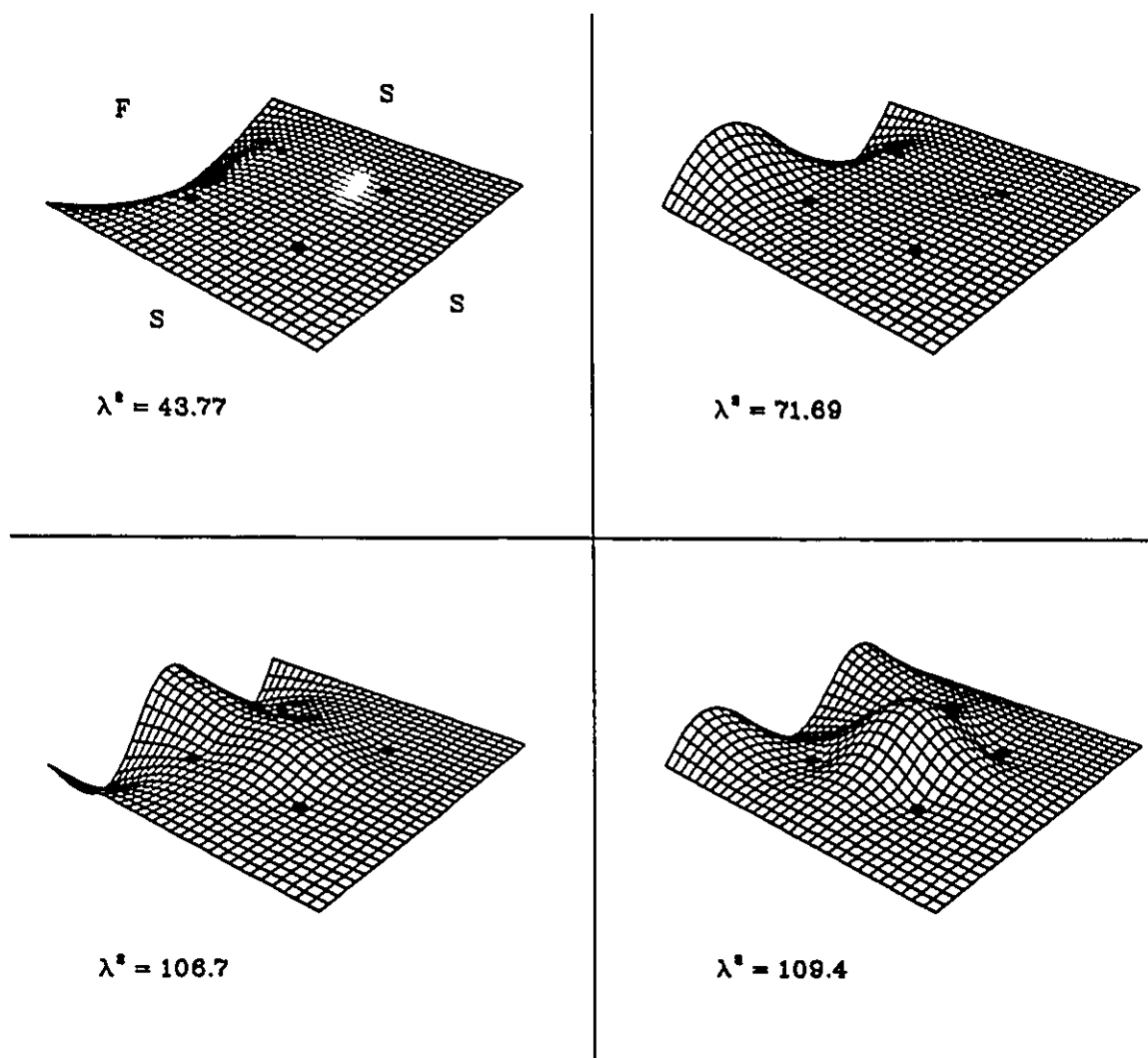


Figure 5.33: First four associated mode shapes for Case 4, SSSF ( $u = v = 0.3$ ,  $\phi = 1.5$ , support type: rigid).

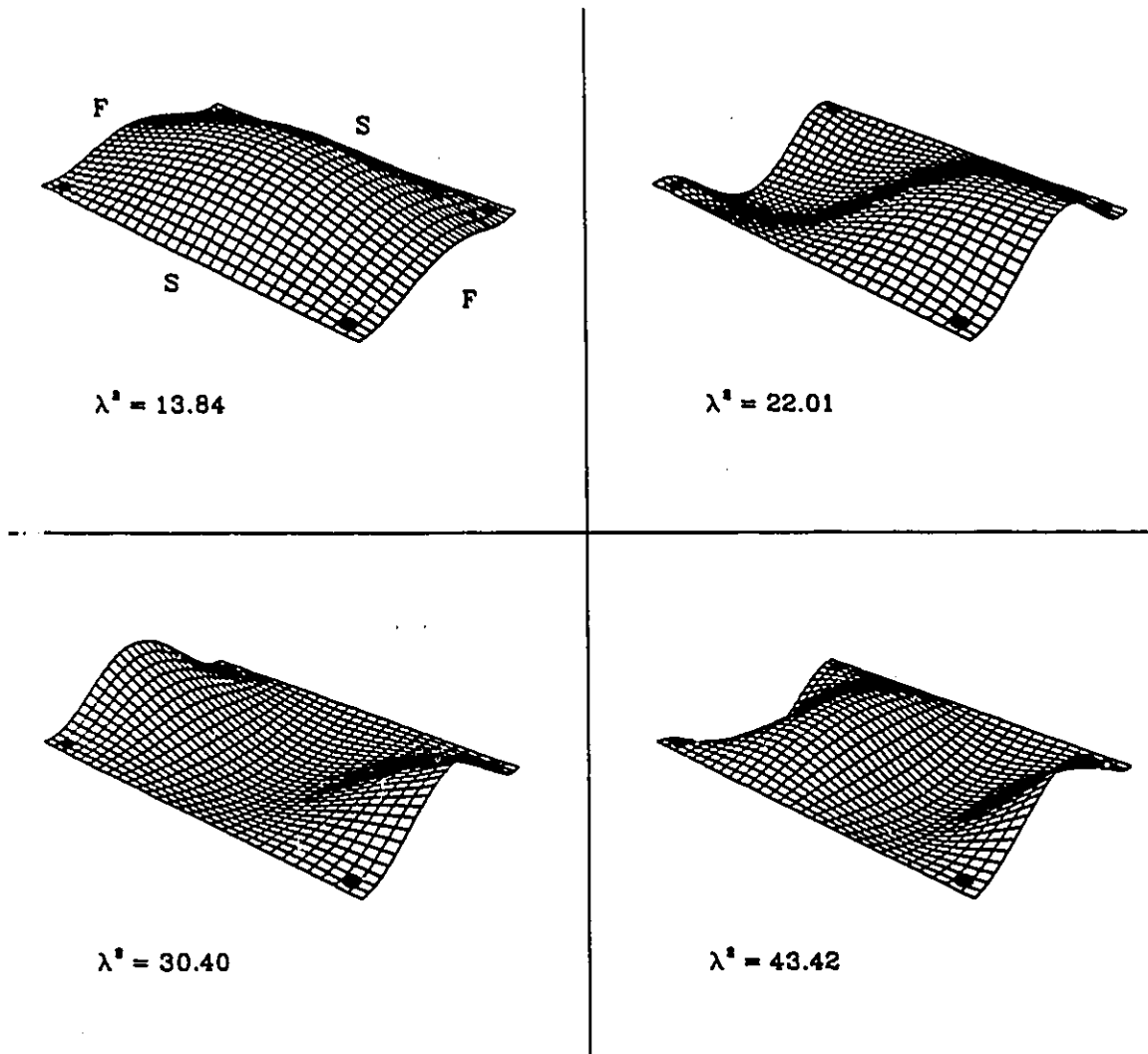


Figure 5.34: First four associated mode shapes for Case 5, SFSF ( $u = v = 0.05$ ,  $\phi = 1.5$ , support type: discrete).

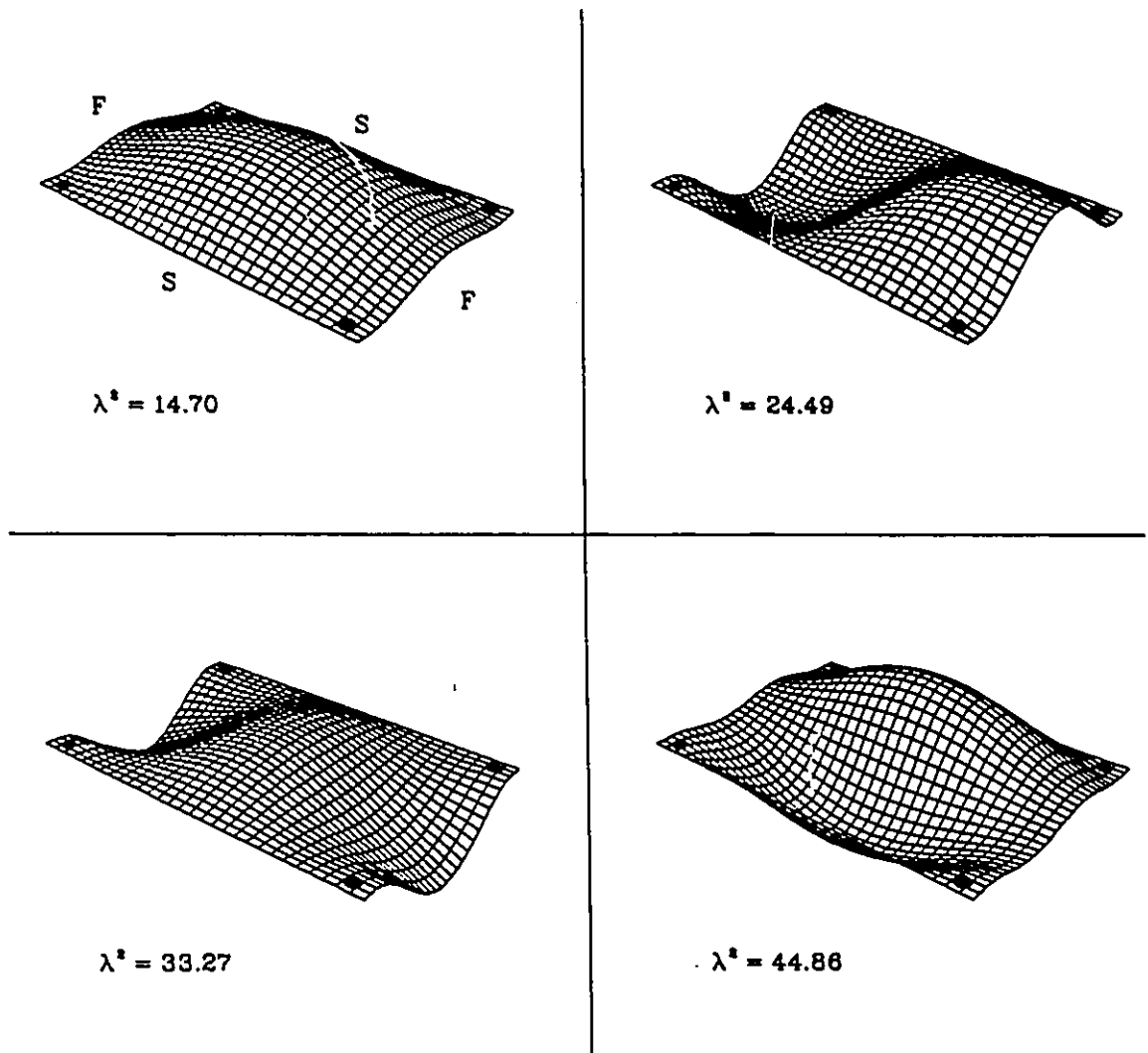


Figure 5.35: First four associated mode shapes for Case 5, SFSF ( $u = v = 0.05$ ,  $\phi = 1.5$ , support type: rigid).

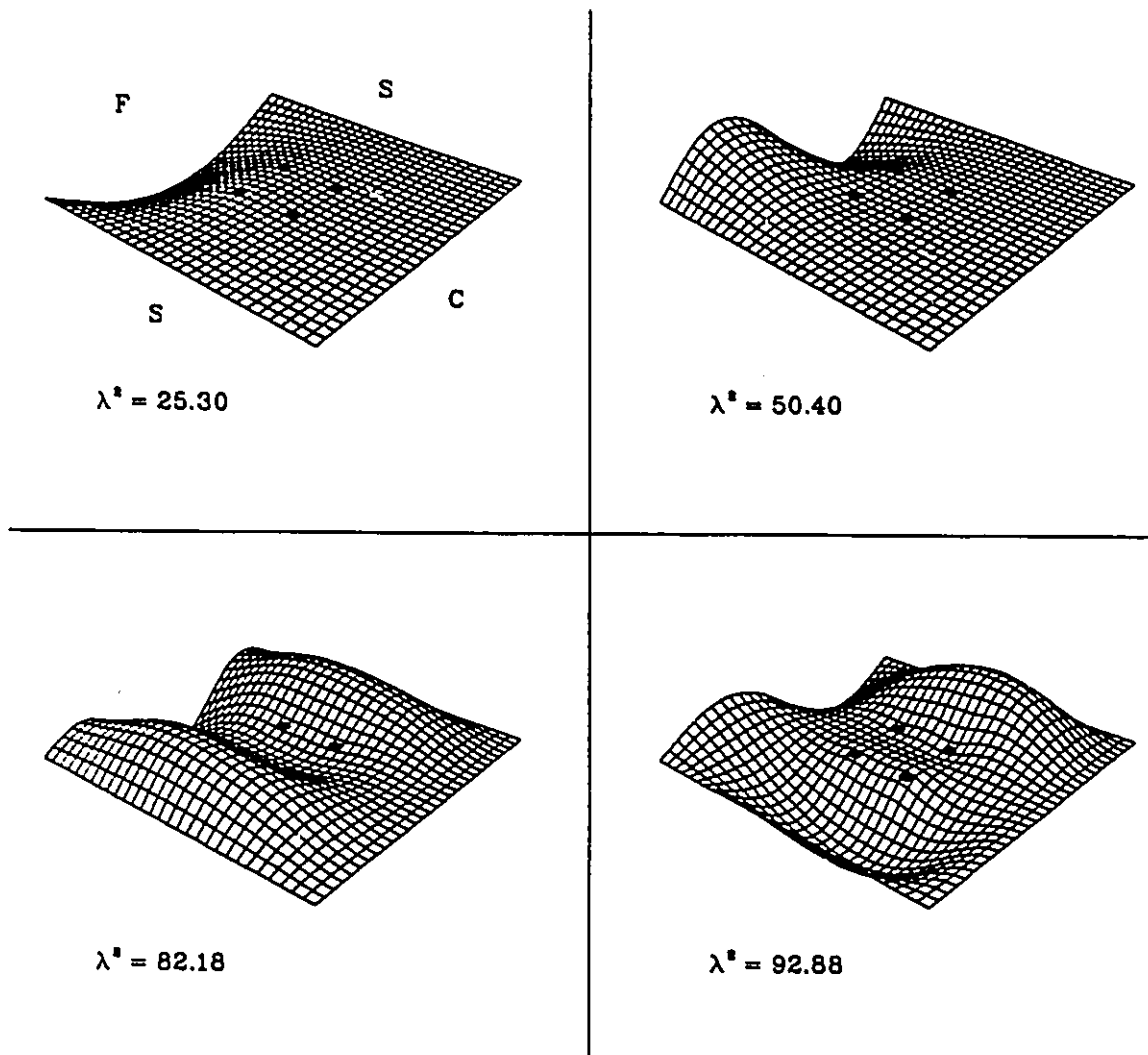


Figure 5.36: First four associated mode shapes for Case 6, SCSF ( $u = v = 0.4$ ,  $\phi = 1.5$ , support type: discrete).

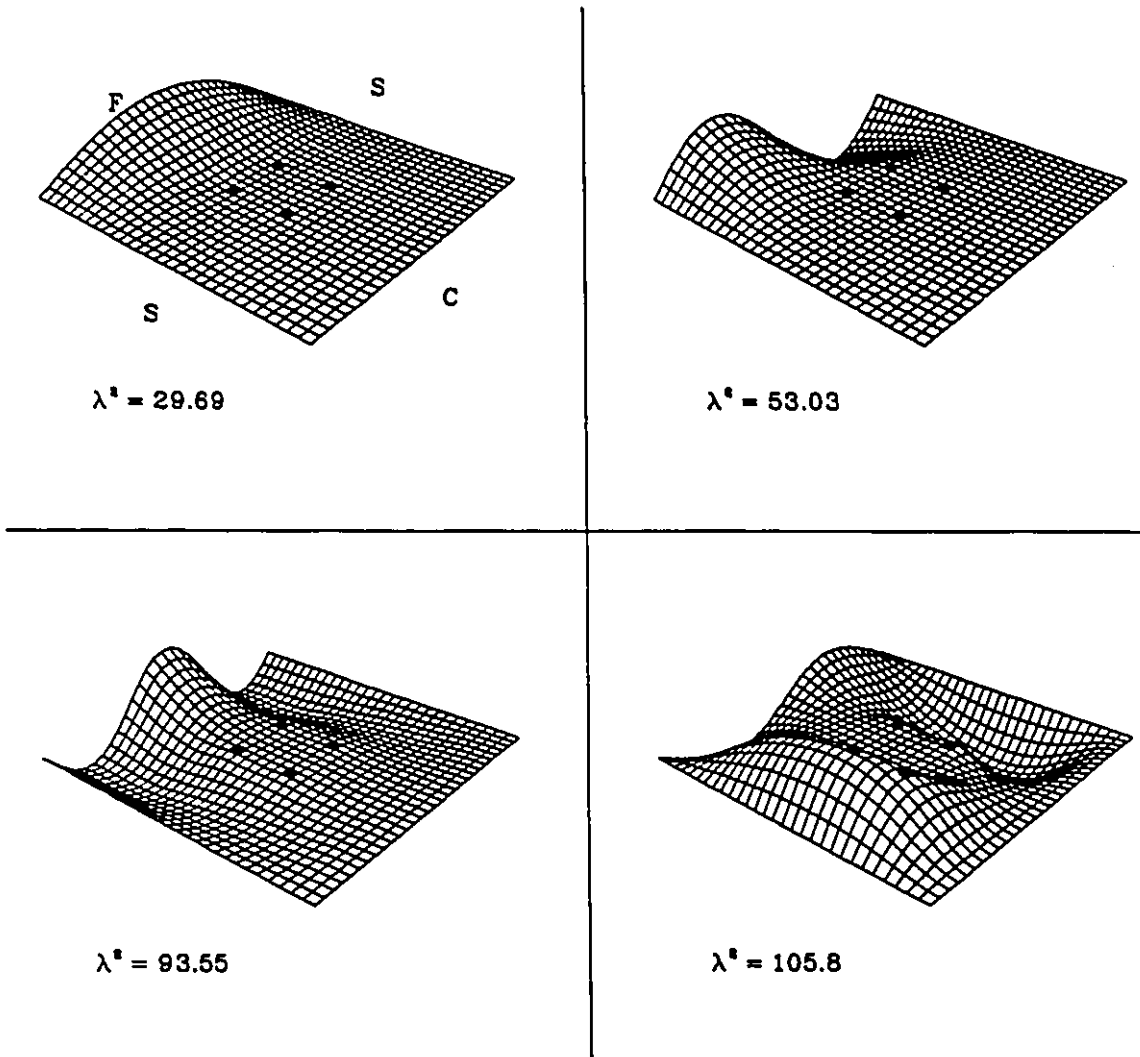


Figure 5.37: First four associated mode shapes for Case 6, SCSF ( $u = v = 0.4$ ,  $\phi = 1.5$ , support type: rigid).

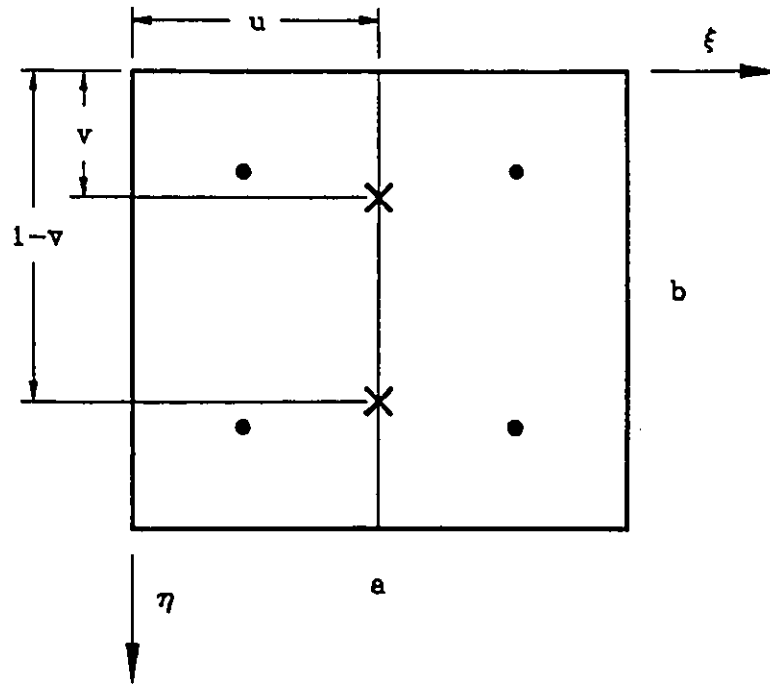


Figure 5.38: Rectangular plate with attached mass and internal point support locations. Attached masses represented by X.

## 5.2 Effects of Attached Masses

The effects of attached masses are investigated for Case 5, SFSF only. For this case, two opposite edges are free and therefore the effects of attached masses will be more substantial than with simply supported or clamped edges. Two problems are investigated for Case 5, SFSF with plate aspect ratios  $\phi = 1.0$  and  $\phi = 1.5$ .

1. Varying mass ratio located at the plate's center.
2. Two fixed mass ratios with varying locations on the line  $u = 0.5$ .

For each problem, there are four discrete point supports symmetrically distributed on the plate's diagonals. The fundamental mode eigenvalue curves and associated mode shapes are presented here. Computed eigenvalues are presented in Appendix B.

### 5.2.1 Eigenvalue Curves

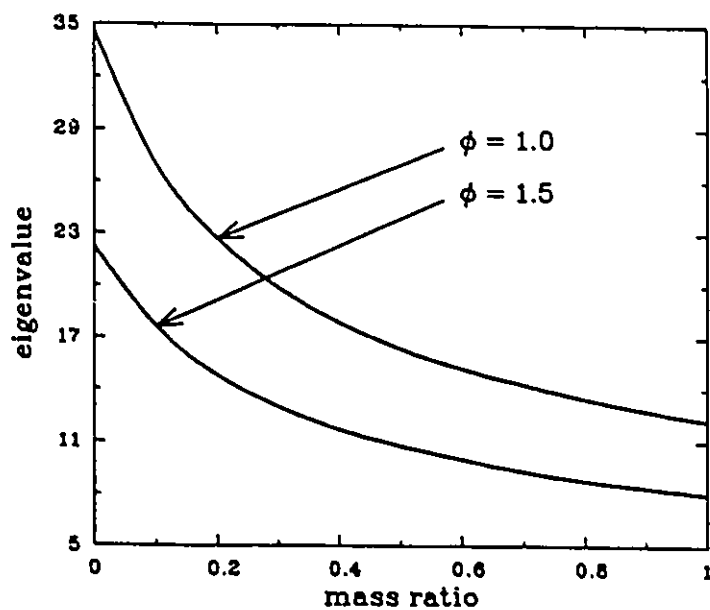


Figure 5.39: Fundamental eigenvalue curve, single attached mass, ( $u = v = 0.2$ ).

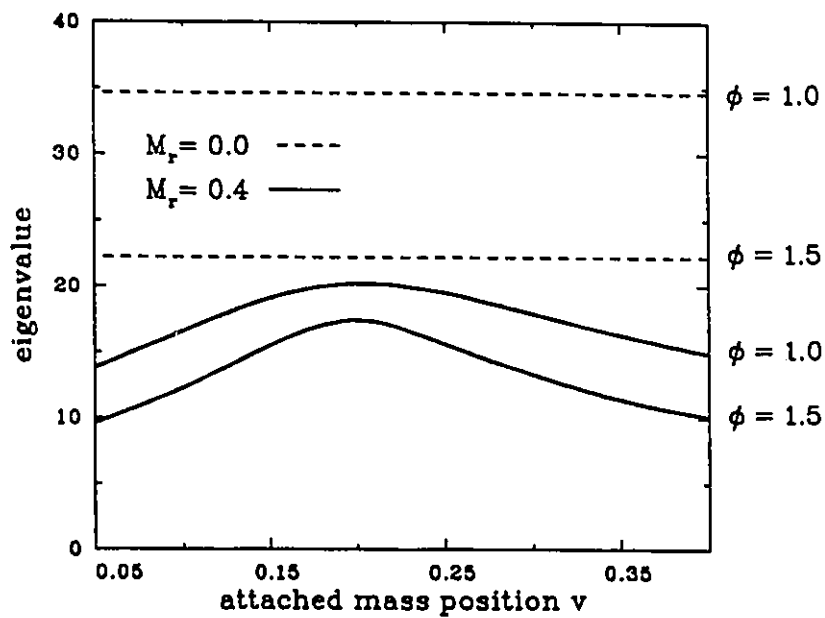


Figure 5.40: Fundamental eigenvalue curves, varying mass location, ( $u = v = 0.25$ ).

5.2.2 Associated Mode Shapes

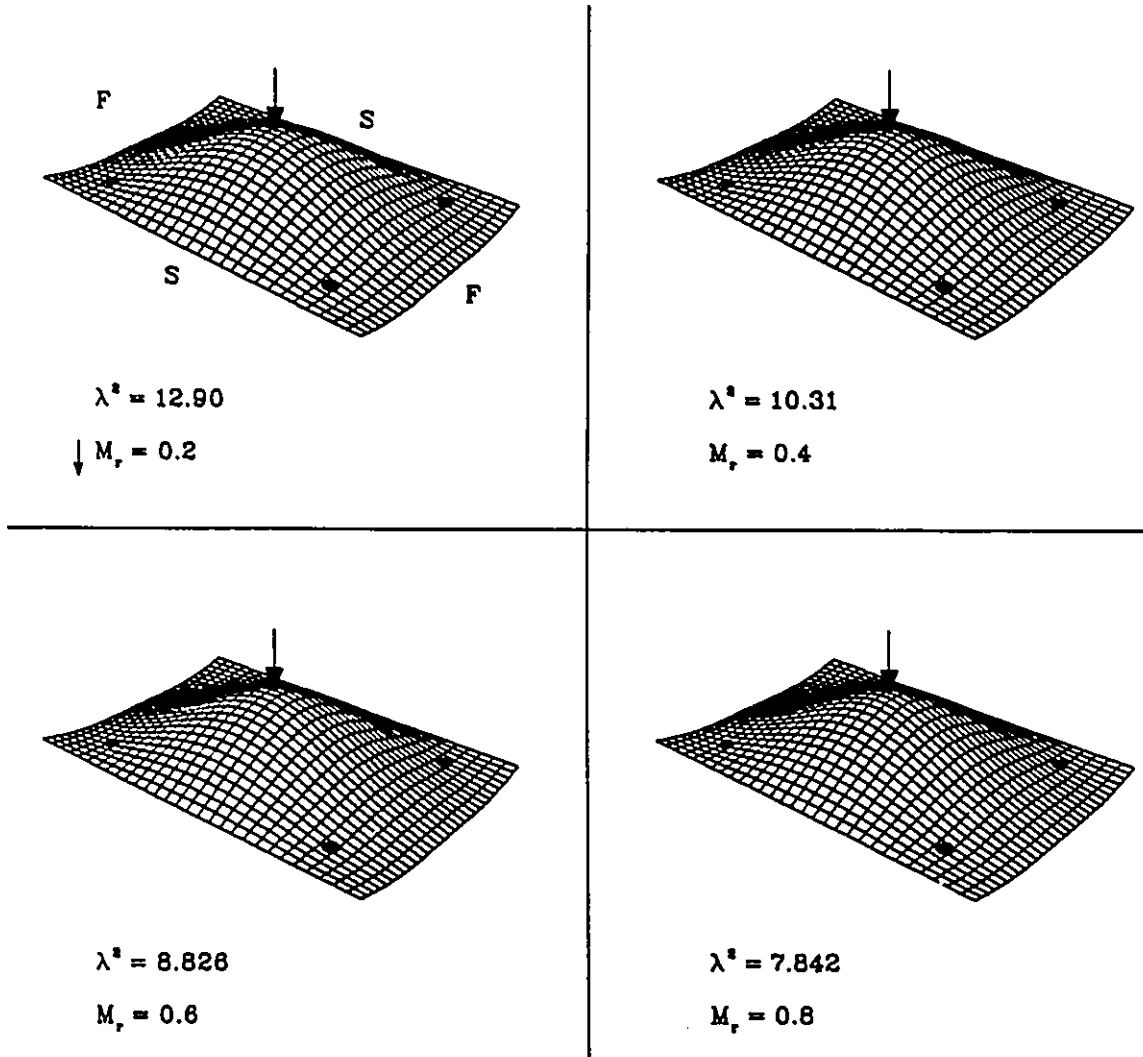


Figure 5.41: Fundamental mode shapes for varying mass ratio.  $M_r$  at  $u = v = 0.5$  (solid arrow), four point supports at  $u = v = 0.15$  (solid dots),  $\phi = 1.5$ .

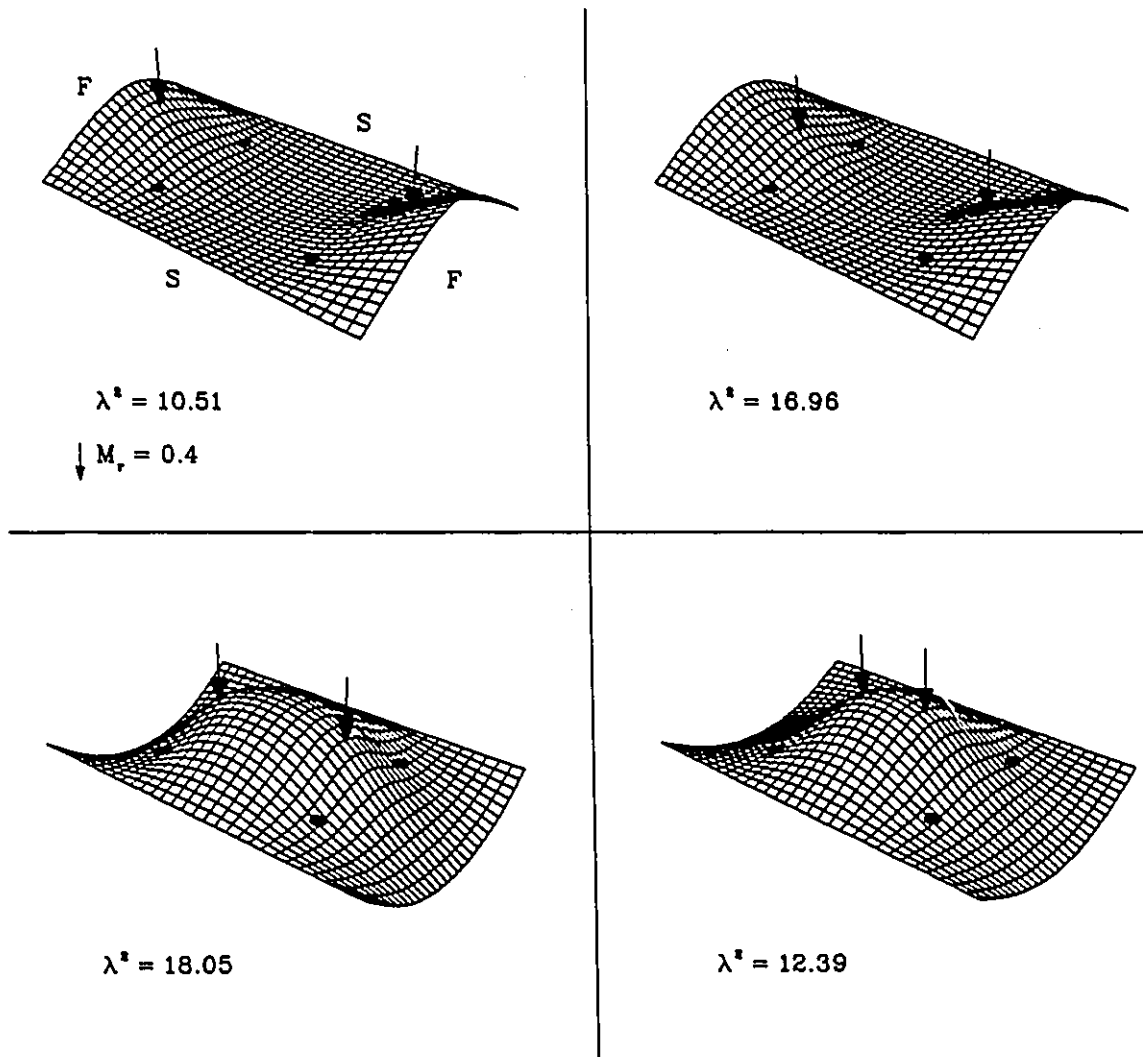


Figure 5.42: Fundamental mode shapes for two varying mass locations on line  $u = 0.5$  and  $v = 0.1, 0.9$   $0.2, 0.8$   $0.3, 0.7$   $0.4, 0.6$  (solid arrow). Four point supports at  $u = v = 0.25$  (solid dots).  $\phi = 1.5$ .

# Chapter 6

## Discussion of Results

The free vibration analysis of the six case studies with varying point support positions and point support types has been presented by means of computed eigenvalues, eigenvalue curves and associated mode shapes. The effects of attached masses were also investigated for Case 5, SFSF, for varying mass ratio and varying mass locations. It should be noted that although the results are quite detailed, there are an infinite number of possible combinations of point support positions, attached mass positions, attached mass ratios and plate boundary conditions. It was desired here to develop a comprehensive set of results to confirm the validity of the mathematical solution and ensure that no inconsistencies were generated by the computer analysis.

### 6.1 Computed Eigenvalues

In Sec. 5.1.1: Comparison of Results, excellent agreement was found between the present solution method and Bapat's [24] solution method, except for the SCSC and SFSF plate where certain of his eigenvalues are considered suspect. For the SCSC plate with two internal point supports the eigenvalues presented by Bapat correspond to the first three eigenvalues for the same plate with no internal point supports.<sup>1</sup> This would be valid

---

<sup>1</sup>Ref.[4], pages 35-36, computed eigenvalues for simple-clamped-simple-clamped plate.

if the point supports were 'inactive' (i.e. point support locations correspond to node lines for the same plate with no internal point supports). But this does not explain the suspect eigenvalues since the two point supports are arbitrarily located and do not fall on any node lines for the same plate with no internal point supports. The present analysis will only generate eigenvalues for plates with active internal point supports. For the SFSF plate with two internal point supports, Bapat's second mode eigenvalues are suspect and his third mode eigenvalues correspond to the second mode eigenvalues obtained by the present analysis. Bapat's third mode eigenvalues are less than the third mode eigenvalues for the same plate with no internal point supports. These results are questionable because with the addition of internal point supports, the plate eigenvalues must be greater than the eigenvalues for the same plate with no internal point supports. Bapat's method of using the Flexibility Function to model internal point supports appears to work successfully for plates with a single internal point support. No attempt has been documented to modify the Flexibility Function approach in order to account for the effects of attached masses.

A comprehensive set of the first four eigenvalue for each case study is tabulated in Appendix B. The eigenvalues are computed for two different plate aspect ratios and various point support positions on the diagonals (discrete and rigid point supports). Convergence tests indicated that the minimum number of terms needed in the series solution,  $k$ , must be equal to 32 in order to obtain four significant digits in the computed eigenvalue. Higher accuracy can be obtained (more significant digits) by using a greater number of terms but with an increase in computer time.

The computed eigenvalues clearly show the increase in the plate's frequency when using a rigid point support instead of a discrete one. This is due to the stiffening effect of the rigid point support which prohibits the local rotation of the plate element as well as the lateral displacement. The increase in the plate's frequency when using a rigid point support instead of a discrete one is more significant as the point support positions move away from the edges of the plate. The point supports will then have greater restriction

on the plate's displacement and consequently the type of point support will be more influential.

The attached mass is seen to notably decrease the plate's computed eigenvalues as the mass ratio  $M_r$  increases. The attached mass is also seen to have the greatest effect on the plate eigenvalue when it is located furthest away from the constrained edges or internal point support positions.

## 6.2 Eigenvalue Curves

Traces of the first four eigenvalues vs. dimensionless distance  $u = v$ , presented in Sec. 5.1.2, demonstrate the sensitivity of the plate's eigenvalues to various point support positions. A comparison of the eigenvalue curves also show how the rigid point support increases the plate eigenvalues when used in place of a discrete point support.

For Case 1, Case 2, and Case 3 eigenvalues were determined as the discrete point supports approached the corners of the plate. The eigenvalue curves are seen to converge to the exact value for the same plate with no internal point support. For Case 4, Case 5, and Case 6 this type of convergence test would not yield any information as to the accuracy of the solution, since a point support at the corner of a simple-free edge would cause a clamped effect and produce an eigenvalue greater than the eigenvalue for the same plate with no internal point support.

In general, observing the eigenvalue curves it is noticed that when the point supports are located near the corners of the plate they do not have a significant influence on the computed eigenvalues other than a moderate increase. The eigenvalues are also well separated, consequently the associated mode shapes are easier to determine. As the point supports approach the center of the plate the eigenvalues are seen to increase significantly and often there are considerable crossings or convergence of the eigenvalue curves. The occurrence of converging or crossing eigenvalue curves represents double roots in the computed eigenvalues. The double roots can cause difficulty in determining

the plate eigenvalues, for the eigenvalue matrix determinant may approach zero with each increment of  $\lambda^2$  and then suddenly begin to increase away from zero without a change in sign at the double root location. These double roots can be easily overlooked and hence the importance of the eigenvalue curves to predict their location. If a plate is vibrating at its double root eigenvalue it will be experiencing two distinct mode shapes at the same frequency. The associated mode shapes were not generated for double root eigenvalues due to the difficulty that is involved in separating or distinguishing between the two associated mode shapes.

For Case 1, Case 2 and Case 3 the lowest eigenvalue is seen to peak at  $u$  equal to .30 to .35. As the point supports approach the center of the plate, at values greater than  $u$  equal to .35, they begin to have a clamping effect on the plate, but only on the central region allowing the remaining areas to be less constrained and therefore the plate can vibrate more freely and consequently at a lower eigenvalue. With the introduction of the free edge in Case 4, Case 5, and Case 6 the lowest eigenvalue peaks at around  $u$  equal to .20 to .25. This is due to the point supports having to be closer to the free edge(s) of the plate in order to have greater constraint on its displacement. As the point supports move closer to the center of the plate, their influence will be less on the free edge(s) and therefore allowing greater displacement of the plate and lower eigenvalues.

The effect of the point support types on the complexity of the eigenvalue curves is minimal. The only conclusive observation here is the increase in the plate eigenvalues when utilizing the rigid point support instead of a discrete point support.

For a single attached mass the eigenvalue curves were seen to decrease as the mass ratio increased. The mass ratio was only considered up to  $M_r = 1.0$ . It was felt that values of  $M_r > 1.0$  were not practical as it must rarely occur that a plate can carry more than its own weight at a single discrete point support.

For two attached masses, the first mode eigenvalue curve is seen to increase to maximum when the attached masses are directly between the point supports of the plate. At this location the effects of the attached masses will be minimized due to the

constraining effects of the point supports. Again it is observed that the attached masses can significantly reduce the plate eigenvalues.

### 6.3 Associated Mode Shapes

The associated mode shapes have been depicted as three-dimensional plots of the vibrating plates at their natural harmonic frequencies. A study of the associated mode shapes for Case 1 to Case 6 show that the mode shapes are always fully symmetric or asymmetric with respect to a center line drawn parallel to the simply supported edges. This is to be expected, since the plate can not experience anti-symmetry when the plate edge boundary conditions and point support positions are symmetric with respect to the center line. With the associated mode shapes, information is available on the locations of the plate's maximum displacement, maximum acceleration and node lines. The associated mode shape also discloses whether the plate boundary and continuity conditions are satisfied. (i.e. the clamped edge is 'seen' to have zero slope, zero displacement, point support locations have zero displacement.) It is difficult to identify the effects of the rigid point support versus the discrete point support in terms of the change of the plate's slope at the point support location. It is observed however that the rigid point support can alter the actual mode shape when used instead of the discrete point support.

The effects of an attached mass are most noticeable on the computed eigenvalues and eigenvalue curves. The effects of increasing mass ratio on the fundamental mode shape is seen to be minimal. For varying mass locations, the mode shapes are also similar but with moderate changes to the locations of maximum displacement and node lines.

# Chapter 7

## Conclusions

The free vibration analysis of rectangular plates with two opposite edges simply supported and with multiple internal point supports has been solved by the method of superposition. The solution method consisted of first determining the complete solution for a plate with a single internal point support. This was obtained by dividing the plate into two segments at the point support location and enforcing four continuity conditions across the partition line of the two segments.  $N$  similar solutions for  $N$  discrete point supports are then superimposed to create an eigenvalue matrix. Once the equations arising from the enforcement of continuity are established (Appendix A), it is a straight forward procedure to generate the eigenvalue matrix for any number and locations of internal point supports. With the eigenvalue matrix available, the plate eigenvalues and associated mode shapes can then be determined by constraining the plate's displacement at the point support locations. It was also shown that the eigenvalue matrix can be easily modified to account for the effects of attached masses.

Due to the nature of the method of superposition, provided the computer analysis is generating the correct eigenvalue for a plate with a single discrete point support, then the analysis will generate the correct eigenvalue for the same plate with  $N$  discrete point supports since only one solution is used, which is superimposed  $N$  times.

Good agreement was obtained in comparison of results with those published by

Bapat[24] but some discrepancies were found. The eigenvalue curves and associated mode shapes indicate that the analysis is accurate and there appear to be no inconsistencies in the computed eigenvalues.

It is hoped that with this type of analysis available, designers of electronic circuit boards and similar industrial type problems will be able to optimize the boards geometry and support locations in order to minimize the dynamic excitation of the electronic components and extend the fatigue life of the entire structure.

# Bibliography

- [1] Kunz, R.J. and Pitarresi, J.M., *Analytical and Experimental Optimization of Support Locations for Vibrating Printed Circuit Boards*, International Electronics Packaging Society Conference, 1989.
- [2] Gorman, D.J. and Singal, R.K., *Analytical and Experimental Study on Vibrating Rectangular Plates on Rigid Point Supports*, Accepted for publication in the American Institute of Aeronautics and Astronautics Journal, April, 1991.
- [3] Timoshenko, S. and Woinowsky-Krieger, S., *Theory of Plates and Shell*, Second Edition, McGraw-Hill Book Company, Inc., U.S.A., 1987.
- [4] Gorman, D.J., *Free Vibration Analysis of Rectangular Plates*, Elsevier North Holland, Inc., New York, New York, 1982.
- [5] Gorman, D.J. and Ohman, H.L., *Free Vibration Analysis of Simply Supported Rectangular Plates with Internal Point Supports*, Engineering Applications of Mechanics Conference, E.A.M. 90, May 1990, pages 409–414.
- [6] Gorman, D.J., *A Note on the Free Vibration of Rectangular Plates Resting on Symmetrically distributed Point Supports*, Journal of Sound and Vibration, 1989, volume 131, number 3, pages 515–519.
- [7] Gorman, D.J., *On use of the Dirac Delta Function for Representing Concentrated Forces and Moments in Structural Mechanics*, International Journal of Mechanical Engineering Education, volume 10, number 3, pages 177–183.

- [8] Nowacki, W., *Dynamics of Elastic Systems*, Chapman and Hall, London, 1963.
- [9] Fenech, H. and Tran, K., *Experimental Study on the Symmetric Modes of Vibration of a Four Bolt Clamped Square Plate*, Journal of Applied Acoustics, 1984, volume 17, pages 209–221.
- [10] Venkateswara, G., *Vibrations of Point Supported Plates*, Journal of Sound and Vibrations, 1973, volume 29, number 3, pages 387–391.
- [11] Raju, I.S. and Amba-Rao, C.L., *Free Vibrations of a Square Plate Symmetrically Supported at Four Points on the Diagonals*, Journal of Sound and Vibrations, 1983, volume 90, number 2, pages 291–297.
- [12] Narita, Y., *Free Vibration Analysis of Orthotropic Elliptical Plates Resting on Arbitrarily Distributed Point Supports*, Journal of Sound and Vibration, 1986, volume 108, number 1, pages 1–10.
- [13] Narita, Y., *Note on Vibrations of Point Supported Rectangular Plates*, Journal of Sound and Vibrations, 1984, volume 93, number 4, pages 593–597.
- [14] Narita, Y., *The Effects of Point Constraints on Transverse Vibration of Cantilever Plates*, Journal of Sound and Vibrations, 1985, volume 102, number 3, 305–313.
- [15] Narita, Y., and Leissa, A.W., *Vibrations of Corner Point Supported Shallow Shells of Rectangular Planform*, Earthquake Engineering and Structural Dynamics, 1984, volume 12, pages 651–661.
- [16] Laura, P.A.A and Cortinez, V.H., *Free Vibrations of a Plate with an Inner Support*, Journal of Sound and Vibrations, 1986, volume 106, number 3, pages 409–413.
- [17] Laura, P.A.A and Cortinez, V.H., *Fundamental Frequency of Point-Supported Square Plates Carrying Concentrated Masses*, Journal of Sound and Vibrations, 1985, volume 100, number 3, pages 456–458.

- [18] Laura, P.A.A and Guitiérrez, R.H., *Transverse Vibrations of Thin, Elastic Plates with Concentrated Masses and Internal Elastic Supports*, Journal of Sound and Vibrations, 1981, volume 75, number 1, pages 135-143.
- [19] Kersten, J.G.M., Laura, P.A.A, Gross, R.O and Ercol, L., *Vibrations of Rectangular Plates with Point Supports: Comparison of Results*, Journal of Sound and Vibrations, 1983, volume 89, number 2, pages 291-293.
- [20] Bapat, A.V., and Suryanarayan, S., *Free Vibrations of Rectangular Plates with Interior Point Supports*, Journal of Sound and Vibration, 1989, volume 134, number 2, pages 291-313.
- [21] Bapat, A.V., Venkatramani, N. and Suryanarayan, S., *Simulation of Classical Edge Conditions by Finite Elastic Restraints in the Vibration Analysis of Plates*, Journal of Sound and Vibration, 1988, volume 120, number 1, pages 127-140.
- [22] Bapat, A.V., Venkatramani, N. and Suryanarayan, S., *A New Approach for the Representation of a Point Support in the Analysis of Plates*, Journal of Sound and Vibration, 1988, volume 120, number 1, pages 107-125.
- [23] Bapat, A.V. and Suryanarayan, S., *The Flexibility Function Approach to Vibration Analysis of Rectangular Plates with Arbitrary Multiple Point Supports on the Edges*, Journal of Sound and Vibrations, 1989, volume 128, number 2 , pages 209-233.
- [24] Bapat, A.V. and Suryanarayan, S., *Free Vibrations of Periodically Point-Supported Rectangular Plates*, Journal of Sound and Vibration, 1989, volume 123, number 3, pages 491-509.
- [25] Gorman, D.J., *An Analytical Solution for the Free Vibration Analysis of Rectangular Plates Resting on Symmetrically Distributed Point Supports*, Journal of Sound and Vibration, 1981, volume 79, number 4, pages 561-574.

- [26] Saliba, H.T., *Free Vibration Analysis of Rectangular Cantilever Plates with Symmetrically Distributed Point Supports Along the Edges*, Journal of Sound and Vibrations, 1984, volume 94, number 3, pages 381-395.
- [27] Gorman, D.J. and Sharma, R.K., *A Comprehensive Approach to the Free Vibration Analysis of Rectangular Plates by use of the Method of Superposition*, Journal of Sound and Vibration, 1976, volume 47, number 1, pages 126-128.
- [28] Leissa, A.W., *Vibration of Plates*, N.A.S.A. SP-160, 1969.
- [29] Leissa, A.W., *Recent Research in Plate Vibrations. 1973-1976: Complicating Effects*, The Shock and Vibration Digest, 1978 volume 10, number 12, pages 21-35.
- [30] Leissa, A.W., *Recent Studies in Plate Vibrations: 1981-1985: Part 1. Classical Theory*, The Shock and Vibration Digest, 1987 volume 19, number 2, pages 11-18.

# Appendix A

## Equations Resulting from Continuity

## A.1 Case 1, SSSS

$$\lambda^2 > (m\pi)^2$$

$$A_m \sinh \beta_m v + B_m \sin \gamma_m v - C_m \sinh \beta_m v^* - D_m \sin \gamma_m v^* = 0$$

$$A_m \beta_m \cosh \beta_m v + B_m \gamma_m \cos \gamma_m v + C_m \beta_m \cosh \beta_m v^* + D_m \gamma_m \cos \gamma_m v^* = 0$$

$$A_m \beta_m^2 \sinh \beta_m v - B_m \gamma_m^2 \sin \gamma_m v - C_m \beta_m^2 \sinh \beta_m v^* + D_m \gamma_m^2 \sin \gamma_m v^* = 0$$

$$A_m \beta_m^3 \cosh \beta_m v - B_m \gamma_m^3 \cos \gamma_m v + C_m \beta_m^3 \cosh \beta_m v^* - D_m \gamma_m^3 \cos \gamma_m v^* = P^* \sin m\pi u$$

$$\lambda^2 < (m\pi)^2$$

$$A_m \sinh \beta_m v + B_m \sinh \gamma_m v - C_m \sinh \beta_m v^* - D_m \sinh \gamma_m v^* = 0$$

$$A_m \beta_m \cosh \beta_m v + B_m \gamma_m \cosh \gamma_m v + C_m \beta_m \cosh \beta_m v^* + D_m \gamma_m \cosh \gamma_m v^* = 0$$

$$A_m \beta_m^2 \sinh \beta_m v + B_m \gamma_m^2 \sinh \gamma_m v - C_m \beta_m^2 \sinh \beta_m v^* - D_m \gamma_m^2 \sinh \gamma_m v^* = 0$$

$$A_m \beta_m^3 \cosh \beta_m v + B_m \gamma_m^3 \cosh \gamma_m v + C_m \beta_m^3 \cosh \beta_m v^* + D_m \gamma_m^3 \cosh \gamma_m v^* = P^* \sin m\pi u$$

## A.2 Case 2, SSSC

$$\lambda^2 > (m\pi)^2$$

$$A_m(\sinh \beta_m v - \frac{\beta_m}{\gamma_m} \sin \gamma_m v) + B_m(\cosh \beta_m v - \cos \gamma_m v) - C_m \sinh \beta_m v^* \\ - D_m \sin \gamma_m v^* = 0$$

$$A_m(\beta_m \cosh \beta_m v - \beta_m \cos \gamma_m v) + B_m(\beta_m \sinh \beta_m v + \gamma_m \sin \gamma_m v) + \beta_m C_m \cosh \beta_m v^* \\ + \gamma_m D_m \cos \gamma_m v^* = 0$$

$$A_m(\beta_m^2 \sinh \beta_m v + \gamma_m \beta_m \sin \gamma_m v) + B_m(\beta_m^2 \cosh \beta_m v + \gamma_m^2 \cos \gamma_m v) - \beta_m^2 C_m \sinh \beta_m v^* \\ + \gamma_m^2 D_m \sin \gamma_m v^* = 0$$

$$A_m(\beta_m^3 \cosh \beta_m v + \gamma_m^2 \beta_m \cos \gamma_m v) + B_m(\beta_m^3 \sinh \beta_m v - \gamma_m^3 \sin \gamma_m v) + \beta_m^3 C_m \cosh \beta_m v^* \\ - \gamma_m^3 D_m \cos \gamma_m v^* = P^* \sin m\pi u$$

$$\lambda^2 < (m\pi)^2$$

$$A_m(\sinh \beta_m v - \frac{\beta_m}{\gamma_m} \sinh \gamma_m v) + B_m(\cosh \beta_m v - \cosh \gamma_m v) - C_m \sinh \beta_m v^* \\ - D_m \sinh \gamma_m v^* = 0$$

$$A_m(\beta_m \cosh \beta_m v - \beta_m \cosh \gamma_m v) + B_m(\beta_m \sinh \beta_m v - \gamma_m \sinh \gamma_m v) + \beta_m C_m \cosh \beta_m v^* \\ + \gamma_m D_m \cosh \gamma_m v^* = 0$$

$$A_m(\beta_m^2 \sinh \beta_m v - \gamma_m \beta_m \sinh \gamma_m v) + B_m(\beta_m^2 \cosh \beta_m v - \gamma_m^2 \cosh \gamma_m v) - \beta_m^2 C_m \sinh \beta_m v^* \\ - \gamma_m^2 D_m \sinh \gamma_m v^* = 0$$

$$A_m(\beta_m^3 \cosh \beta_m v - \gamma_m^2 \beta_m \cosh \gamma_m v) + B_m(\beta_m^3 \sinh \beta_m v - \gamma_m^3 \sinh \gamma_m v) + \beta_m^3 C_m \cosh \beta_m v^* \\ + \gamma_m^3 D_m \cosh \gamma_m v^* = P^* \sin m\pi u$$

### A.3 Case 3, SCSC

$$\lambda^2 > (m\pi)^2$$

$$\begin{aligned}
& A_m(\cosh \beta_m v - \cos \gamma_m v) + B_m(\sinh \beta_m v - \frac{\beta_m}{\gamma_m} \sin \gamma_m v) \\
& - C_m(\cosh \beta_m v^* - \cos \gamma_m v^*) - D_m(\sinh \beta_m v^* - \frac{\beta_m}{\gamma_m} \sin \gamma_m v^*) = 0 \\
& A_m(\beta_m \sinh \beta_m v + \gamma_m \sin \gamma_m v) + B_m(\beta_m \cosh \beta_m v - \beta_m \cos \gamma_m v) \\
& + C_m(\beta_m \sinh \beta_m v^* + \gamma_m \sin \gamma_m v^*) + D_m(\beta_m \cosh \beta_m v^* - \beta_m \cos \gamma_m v) = 0 \\
& A_m(\beta_m^2 \cosh \beta_m v + \gamma_m^2 \cos \gamma_m v) + B_m \beta_m^2 \sinh \beta_m v + \beta_m \gamma_m \sin \gamma_m v) \\
& - C_m(\beta_m^2 \cosh \beta_m v^* + \gamma_m^2 \cos \gamma_m v^*) - D_m(\beta_m^2 \sinh \beta_m v^* + \beta_m \gamma_m \sin \gamma_m v^*) = 0 \\
& A_m(\beta_m^3 \sinh \beta_m v - \gamma_m^3 \sin \gamma_m v) + B_m(\beta_m^3 \cosh \beta_m v + \beta_m \gamma_m^2 \cos \gamma_m v) \\
& + C_m(\beta_m^3 \sinh \beta_m v^* - \gamma_m^3 \sin \gamma_m v^*) + D_m(\beta_m^3 \cosh \beta_m v^* + \beta_m \gamma_m^2 \cos \gamma_m v^*) = P^* \sin m\pi u
\end{aligned}$$

$$\lambda^2 < (m\pi)^2$$

$$\begin{aligned}
& A_m(\cosh \beta_m v - \cosh \gamma_m v) + B_m(\sinh \beta_m v - \frac{\beta_m}{\gamma_m} \sinh \gamma_m v) \\
& - C_m(\cosh \beta_m v^* - \cosh \gamma_m v^*) - D_m(\sinh \beta_m v^* - \frac{\beta_m}{\gamma_m} \sinh \gamma_m v^*) = 0 \\
& A_m(\beta_m \sinh \beta_m v - \gamma_m \sinh \gamma_m v) + B_m(\beta_m \cosh \beta_m v - \beta_m \cosh \gamma_m v) \\
& + C_m(\beta_m \sinh \beta_m v^* - \gamma_m \sinh \gamma_m v^*) + D_m(\beta_m \cosh \beta_m v^* - \beta_m \cosh \gamma_m v) = 0 \\
& A_m(\beta_m^2 \cosh \beta_m v - \gamma_m^2 \cosh \gamma_m v) + B_m \beta_m^2 \sinh \beta_m v - \beta_m \gamma_m \sinh \gamma_m v) \\
& - C_m(\beta_m^2 \cosh \beta_m v^* - \gamma_m^2 \cosh \gamma_m v^*) - D_m(\beta_m^2 \sinh \beta_m v^* - \beta_m \gamma_m \sinh \gamma_m v^*) = 0 \\
& A_m(\beta_m^3 \sinh \beta_m v - \gamma_m^3 \sin \gamma_m v) + B_m(\beta_m^3 \cosh \beta_m v + \beta_m \gamma_m^2 \cos \gamma_m v) \\
& + C_m(\beta_m^3 \sinh \beta_m v^* - \gamma_m^3 \sin \gamma_m v^*) + D_m(\beta_m^3 \cosh \beta_m v^* + \beta_m \gamma_m^2 \cos \gamma_m v^*) = P^* \sin m\pi u
\end{aligned}$$

## A.4 Case 4, SSSF

$$\lambda^2 > (m\pi)^2$$

$$A_m(\cosh \beta_m v + \alpha_m \cos \gamma_m v) + B_m(\sinh \beta_m v + \sigma_m \sin \gamma_m v) - C - m \sinh \beta_m v^* \\ - D_m \sin \gamma_m v^* = 0$$

$$A_m(\beta_m \sinh \beta_m v - \gamma_m \alpha_m \sin \gamma_m v) + B_m(\beta_m \cosh \beta_m v + \gamma_m \sigma_m \cos \gamma_m v) + C_m \beta_m \cosh \beta_m v^* \\ + D_m \gamma_m v^* = 0$$

$$A_m(\beta_m^2 \cosh \beta_m v - \gamma_m^2 \alpha_m \cos \gamma_m v) + B_m(\beta_m \sinh \beta_m v - \gamma_m^2 \sigma_m \sin \gamma_m v) - C_m \beta_m^2 \sinh \beta_m v^* \\ + D_m \gamma_m^2 \sin \gamma_m v^* = 0$$

$$A_m(\beta_m^3 \sinh \beta_m v + \gamma_m^3 \alpha_m \sin \gamma_m v) + B_m(\beta_m^3 \cosh \beta_m v - \gamma_m^3 \sigma_m \cos \gamma_m v) + C_m(\beta_m^3 \cosh \beta_m v^* \\ - D_m \gamma_m^3 \cos \gamma_m v^* = P^* \sin m\pi u$$

where

$$\alpha_m = \frac{\beta_m^2 - \nu \phi^2(m\pi)^2}{\gamma_m^2 + \nu \phi^2(m\pi)^2} \quad \sigma_m = \frac{\beta_m^3 + \beta_m \nu^* \phi^2(m\pi)^2}{\gamma_m^3 - \gamma_m \nu^* \phi^2(m\pi)^2}$$

$$\lambda^2 < (m\pi)^2$$

$$A_m(\cosh \beta_m v - \alpha_m \cosh \gamma_m v) + B_m(\sinh \beta_m v - \sigma_m \sinh \gamma_m v) - C_m \sinh \beta_m v^* \\ - D_m \sinh \gamma_m v^* = 0$$

$$A_m(\beta_m \sinh \beta_m v - \gamma_m \alpha_m \sinh \gamma_m v) + B_m(\beta_m \cosh \beta_m v - \gamma_m \sigma_m \cosh \gamma_m v) + C_m \beta_m \cosh \beta_m v^* \\ + D_m \cosh \gamma_m v^* = 0$$

$$A_m(\beta_m^2 \cosh \beta_m v - \gamma_m^2 \alpha_m \cosh \gamma_m v) + B_m(\beta_m \sinh \beta_m v - \gamma_m^2 \sigma_m \sinh \gamma_m v) - C_m \beta_m^2 \sinh \beta_m v^* \\ - D_m \gamma_m^2 \sinh \gamma_m v^* = 0$$

$$A_m(\beta_m^3 \sinh \beta_m v - \gamma_m^3 \alpha_m \sinh \gamma_m v) + B_m(\beta_m^3 \cosh \beta_m v - \gamma_m^3 \sigma_m \cosh \gamma_m v) + C_m(\beta_m^3 \cosh \beta_m v^* \\ + D_m \gamma_m^3 \cosh \gamma_m v^* = P^* \sin m\pi u$$

where

$$\alpha_m = \frac{\beta_m^2 - \nu \phi^2(m\pi)^2}{\gamma_m^2 - \nu \phi^2(m\pi)^2} \quad \sigma_m = \frac{\beta_m^3 - \beta_m \nu^* \phi^2(m\pi)^2}{\gamma_m^3 - \gamma_m \nu^* \phi^2(m\pi)^2}$$

### A.5 Case 5, SFSF

$$\lambda^2 > (m\pi)^2$$

$$\begin{aligned}
& A_m(\cosh \beta_m v + \alpha_m \cos \gamma_m v) + B_m(\sinh \beta_m v + \sigma_m \sin \gamma_m v) \\
& - C_m(\cosh \beta_m v^* + \alpha_m \cos \gamma_m v^*) - D_m(\sinh \beta_m v^* + \sigma_m \sin \gamma_m v^*) = 0 \\
& A_m(\beta_m \sinh \beta_m v - \gamma_m \alpha_m \sin \gamma_m v) + B_m(\beta_m \cosh \beta_m v + \gamma_m \sigma_m \cos \gamma_m v) \\
& + C_m(\beta_m \sinh \beta_m v^* - \gamma_m \alpha_m \sin \gamma_m v^*) + D_m(\beta_m \cosh \beta_m v^* + \gamma_m \sigma_m \cos \gamma_m v^*) = 0 \\
& A_m(\beta_m^2 \cosh \beta_m v - \gamma_m^2 \alpha_m \cos \gamma_m v) + B_m(\beta_m \sinh \beta_m v - \gamma_m^2 \sigma_m \sin \gamma_m v) \\
& - C_m(\beta_m^2 \cosh \beta_m v^* - \gamma_m^2 \alpha_m \cos \gamma_m v^*) - D_m(\beta_m \sinh \beta_m v^* - \gamma_m^2 \sigma_m \sin \gamma_m v^*) = 0 \\
& A_m(\beta_m^3 \sinh \beta_m v + \gamma_m^3 \alpha_m \sin \gamma_m v) + B_m(\beta_m^3 \cosh \beta_m v - \gamma_m^3 \sigma_m \cos \gamma_m v) \\
& + C_m(\beta_m^3 \sinh \beta_m v^* + \gamma_m^3 \alpha_m \sin \gamma_m v^*) + D_m(\beta_m^3 \cosh \beta_m v^* - \gamma_m^3 \sigma_m \cos \gamma_m v^*) = P^* \sin m\pi u
\end{aligned}$$

where

$$\alpha_m = \frac{\beta_m^2 - \nu \phi^2 (m\pi)^2}{\gamma_m^2 + \nu \phi^2 (m\pi)^2} \quad \sigma_m = \frac{\beta_m^3 + \beta_m \nu^* \phi^2 (m\pi)^2}{\gamma_m^3 - \gamma_m \nu^* \phi^2 (m\pi)^2}$$

$$\lambda^2 < (m\pi)^2$$

$$\begin{aligned}
& A_m(\cosh \beta_m v - \alpha_m \cosh \gamma_m v) + B_m(\sinh \beta_m v - \sigma_m \sinh \gamma_m v) \\
& - C_m(\cosh \beta_m v^* - \alpha_m \cosh \gamma_m v^*) - D_m(\sinh \beta_m v^* - \sigma_m \sinh \gamma_m v^*) = 0 \\
& A_m(\beta_m \sinh \beta_m v - \gamma_m \alpha_m \sinh \gamma_m v) + B_m(\beta_m \cosh \beta_m v - \gamma_m \sigma_m \cosh \gamma_m v) \\
& + C_m(\beta_m \sinh \beta_m v^* - \gamma_m \alpha_m \sinh \gamma_m v^*) + D_m(\beta_m \cosh \beta_m v^* - \gamma_m \sigma_m \cosh \gamma_m v^*) = 0 \\
& A_m(\beta_m^2 \cosh \beta_m v - \gamma_m^2 \alpha_m \cosh \gamma_m v) + B_m(\beta_m \sinh \beta_m v - \gamma_m^2 \sigma_m \sinh \gamma_m v) \\
& - C_m(\beta_m^2 \cosh \beta_m v^* - \gamma_m^2 \alpha_m \cosh \gamma_m v^*) - D_m(\beta_m \sinh \beta_m v^* - \gamma_m^2 \sigma_m \sinh \gamma_m v^*) = 0 \\
& A_m(\beta_m^3 \sinh \beta_m v - \gamma_m^3 \alpha_m \sinh \gamma_m v) + B_m(\beta_m^3 \cosh \beta_m v - \gamma_m^3 \sigma_m \cosh \gamma_m v) \\
& + C_m(\beta_m^3 \sinh \beta_m v^* - \gamma_m^3 \alpha_m \sinh \gamma_m v^*) + D_m(\beta_m^3 \cosh \beta_m v^* - \gamma_m^3 \sigma_m \cosh \gamma_m v^*) = P^* \sin m\pi u
\end{aligned}$$

where

$$\alpha_m = \frac{\beta_m^2 - \nu \phi^2 (m\pi)^2}{\gamma_m^2 - \nu \phi^2 (m\pi)^2} \quad \sigma_m = \frac{\beta_m^3 - \beta_m \nu^* \phi^2 (m\pi)^2}{\gamma_m^3 - \gamma_m \nu^* \phi^2 (m\pi)^2}$$

## A.6 Case 6, SCSF

$$\lambda^2 > (m\pi)^2$$

$$\begin{aligned} & A_m(\cosh \beta_m v + \alpha_m \cos \gamma_m v) + B_m(\sinh \beta_m v + \sigma_m \sin \gamma_m v) \\ & - C_m(\cosh \beta_m v^* - \cos \gamma_m v^*) - D_m(\sinh \beta_m v^* - \frac{\beta_m}{\gamma_m} \sin \gamma_m v^*) = 0 \\ & A_m(\beta_m \sinh \beta_m v - \gamma_m \alpha_m \sin \gamma_m v) + B_m(\beta_m \cosh \beta_m v + \gamma_m \sigma_m \cos \gamma_m v) \\ & + C_m(\beta_m \sinh \beta_m v^* + \gamma_m \sin \gamma_m v^*) + D_m(\beta_m \cosh \beta_m v^* - \beta_m \cos \gamma_m v) = 0 \\ & A_m(\beta_m^2 \cosh \beta_m v - \gamma_m^2 \alpha_m \cos \gamma_m v) + B_m(\beta_m \sinh \beta_m v - \gamma_m^2 \sigma_m \sin \gamma_m v) \\ & - C_m(\beta_m^2 \cosh \beta_m v^* + \gamma_m^2 \cos \gamma_m v^*) - D_m(\beta_m^2 \sinh \beta_m v^* + \beta_m \gamma_m \sin \gamma_m v^*) = 0 \\ & A_m(\beta_m^3 \sinh \beta_m v + \gamma_m^3 \alpha_m \sin \gamma_m v) + B_m(\beta_m^3 \cosh \beta_m v - \gamma_m^3 \sigma_m \cos \gamma_m v) \\ & + C_m(\beta_m^3 \sinh \beta_m v^* - \gamma_m^3 \sin \gamma_m v^*) + D_m(\beta_m^3 \cosh \beta_m v^* + \beta_m \gamma_m^2 \cos \gamma_m v^*) = P^* \sin m\pi u \end{aligned}$$

where

$$\alpha_m = \frac{\beta_m^2 - \nu \phi^2 (m\pi)^2}{\gamma_m^2 + \nu \phi^2 (m\pi)^2} \quad \sigma_m = \frac{\beta_m^3 + \beta_m \nu^* \phi^2 (m\pi)^2}{\gamma_m^3 - \gamma_m \nu^* \phi^2 (m\pi)^2}$$

$$\lambda^2 < (m\pi)^2$$

$$\begin{aligned} & A_m(\cosh \beta_m v - \alpha_m \cosh \gamma_m v) + B_m(\sinh \beta_m v - \sigma_m \sinh \gamma_m v) \\ & - C_m(\cosh \beta_m v^* - \cosh \gamma_m v^*) - D_m(\sinh \beta_m v^* - \frac{\beta_m}{\gamma_m} \sinh \gamma_m v^*) = 0 \\ & A_m(\beta_m \sinh \beta_m v - \gamma_m \alpha_m \sinh \gamma_m v) + B_m(\beta_m \cosh \beta_m v - \gamma_m \sigma_m \cosh \gamma_m v) \\ & + C_m(\beta_m \sinh \beta_m v^* - \gamma_m \sinh \gamma_m v^*) + D_m(\beta_m \cosh \beta_m v^* - \beta_m \cosh \gamma_m v) = 0 \\ & A_m(\beta_m^2 \cosh \beta_m v - \gamma_m^2 \alpha_m \cosh \gamma_m v) + B_m(\beta_m \sinh \beta_m v - \gamma_m^2 \sigma_m \sinh \gamma_m v) \\ & - C_m(\beta_m^2 \cosh \beta_m v^* - \gamma_m^2 \cosh \gamma_m v^*) - D_m(\beta_m^2 \sinh \beta_m v^* - \beta_m \gamma_m \sinh \gamma_m v^*) = 0 \\ & A_m(\beta_m^3 \sinh \beta_m v - \gamma_m^3 \alpha_m \sinh \gamma_m v) + B_m(\beta_m^3 \cosh \beta_m v - \gamma_m^3 \sigma_m \cosh \gamma_m v) \\ & + C_m(\beta_m^3 \sinh \beta_m v^* - \gamma_m^3 \sinh \gamma_m v^*) + D_m(\beta_m^3 \cosh \beta_m v^* - \beta_m \gamma_m^2 \cosh \gamma_m v^*) = P^* \sin m\pi u \end{aligned}$$

where

$$\alpha_m = \frac{\beta_m^2 - \nu \phi^2 (m\pi)^2}{\gamma_m^2 - \nu \phi^2 (m\pi)^2} \quad \sigma_m = \frac{\beta_m^3 - \beta_m \nu^* \phi^2 (m\pi)^2}{\gamma_m^3 - \gamma_m \nu^* \phi^2 (m\pi)^2}$$

# Appendix B

## Computed Eigenvalues

## **B.1 Multiple Internal Point Supports**

Computed Eigenvalues  $\lambda^2$  for each case study with various point support positions (discrete and rigid). Number of terms taken in series,  $k = 32$ . Note: all internal supports lie on diagonal lines across the plate surface.

Table B.1: Computed Eigenvalues  $\lambda^2$ , Case 1, SSSS ( $\phi = 1.0$ , support type: discrete).

mode	$u = v$							
	0.05	0.10	0.15	0.20	0.25	0.30	0.35	0.40
1	20.65	23.50	28.79	37.65	52.66	79.37	94.19	73.78
2	50.79	55.13	62.74	74.50	91.24	109.9	102.9	81.94
3	50.79	55.13	62.74	74.50	91.24	109.9	102.9	81.94
4	82.56	93.48	113.5	136.3	146.8	131.5	113.5	133.7

Table B.2: Computed Eigenvalues  $\lambda^2$ , Case 1, SSSS ( $\phi = 1.0$ , support type: rigid).

mode	$u = v$							
	0.05	0.10	0.15	0.20	0.25	0.30	0.35	0.40
1	21.59	25.79	33.21	45.63	67.17	108.5	116.4	89.51
2	52.25	58.49	69.10	86.19	112.6	138.6	120.2	93.48
3	52.25	58.49	69.10	86.22	112.6	138.6	120.2	93.50
4	86.18	99.45	102.7	111.0	126.2	141.4	137.4	101.8

Table B.3: Computed Eigenvalues  $\lambda^2$ , Case 1, SSSS ( $\phi = 1.5$ , support type: discrete).

mode	$u = v$							
	0.05	0.10	0.15	0.20	0.25	0.30	0.35	0.40
1	14.83	16.58	19.68	24.63	32.52	44.45	48.41	41.69
2	28.62	32.34	39.15	50.38	61.61	64.99	53.66	43.96
3	44.59	46.57	49.73	54.46	67.21	67.70	76.26	64.83
4	50.81	54.92	61.00	67.09	69.53	72.23	76.74	65.77

Table B.4: Computed Eigenvalues  $\lambda^2$ , Case 1, SSSS ( $\phi = 1.5$ , support type: rigid).

mode	$u = v$							
	0.05	0.10	0.15	0.20	0.25	0.30	0.35	0.40
1	15.31	17.71	21.77	28.35	39.64	60.85	61.62	49.16
2	29.63	34.84	43.98	58.34	69.10	86.14	61.71	49.21
3	45.14	47.71	51.80	59.02	81.90	77.19	83.06	69.05
4	52.01	57.71	66.42	77.75	86.25	76.98	83.29	69.51

Table B.5: Computed Eigenvalues  $\lambda^2$ , Case 2, SSSC ( $\phi = 1.0$ , support type: discrete).

mode	$u = v$							
	0.05	0.10	0.15	0.20	0.25	0.30	0.35	0.40
1	24.25	26.34	38.80	53.80	53.28	80.02	96.77	76.44
2	52.66	56.12	63.10	74.74	91.77	101.6	100.7	84.40
3	59.49	62.57	68.92	79.53	94.20	110.3	104.8	93.00
4	88.45	97.22	105.3	106.3	108.4	119.4	120.5	103.4

Table B.6: Computed Eigenvalues  $\lambda^2$ , Case 2, SSSC ( $\phi = 1.0$ , support type: rigid).

mode	$u = v$							
	0.05	0.10	0.15	0.20	0.25	0.30	0.35	0.40
1	24.91	28.17	34.64	46.32	67.42	108.7	117.9	91.06
2	53.75	59.10	69.23	86.23	112.7	138.9	122.3	95.77
3	60.44	65.25	74.53	90.59	116.6	140.3	133.3	109.8
4	91.14	104.6	108.9	116.9	132.1	144.2	139.6	113.7

Table B.7: Computed Eigenvalues  $\lambda^2$ , Case 2, SSSC ( $\phi = 1.5$ , support type: discrete).

mode	$u = v$							
	0.05	0.10	0.15	0.20	0.25	0.30	0.35	0.40
1	15.97	17.29	19.97	24.71	32.68	45.45	50.42	42.71
2	31.80	34.58	40.55	51.30	61.80	66.42	67.07	56.70
3	45.05	46.71	49.77	54.53	67.88	72.66	76.50	65.25
4	56.28	59.48	64.97	70.78	74.26	85.58	83.00	72.80

Table B.8: Computed Eigenvalues  $\lambda^2$ , Case 2, SSSC ( $\phi = 1.5$ , support type: rigid).

mode	$u = v$							
	0.05	0.10	0.15	0.20	0.25	0.30	0.35	0.40
1	16.31	18.21	21.90	28.35	39.63	60.85	100.1	49.21
2	32.49	36.64	44.98	58.33	69.09	77.03	106.2	65.26
3	45.47	47.77	51.79	59.63	91.19	86.22	120.2	69.41
4	57.12	61.81	69.82	80.84	104.9	104.8	126.7	78.57

Table B.9: Computed Eigenvalues  $\lambda^2$ , Case 3, SCSC ( $\phi = 1.0$ , support type: discrete).

mode	$u = v$							
	0.05	0.10	0.15	0.20	0.25	0.30	0.35	0.40
1	28.99	29.95	33.05	40.10	53.96	80.71	99.93	85.66
2	54.98	57.22	63.48	75.00	92.32	108.6	108.7	90.31
3	69.53	71.51	77.02	87.45	104.7	110.8	128.0	108.7
4	95.30	101.5	108.5	110.5	110.6	128.4	134.1	112.5

Table B.10: Computed Eigenvalues  $\lambda^2$ , Case 3, SCSC ( $\phi = 1.0$ , support type: rigid).

mode	$u = v$							
	0.05	0.10	0.15	0.20	0.25	0.30	0.35	0.40
1	29.24	31.11	36.29	47.07	67.71	108.8	128.9	103.7
2	55.53	59.75	69.37	86.20	112.7	139.1	128.9	103.8
3	70.01	73.59	81.81	97.25	125.1	144.0	153.2	121.1
4	96.88	107.1	112.2	119.9	133.4	158.5	153.8	122.5

Table B.11: Computed Eigenvalues  $\lambda^2$ , Case 3, SCSC ( $\phi = 1.5$ , support type: discrete).

mode	$u = v$							
	0.05	0.10	0.15	0.20	0.25	0.30	0.35	0.40
1	17.43	18.11	20.27	24.79	32.85	46.58	61.82	55.13
2	35.52	37.21	42.22	52.42	70.65	73.12	72.54	58.09
3	45.58	46.85	49.80	54.52	82.02	84.58	84.69	71.64
4	62.63	64.80	70.18	76.96	99.04	87.18	87.42	73.94

Table B.12: Computed Eigenvalues  $\lambda^2$ , Case 3, SCSC ( $\phi = 1.5$ , support type: rigid).

mode	$u = v$							
	0.05	0.10	0.15	0.20	0.25	0.30	0.35	0.40
1	17.55	18.77	22.04	28.36	39.63	60.96	83.31	65.24
2	35.82	38.75	46.16	58.33	69.09	86.22	83.41	65.28
3	45.83	47.83	51.79	60.38	85.83	103.8	97.15	78.00
4	62.84	66.71	74.31	85.63	99.57	103.8	98.26	79.14

Table B.13: Computed Eigenvalues  $\lambda^2$ , Case 4, SSSF ( $\phi = 1.0$ , support type: discrete).

mode	$u = v$							
	0.05	0.10	0.15	0.20	0.25	0.30	0.35	0.40
1	17.66	21.72	27.54	36.21	37.36	33.16	28.93	25.28
2	33.03	37.14	40.54	51.32	52.25	62.61	55.58	50.40
3	58.96	54.28	61.76	71.13	70.96	78.12	89.11	76.04
4	63.55	64.95	68.09	76.00	89.35	96.99	98.82	85.33

Table B.14: Computed Eigenvalues  $\lambda^2$ , Case 4, SSSF ( $\phi = 1.0$ , support type: rigid).

mode	$u = v$							
	0.05	0.10	0.15	0.20	0.25	0.30	0.35	0.40
1	19.63	24.90	32.81	45.44	51.18	43.77	36.05	29.71
2	35.77	42.06	49.13	53.66	67.08	71.69	60.33	53.03
3	51.35	58.30	69.06	86.20	89.10	106.7	101.0	90.30
4	65.12	69.23	76.56	90.17	112.7	109.4	118.2	95.42

Table B.15: Computed Eigenvalues  $\lambda^2$ , Case 4, SSSF ( $\phi = 1.5$ , support type: discrete).

mode	$u = v$							
	0.05	0.10	0.15	0.20	0.25	0.30	0.35	0.40
1	14.24	16.32	19.33	23.26	23.30	20.59	18.32	16.59
2	24.07	28.90	32.09	29.86	33.85	46.15	46.65	42.76
3	36.86	37.92	39.84	50.32	53.85	49.75	50.61	44.44
4	44.25	46.45	49.50	53.57	63.07	66.47	70.26	60.97

Table B.16: Computed Eigenvalues  $\lambda^2$ , Case 4, SSSF ( $\phi = 1.5$ , support type: rigid).

mode	$u = v$							
	0.05	0.10	0.15	0.20	0.25	0.30	0.35	0.40
1	15.00	17.63	21.68	28.11	29.70	24.80	21.02	18.24
2	26.27	32.57	38.76	35.82	60.00	52.75	48.21	45.30
3	38.79	41.97	45.42	58.32	69.10	60.92	61.67	49.21
4	45.00	47.69	51.78	59.27	82.65	77.03	83.29	69.24

Table B.17: Computed eigenvalues  $\lambda^2$ , Case 5, SFSF ( $\phi = 1.0$ , support type: discrete).

mode	$u = v$							
	0.05	0.10	0.15	0.20	0.25	0.30	0.35	0.40
1	16.41	20.56	26.49	34.66	34.99	31.03	27.37	24.46
2	26.89	32.75	38.49	41.15	39.75	35.32	30.50	26.11
3	42.28	43.45	42.79	41.50	51.91	61.67	55.29	50.21
4	47.72	53.53	60.83	68.64	68.52	63.58	55.88	50.59

Table B.18: Computed eigenvalues  $\lambda^2$ , Case 5, SFSF ( $\phi = 1.0$ , support type: rigid).

mode	$u = v$							
	0.05	0.10	0.15	0.20	0.25	0.30	0.35	0.40
1	18.37	24.19	32.45	45.26	51.06	43.66	36.02	29.66
2	30.29	38.21	46.79	53.01	51.31	43.88	36.08	29.76
3	44.76	48.57	52.44	54.34	67.00	71.69	60.31	52.99
4	50.59	58.11	69.03	86.14	89.12	71.69	60.36	53.06

Table B.19: Computed eigenvalues  $\lambda^2$ , Case 5, SFSF ( $\phi = 1.5$ , support type: discrete).

mode	$u = v$							
	0.05	0.10	0.15	0.20	0.25	0.30	0.35	0.40
1	13.84	16.08	18.97	22.20	22.08	19.77	17.73	16.23
2	22.01	27.54	31.92	28.96	24.81	21.46	18.92	16.96
3	30.40	32.94	32.27	30.45	34.88	47.99	46.56	44.42
4	43.42	41.72	40.63	50.24	53.06	49.48	46.74	44.46

Table B.20: Computed eigenvalues  $\lambda^2$ , Case 5, SFSF ( $\phi = 1.5$ , support type: rigid).

mode	$u = v$							
	0.05	0.10	0.15	0.20	0.25	0.30	0.35	0.40
1	14.70	17.54	21.59	27.89	29.53	24.76	21.01	18.24
2	24.49	31.43	38.34	35.72	29.87	24.84	21.03	18.24
3	33.27	37.90	39.36	35.92	39.89	52.74	48.21	45.29
4	44.86	46.07	46.91	58.31	60.00	52.74	48.21	45.31

Table B.21: Computed eigenvalues  $\lambda^2$ , Case 6, SCSF ( $\phi = 1.0$ , support type: discrete).

mode	$u = v$							
	0.05	0.10	0.15	0.20	0.25	0.30	0.35	0.40
1	19.60	23.73	29.18	37.28	37.41	31.19	28.96	25.30
2	37.09	39.47	41.27	41.32	52.76	62.61	55.58	50.40
3	50.32	55.19	62.10	71.32	71.01	78.61	89.49	82.18
4	73.06	73.50	75.97	82.86	95.52	97.41	109.0	92.88

Table B.22: Computed eigenvalues  $\lambda^2$ , Case 6, SCSF ( $\phi = 1.0$ , support type: rigid).

mode	$u = v$							
	0.05	0.10	0.15	0.20	0.25	0.30	0.35	0.40
1	21.77	26.82	34.10	46.09	51.16	43.74	36.04	29.69
2	39.23	43.95	49.79	53.74	67.33	71.66	60.33	53.03
3	52.65	58.89	69.19	86.17	89.10	106.7	101.0	93.55
4	74.16	77.41	84.00	96.49	112.7	109.5	131.3	105.8

Table B.23: Computed eigenvalues  $\lambda^2$ , Case 6, SCSF ( $\phi = 1.5$ , support type: discrete).

mode	$u = v$							
	0.05	0.10	0.15	0.20	0.25	0.30	0.35	0.40
1	15.13	16.98	19.60	23.32	23.32	20.61	18.33	16.59
2	25.75	29.82	32.11	29.87	33.99	47.29	46.65	44.44
3	40.09	39.96	41.41	51.29	53.87	49.75	63.28	56.18
4	44.66	46.59	49.53	53.64	63.25	73.62	74.92	61.34

Table B.24: Computed eigenvalues  $\lambda^2$ , Case 6, SCSF ( $\phi = 1.5$ , support type: rigid).

mode	$u = v$							
	0.05	0.10	0.15	0.20	0.25	0.30	0.35	0.40
1	15.88	18.12	21.81	28.12	29.69	24.79	21.02	18.23
2	27.89	33.53	38.82	35.82	39.76	52.73	48.20	45.30
3	41.54	43.49	46.54	58.31	60.00	60.95	87.15	65.23
4	45.32	47.75	51.78	59.98	69.10	86.18	83.35	69.22

## B.2 Effects of Attached Mass

Computed eigenvalues  $\lambda^2$  for Case 5, SFSF having varying mass ratios and varying mass locations.

For varying mass ratio, mass location is at plate's center at  $u = v = 0.5$ . Plate is also supported by four discrete point supports.

For varying mass location, two attached masses are considered with mass ratio  $M_r = 0.4$ . Attached masses are located on the line  $u = 0.5$  at varying values of  $v$  and  $1 - v$ . Plate is also supported by four discrete point supports.

Table B.25: Computed eigenvalues  $\lambda^2$ , varying mass ratios ( $\phi = 1.0$ ).

$u = v$	mass ratio $M_r$									
	0.1	0.2	0.3	0.4	0.5	0.6	0.7	0.8	0.9	1.0
0.05	14.39	12.89	11.76	10.86	10.14	9.500	9.037	8.610	8.236	7.907
0.10	17.47	15.35	13.81	12.65	11.73	10.98	10.36	9.837	9.357	8.974
0.15	21.61	18.55	16.46	14.95	13.77	12.84	12.07	11.42	10.87	10.39
0.20	27.01	22.68	19.88	17.90	16.41	15.24	14.29	13.49	12.82	12.23
0.25	31.71	27.40	24.09	21.67	19.83	18.39	17.21	16.24	15.40	14.69
0.30	30.30	29.13	27.48	25.63	23.88	22.35	21.03	19.91	18.93	18.08
0.35	27.17	26.91	26.60	26.21	25.73	25.17	24.52	23.81	23.09	22.36
0.40	24.41	24.36	24.30	24.23	24.17	24.09	24.01	23.92	23.82	23.72

Table B.26: Computed eigenvalues  $\lambda^2$ , varying mass ratios ( $\phi = 1.5$ ).

$u = v$	mass ratio $M_r$									
	0.1	0.2	0.3	0.4	0.5	0.6	0.7	0.8	0.9	1.0
0.05	11.79	10.37	9.324	8.543	7.924	7.419	6.999	6.642	6.334	6.065
0.10	13.26	11.46	10.22	9.290	8.583	8.013	7.542	7.144	6.803	6.506
0.15	15.15	12.90	11.39	10.31	9.468	8.826	8.291	7.842	7.458	7.126
0.20	17.59	14.82	13.01	11.73	10.76	9.993	9.356	8.844	8.404	8.023
0.25	19.75	17.18	15.19	13.71	12.57	11.68	10.94	10.33	9.815	9.346
0.30	19.23	18.39	17.27	16.09	14.99	14.03	13.21	12.51	11.90	11.37
0.35	17.60	17.42	17.21	16.93	16.59	16.18	15.72	15.22	14.72	14.23
0.40	16.20	16.17	16.13	16.09	16.04	16.00	15.94	15.88	15.81	15.74

Table B.27: Computed eigenvalues  $\lambda^2$ , varying mass locations ( $M_r = 0.4$ ,  $\phi = 1.0$ ).

$u = v$	attached mass location $v$ ( $u = 0.5$ )							
	0.05	0.10	0.15	0.20	0.25	0.30	0.35	0.40
0.05	9.959	10.26	10.26	10.08	9.813	9.480	9.194	8.925
0.10	12.13	12.78	12.79	12.44	11.93	11.36	10.82	10.35
0.15	13.59	15.44	16.11	19.05	14.99	14.01	13.06	12.27
0.20	13.80	16.57	19.06	20.15	19.48	17.91	16.27	14.91
0.25	12.87	15.69	19.06	22.66	25.07	23.91	21.09	18.67
0.30	11.68	14.09	17.13	20.92	25.38	29.73	28.24	23.99
0.35	10.64	12.60	15.02	18.08	21.85	25.60	27.35	26.67
0.40	9.841	11.43	13.33	15.65	18.53	21.70	23.93	24.46

Table B.28: Computed eigenvalues  $\lambda^2$ , varying mass locations ( $M_r = 0.4$ ,  $\phi = 1.5$ ).

$u = v$	attached mass location $v$ ( $u = 0.5$ )							
	0.05	0.10	0.15	0.20	0.25	0.30	0.35	0.40
0.05	9.039	9.331	9.117	8.710	8.257	7.819	7.418	7.066
0.10	10.63	11.57	11.28	10.51	9.620	8.900	8.255	7.729
0.15	10.71	13.22	14.22	13.30	11.87	10.55	9.475	8.679
0.20	9.581	12.31	15.46	17.39	15.60	13.27	11.44	10.12
0.25	8.462	10.61	13.38	16.96	20.91	18.05	14.68	12.39
0.30	7.577	9.195	11.26	13.98	17.36	19.70	18.64	15.79
0.35	6.968	8.229	10.46	11.67	14.18	16.75	17.73	17.31
0.40	6.570	7.601	8.757	10.16	11.93	14.10	15.81	16.23

## Appendix C

### Illustrative Convergence Test

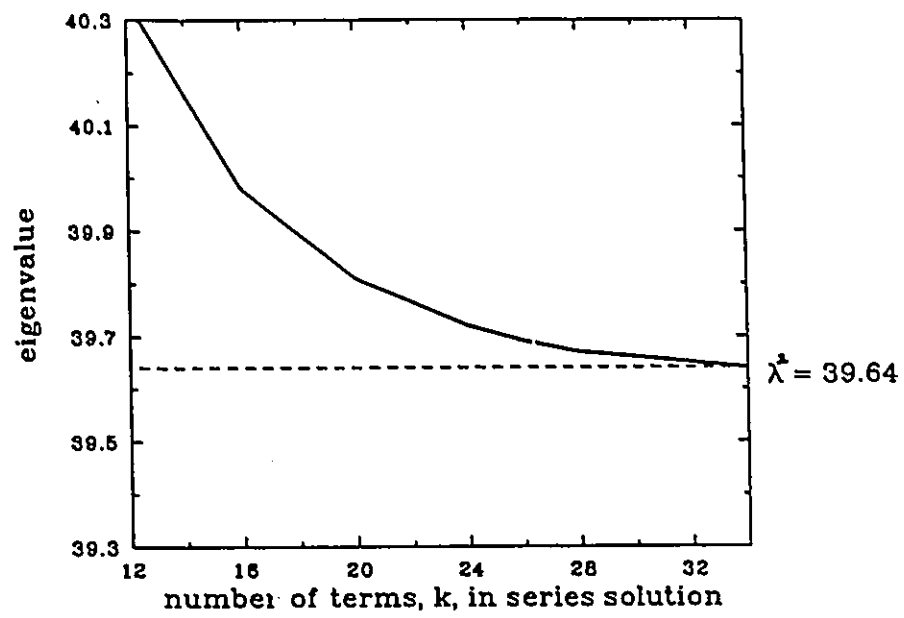


Figure C.1: Convergence curve for Case 1, SSSS,  $u = v = 0.25$ ,  $\phi = 1.5$ , support type: rigid

## Appendix D

# Computer Program for Plate Vibration Analysis

## List of Computer Program Symbols

A	equation elements determined from enforcement of continuity
ALMDS	eigenvalue $\lambda^2$
AMR	attached mass ratio
B	eigenvalue matrix
BM	$\phi\sqrt{\lambda^2 + (m\pi)^2}$
CF	four unknowns from equations of continuity
CP	internal point support coordinate
DEL	increment of eigenvalue
DLIM	upper limit in eigenvalue search
ETA	dimensionless coordinate $\eta$
FAC	value subtracted for an attached mass
GM	$\phi\sqrt{\lambda^2 - (m\pi)^2}$ or $\phi\sqrt{(m\pi)^2 - \lambda^2}$
K	number of terms in fourier expansions
KN	number of discrete point supports
P	point support driving force
PHI	plate aspect ratio $\phi$
PI	$\pi$
PSI	dimensionless coordinate $\xi$
PSR	Poisson's ratio
UV	point support coordinate $u = v$
W(I, J)	stored displacement values
Y	eigenvalue determinant

```

C *****
C * * Listing of computer program used to calculate the eigenvalues
C * * and mode shape data for rectangular plates with two opposite
C * * edges simply supported and the remaining edges simply supported,
C * * clamped or free. There can be any number of point supports and/or
C * * attached masses. Note: must set program subroutine call
C * * statements to correspond with appropriate plate boundary
C * * conditions. Program is set to analyse Case 1, SSSS.
C ***** subroutine definitions *****
C * * equation elements from enforcement of continuity conditions:
C * * SUBROUTINE ABCD1 - SSSS plate
C * * SUBROUTINE ABCD2 - SSSC plate
C * * SUBROUTINE ABCD3 - SCSC plate
C * * SUBROUTINE ABCD4 - SSSF plate
C * * SUBROUTINE ABCD5 - SFSF plate
C * * SUBROUTINE ABCD6 - SCSF plate
C * * modified Levy type series solution
C * * SUBROUTINE SSSS - SSSS plate
C * * SUBROUTINE SCSS - SSSC plate
C * * SUBROUTINE SCSC - SCSC plate
C * * SUBROUTINE SFSS - SSSF plate
C * * SUBROUTINE SFSF - SFSF plate
C * * SUBROUTINE SFSC - SCSF plate
C * * SUBROUTINE SIMQ - calculates unknowns A,B,C,D
C * * SUBROUTINE DETERM - calculates determinant for eigenvalue search
C * * SUBROUTINE DETR - calculates point supports P value
C***** start of main program *****
      IMPLICIT DOUBLE PRECISION (A-H,O-Z)
      DIMENSION W(61,61), B(16,16),P(16),CP(16,3)
      DIMENSION A(4,5), CF(5)
      1 FORMAT (7(E13.6,3X))
C * * terminal input section
      READ (6,*) UV, SS, AMR,PHI
      READ (6,*) ALMDS, DEL, DLIM
C * * initialize remaining input variables
      SS = 1.0
      K = 32
      JL = 21
      C = 1.
      PI = 4.*DATAN(C)
      PS = 1
      PHIS = PHI**2
      PSR = 0.333
C * * X1,Y1,X2,Y2,...are the rigid support positions
C * * EP1,EP2 define the radius of rigid support
C * * note: 1 rigid support = 4 point supports.
      EP1 = 5./160.

```

```

EP2 = 5./240.
IF (PHI.EQ.1) THEN
EP2 = EP1
END IF
X1 = UV
Y1 = X1
X2 = 1 - X1
Y2 = Y1
X3 = X1
Y3 = 1 - Y1
X4 = 1 - X1
Y4 = 1 - Y1

```

```

C * * now generate U,V,and AMR(mass ratios) associated with each pt.
C * * note third value AMR will always = 0 unless we wish to attach
C * * masses at the points of interest.

```

```

C * * CP represents point load location. Note four points generate
C * * a cluster of points which simulates a bolt fastner

```

```

C * * K represents number of terms of series, 20 to 30 terms usually
C * * gives good convergence. Final pass k=32.

```

```

C * * SS defines the point support type.
C * * SS = 1 - discrete SS = 2 - rigid

```

```

IF(SS.EQ.1) THEN
KN = 4
CP(1,1)= X1
CP(1,2)= Y1
CP(1,3)= 0.

```

```

CP(2,1)= X2
CP(2,2)= Y2
CP(2,3)= 0.

```

```

CP(3,1)= X3
CP(3,2)= Y3
CP(3,3)= 0.

```

```

CP(4,1)= X4
CP(4,2)= Y4
CP(4,3)= 0.

```

```

ELSE
KN = 16
CP(1,1)= X1+EP1
CP(1,2)= Y1
CP(1,3)= 0.

```

```

CP(2,1)= X1-EP1
CP(2,2)= Y1
CP(2,3)= 0.

```

```

CP(3,1)= X1
CP(3,2)= Y1+EP2
CP(3,3)= 0.

```

```

CP(4,1)= X1

```

```
CP(4,2)= Y1-EP2
CP(4,3)= 0.

CP(5,1)= X2+EP1
CP(5,2)= Y2
CP(5,3)= 0.

CP(6,1)= X2-EP1
CP(6,2)= Y2
CP(6,3)= 0.

CP(7,1)= X2
CP(7,2)= Y2+EP2
CP(7,3)= 0.

CP(8,1)= X2
CP(8,2)= Y2-EP2
CP(8,3)= 0.

CP(9,1)= X3+EP1
CP(9,2)= Y3
CP(9,3)= 0.

CP(10,1)= X3-EP1
CP(10,2)= Y3
CP(10,3)= 0.

CP(11,1)= X3
CP(11,2)= Y3+EP2
CP(11,3)= 0.

CP(12,1)= X3
CP(12,2)= Y3-EP2
CP(12,3)= 0.

CP(13,1)= X4+EP1
CP(13,2)= Y4
CP(13,3)= 0.

CP(14,1)= X4-EP1
CP(14,2)= Y4
CP(14,3)= 0.

CP(15,1)= X4
CP(15,2)= Y4+EP2
CP(15,3)= 0.

CP(16,1)= X4
CP(16,2)= Y4-EP2
CP(16,3)= 0.
ENDIF

9 DO 55 I = 1,KN
DO 55 J = 1,KN
55 B(I,J) = 0.
DO 53 I = 1,KN
DO 53 J = 1,KN
U1 = CP(I,1)
V1 = CP(I,2)
```

```

      U2 = CP(J,1)
      V2 = CP(J,2)

C * * calculate the series summation of the modified Levy solution for
C * * for point support location U1, V1.

      DO 54 M = 1,K
      CALL ABCD1 (M,PHIS,ALMDS,PS,U1,V1,A,PSR)
      CALL SIMQ (A,CF)
      CALL SSSS (M,PHIS,ALMDS,U2,V2,V1,CF,WS,PSR)
      B(I,J) = B(I,J) + WS
54    CONTINUE

C * * if point support is an attached mass than subtract the
C * * appropriate quantity FAC.

      IF (I.EQ.J) THEN
      IF (CP(I,3).NE.0.) THEN
      FAC=-1./(2.*PHIS*PHIS*CP(I,3)*ALMDS*ALMDS)
      B(I,I)=B(I,I)-FAC
      END IF
      ENDIF
53    CONTINUE

C * * if DEL.NE.0 perform an eigenvalue search

      IF (DEL.NE.0) THEN
      IF (ALMDS.LT.DLIM) THEN
      CALL DETERM(B,KN,Y)
      WRITE (4,1) ALMDS,Y
      ALMDS = ALMDS + DEL
      GOTO 9
      END IF

C * * if DEL.EQ.0 calculate displacement data for three-dimensional
C * * mode plots.

      ELSE
      WRITE (4,1) ALMDS, UV, SS, PHI
      DO 18 I = 1,KN
18    P(I) = 0
      CALL DETR (B,KN,P)
      DO 99 I = 1,JL
      DO 99 J = 1,JL
99    W(I,J) = 0.

C * * calculate plate displacement at incremental values of
C * * PSI and ETA.

      DO 44 I = 1,JL
      ETA = (FLOAT(I)-1.)/(FLOAT(JL)-1.)
      DO 44 J = 1,1
      PSI = (FLOAT(J)-1.)/(FLOAT(JL)-1.)
      DO 44 N = 1,KN
      U = CP(N,1)
      V = CP(N,2)
      PN = -P(N)

      DO 44 M = 1,K
      CALL ABCD1 (M,PHIS,ALMDS,PN,U,V,A,PSR)

```

```

      CALL SIMQ (A,CF)
      CALL SSSS (M,PHIS,ALMDS,PSI,ETA,V,CF,WS,PSR)
44   W(I,J) = W(I,J) + WS

C * * print out IxJ array of W(I,J): mode shape data
C * * TST2,TST1 are used to normalize the displacement so that
C * * the plate's maximum displacement is always equal to one.

      TST2 = 0.0
      DO 77 I= 1,JL
      DO 77 J= 1,1
      TST1 = ABS(W(I,J))
      IF (TST1.GT.TST2) THEN
      TST2 = TST1
      END IF
77   CONTINUE
      DO 88 I = 1,JL
      DO 88 J = 1,1
      DISP = W(I,J) / TST2
88   WRITE (4,1) DISP
      ENDIF
      STOP
      END

C ***** end of main program *****

C *****
C *****
C *****
      SUBROUTINE ABCD1(M,PHIS,ALMDS,P,U,V,A,PSR)
C *****
C *****
      IMPLICIT DOUBLE PRECISION (A-H,O-Z)
      DIMENSION A(4,5)

      C      = 1
      PI      = 4.*DATAN(C)
      VS      = 1 - V
      EMP     = M*PI
      EMPS    = EMP*EMP
      BMS     = PHIS*(ALMDS+EMPS)
      BM      = DSQRT(BMS)

      IF (ALMDS.GT.EMPS) THEN
      GMS     = PHIS*(ALMDS-EMPS)
      GM      = DSQRT(GMS)
      A(1,1)  = DSINH(BM*V)
      A(1,2)  = DSIN(GM*V)
      A(1,3)  = -DSINH(BM*VS)
      A(1,4)  = -DSIN(GM*VS)
      A(1,5)  = 0

      A(2,1)  = BM*DCOSH(BM*V)
      A(2,2)  = GM*DCOS(GM*V)
      A(2,3)  = BM*DCOSH(BM*VS)
      A(2,4)  = GM*DCOS(GM*VS)
      A(2,5)  = 0

      A(3,1)  = BMS*DSINH(BM*V)
      A(3,2)  = -GMS*DSIN(GM*V)
      A(3,3)  = -BMS*DSINH(BM*VS)
      A(3,4)  = GMS*DSIN(GM*VS)

```

```

A(3,5) = 0
A(4,1) = BM**3*DCOSH(BM*V)
A(4,2) = -GM**3*DCOS(GM*V)
A(4,3) = BM**3*DCOSH(BM*VS)
A(4,4) = -GM**3*DCOS(GM*VS)
A(4,5) = P*DSIN(EMP*U)

```

```

ELSE
GMS = PHIS*(EMPS-ALMDS)
GM = SQRT(GMS)
A(1,1) = DSINH(BM*V)
A(1,2) = DSINH(GM*V)
A(1,3) = -DSINH(BM*VS)
A(1,4) = -DSINH(GM*VS)
A(1,5) = 0

```

```

A(2,1) = BM*DCOSH(BM*V)
A(2,2) = GM*DCOSH(GM*V)
A(2,3) = BM*DCOSH(BM*VS)
A(2,4) = GM*DCOSH(GM*VS)
A(2,5) = 0

```

```

A(3,1) = BMS*DSINH(BM*V)
A(3,2) = GMS*DSINH(GM*V)
A(3,3) = -BMS*DSINH(BM*VS)
A(3,4) = -GMS*DSINH(GM*VS)
A(3,5) = 0

```

```

A(4,1) = BM**3*DCOSH(BM*V)
A(4,2) = GM**3*DCOSH(GM*V)
A(4,3) = BM**3*DCOSH(BM*VS)
A(4,4) = GM**3*DCOSH(GM*VS)
A(4,5) = P*DSIN(EMP*U)
END IF
RETURN
END

```

```

C *****
C SUBROUTINE ABCD2(M,PHIS,ALMDS,P,U,V,A,PSR)
C *****

```

```

IMPLICIT DOUBLE PRECISION (A-H,O-Z)
DIMENSION A(4,5)

```

```

C = 1
PI = 4.*DATAN(C)
VS = 1 - V
EMP = M*PI
EMPS = EMP*EMP
BMS = PHIS*(ALMDS+EMPS)
BM = DSQRT(BMS)

```

```

IF (ALMDS.GT.EMPS) THEN
GMS = PHIS*(ALMDS-EMPS)
GM = DSQRT(GMS)
A(1,1) = DCOSH(BM*V) - DCOS(GM*V)
A(1,2) = DSINH(BM*V) - BM/GM * DSIN(GM*V)
A(1,3) = -DSINH(BM*VS)

```

```

A(1,4) = -DSIN(GM*VS)
A(1,5) = 0

A(2,1) = BM*DSINH(BM*V) + GM*DSIN(GM*V)
A(2,2) = BM*DCOSH(BM*V) - BM*DCOS(GM*V)
A(2,3) = BM*DCOSH(BM*VS)
A(2,4) = GM*DCOS(GM*VS)
A(2,5) = 0

A(3,1) = BMS*DCOSH(BM*V) + GMS*DCOS(GM*V)
A(3,2) = BMS*DSINH(BM*V) + GM*BM*DSIN(GM*V)
A(3,3) = -BMS*DSINH(BM*VS)
A(3,4) = GMS*DSIN(GM*VS)
A(3,5) = 0

A(4,1) = BM**3*DSINH(BM*V) - GM**3*DSIN(GM*V)
A(4,2) = BM**3*DCOSH(BM*V) + GMS*BM*DCOS(GM*V)
A(4,3) = BM**3*DCOSH(BM*VS)
A(4,4) = -GM**3*DCOS(GM*VS)
A(4,5) = P*DSIN(EMP*U)

ELSE
GMS = PHIS*(EMPS-ALMDS)
GM = SQRT(GMS)
A(1,1) = DCOSH(BM*V) - DCOSH(GM*V)
A(1,2) = DSINH(BM*V) - BM/GM*DSINH(GM*V)
A(1,3) = -DSINH(BM*VS)
A(1,4) = -DSINH(GM*VS)
A(1,5) = 0

A(2,1) = BM*DSINH(BM*V) - GM*DSINH(GM*V)
A(2,2) = BM*DCOSH(BM*V) - BM*DCOSH(GM*V)
A(2,3) = BM*DCOSH(BM*VS)
A(2,4) = GM*DCOSH(GM*VS)
A(2,5) = 0

A(3,1) = BMS*DCOSH(BM*V) - GMS*DCOSH(GM*V)
A(3,2) = BMS*DSINH(BM*V) - GM*BM*DSINH(GM*V)
A(3,3) = -BMS*DSINH(BM*VS)
A(3,4) = -GMS*DSINH(GM*VS)
A(3,5) = 0

A(4,1) = BM**3*DSINH(BM*V) - GM**3*DSINH(GM*V)
A(4,2) = BM**3*DCOSH(BM*V) - GMS*BM*DCOSH(GM*V)
A(4,3) = BM**3*DCOSH(BM*VS)
A(4,4) = GM**3*DCOSH(GM*VS)
A(4,5) = P*DSIN(EMP*U)
END IF
RETURN
END

```

```

C *****
C SUBROUTINE ABCD3(M,PHIS,ALMDS,P,U,V,A,PSR)
C *****

```

```

IMPLICIT DOUBLE PRECISION (A-H,O-Z)
DIMENSION A(4,5)

```

```

C      = 1
PI     = 4.*DATAN(C)
VS     = 1 - V
EMP    = M*PI
EMPS   = EMP*EMP
BMS    = PHIS*(ALMDS+EMPS)
BM     = DSQRT(BMS)
BMV    = BM*V
BMVS   = BM*VS

IF (ALMDS.GT.EMPS) THEN
GMS    = PHIS*(ALMDS-EMPS)
GM     = DSQRT(GMS)
GMV    = GM*V
GMVS   = GM*VS

A(1,1) = DCOSH(BMV) - DCOS(GMV)
A(1,2) = DSINH(BMV) - BM/GM * DSIN(GMV)
A(1,3) = -DCOSH(BMVS) + DCOS(GMVS)
A(1,4) = -DSINH(BMVS) + BM/GM * DSIN(GMVS)
A(1,5) = 0

A(2,1) = BM*DSINH(BMV) + GM*DSIN(GMV)
A(2,2) = BM*DCOSH(BMV) - BM*DCOS(GMV)
A(2,3) = BM*DSINH(BMVS) + GM*DSIN(GMVS)
A(2,4) = BM*DCOSH(BMVS) - BM*DCOS(GMVS)
A(2,5) = 0

A(3,1) = BMS*DCOSH(BMV) + GMS*DCOS(GMV)
A(3,2) = BMS*DSINH(BMV) + GM*BM*DSIN(GMV)
A(3,3) = -BMS*DCOSH(BMVS) - GMS*DCOS(GMVS)
A(3,4) = -BMS*DSINH(BMVS) - GM*BM*DSIN(GMVS)
A(3,5) = 0

A(4,1) = BM**3*DSINH(BMV) - GM**3*DSIN(GMV)
A(4,2) = BM**3*DCOSH(BMV) + GMS*BM*DCOS(GMV)
A(4,3) = BM**3*DSINH(BMVS) - GM**3*DSIN(GMVS)
A(4,4) = BM**3*DCOSH(BMVS) + GMS*BM*DCOS(GMVS)
A(4,5) = P*DSIN(EMP*U)

ELSE
GMS    = PHIS*(EMPS-ALMDS)
GM     = SQRT(GMS)
GMV    = GM*V
GMVS   = GM*VS

A(1,1) = DCOSH(BMV) - DCOSH(GMV)
A(1,2) = DSINH(BMV) - BM/GM*DSINH(GMV)
A(1,3) = -DCOSH(BMVS) + DCOSH(GMVS)
A(1,4) = -DSINH(BMVS) + BM/GM*DSINH(GMVS)
A(1,5) = 0

A(2,1) = BM*DSINH(BMV) - GM*DSINH(GMV)
A(2,2) = BM*DCOSH(BMV) - BM*DCOSH(GMV)
A(2,3) = BM*DSINH(BMVS) - GM*DSINH(GMVS)
A(2,4) = BM*DCOSH(BMVS) - BM*DCOSH(GMVS)
A(2,5) = 0

A(3,1) = BMS*DCOSH(BMV) - GMS*DCOSH(GMV)

```

```

A(3,2) = BMS*DSINH(BMV) - GM*BM*DSINH(GMV)
A(3,3) = -BMS*DCOSH(BMVS) + GMS*DCOSH(GMVS)
A(3,4) = -BMS*DSINH(BMVS) + GM*BM*DSINH(GMVS)
A(3,5) = 0

A(4,1) = BM**3*DSINH(BMV) - GM**3*DSINH(GMV)
A(4,2) = BM**3*DCOSH(BMV) - GMS*BM*DCOSH(GMV)
A(4,3) = BM**3*DSINH(BMVS) - GM**3*DSINH(GMVS)
A(4,4) = BM**3*DCOSH(BMVS) - GMS*BM*DCOSH(GMVS)
A(4,5) = P*DSIN(EMP*U)
END IF
RETURN
END

```

```

C *****
C SUBROUTINE ABCD4(M,PHIS,ALMDS,P,U,V,A,PSR)
C *****

```

```

IMPLICIT DOUBLE PRECISION (A-H,O-Z)
DIMENSION A(4,5)

```

```

C      = 1
PI     = 4*DATAN(C)
PSRS   = 2 - PSR
VS     = 1 - V
EMP    = M*PI
EMPS   = EMP*EMP
BMS    = PHIS*(ALMDS+EMPS)
BM     = DSQRT(BMS)
BMV    = BM*V
BMVS   = BM*VS

```

```

IF (ALMDS.GT.EMPS) THEN

```

```

GMS    = PHIS*(ALMDS-EMPS)
GM     = DSQRT(GMS)
GMV    = GM*V
GMVS   = GM*VS
ALPH1  = BMS-PSR*PHIS*EMPS
ALPH2  = GMS+PSR*PHIS*EMPS
ALPHA  = ALPH1/ALPH2
OMEG1  = BM**3 - BM*PSRS*PHIS*EMPS
OMEG2  = GM**3 + GM*PSRS*PHIS*EMPS
OMEGA  = OMEG1/OMEG2

```

```

A(1,1) = DCOSH(BMV) + ALPHA*DCOS(GMV)
A(1,2) = DSINH(BMV) + OMEGA*DSIN(GMV)
A(1,3) = -DSINH(BMVS)
A(1,4) = -DSIN(GMVS)
A(1,5) = 0

```

```

A(2,1) = BM*DSINH(BMV) - GM*ALPHA*DSIN(GMV)
A(2,2) = BM*DCOSH(BMV) + GM*OMEGA*DCOS(GMV)
A(2,3) = BM*DCOSH(BMVS)
A(2,4) = GM*DCOS(GMVS)
A(2,5) = 0

```

```

A(3,1) = BMS*DCOSH(BMV) - GMS*ALPHA*DCOS(GMV)
A(3,2) = BMS*DSINH(BMV) - GMS*OMEGA*DSIN(GMV)

```

```

A(3,3) = -BMS*DSINH(BMVS)
A(3,4) = GMS*DSIN(GMVS)
A(3,5) = 0

A(4,1) = BM**3*DSINH(BMV) + GM**3*ALPHA*DSIN(GMV)
A(4,2) = BM**3*DCOSH(BMV) - GM**3*OMEGA*DCOS(GMV)
A(4,3) = BM**3*DCOSH(BM*VS)
A(4,4) = -GM**3*DCOS(GM*VS)
A(4,5) = P*DSIN(EMP*U)

ELSE

GMS = PHIS*(EMPS-ALMDS)
GM = SQRT(GMS)
GMV = GM*V
GMVS = GM*VS

ALPH1 = BMS-PSR*PHIS*EMPS
ALPH2 = GMS-PSR*PHIS*EMPS
ALPHA = ALPH1/ALPH2
OMEG1 = BM**3 - BM*PSRS*PHIS*EMPS
OMEG2 = GM**3 - GM*PSRS*PHIS*EMPS
OMEGA = OMEG1/OMEG2

A(1,1) = DCOSH(BMV) - ALPHA*DCOSH(GMV)
A(1,2) = DSINH(BMV) - OMEGA*DSINH(GMV)
A(1,3) = -DSINH(BMVS)
A(1,4) = -DSINH(GMVS)
A(1,5) = 0

A(2,1) = BM*DSINH(BMV) - GM*ALPHA*DSINH(GMV)
A(2,2) = BM*DCOSH(BMV) - GM*OMEGA*DCOSH(GMV)
A(2,3) = BM*DCOSH(BMVS)
A(2,4) = GM*DCOSH(GMVS)
A(2,5) = 0

A(3,1) = BMS*DCOSH(BMV) - GMS*ALPHA*DCOSH(GMV)
A(3,2) = BMS*DSINH(BMV) - GMS*OMEGA*DSINH(GMV)
A(3,3) = -EMS*DSINH(BMVS)
A(3,4) = -GMS*DSINH(GMVS)
A(3,5) = 0

A(4,1) = BM**3*DSINH(BMV) - GM**3*ALPHA*DSINH(GMV)
A(4,2) = BM**3*DCOSH(BMV) - GM**3*OMEGA*DCOSH(GMV)
A(4,3) = BM**3*DCOSH(BMVS)
A(4,4) = GM**3*DCOSH(GMVS)
A(4,5) = P*DSIN(EMP*U)
END IF
RETURN
END

```

```

C *****
C SUBROUTINE ABCD5(M,PHIS,ALMDS,P,U,V,A,PSR)
C *****

```

```

IMPLICIT DOUBLE PRECISION (A-H,O-Z)
DIMENSION A(4,5)

```

```

C = 1

```

```

PI      = 4*DATAN(C)
PSRS   = 2 - PSR
VS     = 1 - V
EMP    = M*PI
EMPS   = EMP*EMP
BMS    = PHIS*(ALMDS+EMPS)
BM     = DSQRT(BMS)
BMV    = BM*V
BMVS   = BM*VS

IF (ALMDS.GT.EMPS) THEN

GMS    = PHIS*(ALMDS-EMPS)
GM     = DSQRT(GMS)
GMV    = GM*V
GMVS   = GM*VS
ALPH1  = BMS-PSR*PHIS*EMPS
ALPH2  = GMS+PSR*PHIS*EMPS
ALPHA  = ALPH1/ALPH2
OMEG1  = BM**3 - BM*PSRS*PHIS*EMPS
OMEG2  = GM**3 + GM*PSRS*PHIS*EMPS
OMEGA  = OMEG1/OMEG2

A(1,1) = DCOSH(BMV) + ALPHA*DCOS(GMV)
A(1,2) = DSINH(BMV) + OMEGA*DSIN(GMV)
A(1,3) = -DCOSH(BMVS) - ALPHA*DCOS(GMVS)
A(1,4) = -DSINH(BMVS) - OMEGA*DSIN(GMVS)
A(1,5) = 0

A(2,1) = BM*DSINH(BMV) - GM*ALPHA*DSIN(GMV)
A(2,2) = BM*DCOSH(BMV) + GM*OMEGA*DCOS(GMV)
A(2,3) = BM*DSINH(BMVS) - GM*ALPHA*DSIN(GMVS)
A(2,4) = BM*DCOSH(BMVS) + GM*OMEGA*DCOS(GMVS)
A(2,5) = 0

A(3,1) = BMS*DCOSH(BMV) - GMS*ALPHA*DCOS(GMV)
A(3,2) = BMS*DSINH(BMV) - GMS*OMEGA*DSIN(GMV)
A(3,3) = -BMS*DCOSH(BMVS) + GMS*ALPHA*DCOS(GMVS)
A(3,4) = -BMS*DSINH(BMVS) + GMS*OMEGA*DSIN(GMVS)
A(3,5) = 0

A(4,1) = BM**3*DSINH(BMV) + GM**3*ALPHA*DSIN(GMV)
A(4,2) = BM**3*DCOSH(BMV) - GM**3*OMEGA*DCOS(GMV)
A(4,3) = BM**3*DSINH(BMVS) + GM**3*ALPHA*DSIN(GMVS)
A(4,4) = BM**3*DCOSH(BMVS) - GM**3*OMEGA*DCOS(GMVS)
A(4,5) = P*DSIN(EMP*U)

ELSE

GMS    = PHIS*(EMPS-ALMDS)
GM     = SQRT(GMS)
GMV    = GM*V
GMVS   = GM*VS

ALPH1  = BMS-PSR*PHIS*EMPS
ALPH2  = GMS-PSR*PHIS*EMPS
ALPHA  = ALPH1/ALPH2
OMEG1  = BM**3 - BM*PSRS*PHIS*EMPS
OMEG2  = GM**3 - GM*PSRS*PHIS*EMPS
OMEGA  = OMEG1/OMEG2

```

```

A(1,1) = DCOSH(BMV) - ALPHA*DCOSH(GMV)
A(1,2) = DSINH(BMV) - OMEGA*DSINH(GMV)
A(1,3) = -DCOSH(BMVS) + ALPHA*DCOSH(GMVS)
A(1,4) = -DSINH(BMVS) + OMEGA*DSINH(GMVS)
A(1,5) = 0

A(2,1) = BM*DSINH(BMV) - GM*ALPHA*DSINH(GMV)
A(2,2) = BM*DCOSH(BMV) - GM*OMEGA*DCOSH(GMV)
A(2,3) = BM*DSINH(BMVS) - GM*ALPHA*DSINH(GMVS)
A(2,4) = BM*DCOSH(BMVS) - GM*OMEGA*DCOSH(GMVS)
A(2,5) = 0

A(3,1) = BMS*DCOSH(BMV) - GMS*ALPHA*DCOSH(GMV)
A(3,2) = BMS*DSINH(BMV) - GMS*OMEGA*DSINH(GMV)
A(3,3) = -BMS*DCOSH(BMVS) + GMS*ALPHA*DCOSH(GMVS)
A(3,4) = -BMS*DSINH(BMVS) + GMS*OMEGA*DSINH(GMVS)
A(3,5) = 0

A(4,1) = BM**3*DSINH(BMV) - GM**3*ALPHA*DSINH(GMV)
A(4,2) = BM**3*DCOSH(BMV) - GM**3*OMEGA*DCOSH(GMV)
A(4,3) = BM**3*DSINH(BMVS) - GM**3*ALPHA*DSINH(GMVS)
A(4,4) = BM**3*DCOSH(BMVS) - GM**3*OMEGA*DSINH(GMVS)
A(4,5) = P*DSIN(EMP*U)
END IF
RETURN
END

```

```

C *****
C SUBROUTINE ABCD6(M,PHIS,ALMDS,P,U,V,A,PSR)
C *****

```

```

IMPLICIT DOUBLE PRECISION (A-H,O-Z)
DIMENSION A(4,5)

```

```

C = 1
PI = 4*DATAN(C)
PSRS = 2 - PSR
VS = 1 - V
EMP = M*PI
EMPS = EMP*EMP
BMS = PHIS*(ALMDS+EMPS)
BM = DSQRT(BMS)
BMV = BM*V
BMVS = BM*VS

```

```

IF (ALMDS.GT.EMPS) THEN

```

```

GMS = PHIS*(ALMDS-EMPS)
GM = DSQRT(GMS)
GMV = GM*V
GMVS = GM*VS
ALPH1 = BMS-PSR*PHIS*EMPS
ALPH2 = GMS+PSR*PHIS*EMPS
ALPHA = ALPH1/ALPH2
OMEG1 = BM**3 - BM*PSRS*PHIS*EMPS
OMEG2 = GM**3 + GM*PSRS*PHIS*EMPS
OMEGA = OMEG1/OMEG2

```

```

A(1,1) = DCOSH(BMV) + ALPHA*DCOS(GMV)
A(1,2) = DSINH(BMV) + OMEGA*DSIN(GMV)

```

```

A(1,3) = -DCOSH(BMVS) + DCOS(GMVS)
A(1,4) = -DSINH(BMVS) + BM/GM*DSIN(GMVS)
A(1,5) = 0

A(2,1) = BM*DSINH(BMV) - GM*ALPHA*DSIN(GMV)
A(2,2) = BM*DCOSH(BMV) + GM*OMEGA*DCOS(GMV)
A(2,3) = BM*DSINH(BMVS) + GM*DSIN(GMVS)
A(2,4) = BM*DCOSH(BMVS) - BM*DCOS(GMVS)
A(2,5) = 0

A(3,1) = BMS*DCOSH(BMV) - GMS*ALPHA*DCOS(GMV)
A(3,2) = BMS*DSINH(BMV) - GMS*OMEGA*DSIN(GMV)
A(3,3) = -BMS*DCOSH(BMVS) - GMS*DCOS(GMVS)
A(3,4) = -BMS*DSINH(BMVS) - GM*BM*DSIN(GMVS)
A(3,5) = 0

A(4,1) = BM**3*DSINH(BMV) + GM**3*ALPHA*DSIN(GMV)
A(4,2) = BM**3*DCOSH(BMV) - GM**3*OMEGA*DCOS(GMV)
A(4,3) = BM**3*DSINH(BMVS) - GM**3*DSIN(GMVS)
A(4,4) = BM**3*DCOSH(BMVS) + GMS*BM*DCOS(GMVS)
A(4,5) = P*DSIN(EMP*U)

ELSE

GMS = PHIS*(EMPS-ALMDS)
GM = SQRT(GMS)
GMV = GM*V
GMVS = GM*VS

ALPH1 = BMS-PSR*PHIS*EMPS
ALPH2 = GMS-PSR*PHIS*EMPS
ALPHA = ALPH1/ALPH2
OMEG1 = BM**3 - BM*PSRS*PHIS*EMPS
OMEG2 = GM**3 - GM*PSRS*PHIS*EMPS
OMEGA = OMEG1/OMEG2

A(1,1) = DCOSH(BMV) - ALPHA*DCOSH(GMV)
A(1,2) = DSINH(BMV) - OMEGA*DSINH(GMV)
A(1,3) = -DCOSH(BMVS) + DCOSH(GMVS)
A(1,4) = -DSINH(BMVS) + BM/GM*DSINH(GMVS)
A(1,5) = 0

A(2,1) = BM*DSINH(BMV) - GM*ALPHA*DSINH(GMV)
A(2,2) = BM*DCOSH(BMV) - GM*OMEGA*DCOSH(GMV)
A(2,3) = BM*DSINH(BMVS) - GM*DSINH(GMVS)
A(2,4) = BM*DCOSH(BMVS) - BM*DCOSH(GMVS)
A(2,5) = 0

A(3,1) = BMS*DCOSH(BMV) - GMS*ALPHA*DCOSH(GMV)
A(3,2) = BMS*DSINH(BMV) - GMS*OMEGA*DSINH(GMV)
A(3,3) = -BMS*DCOSH(BMVS) + GMS*DCOSH(GMVS)
A(3,4) = -BMS*DSINH(BMVS) + GM*BM*DSINH(GMVS)
A(3,5) = 0

A(4,1) = BM**3*DSINH(BMV) - GM**3*ALPHA*DSINH(GMV)
A(4,2) = BM**3*DCOSH(BMV) - GM**3*OMEGA*DCOSH(GMV)
A(4,3) = BM**3*DSINH(BMVS) - GM**3*DSINH(GMVS)
A(4,4) = BM**3*DCOSH(BMVS) - GMS*BM*DCOSH(GMVS)
A(4,5) = P*DSIN(EMP*U)

```

```

END IF
RETURN
END

```

```

C*****
SUBROUTINE SSSC (M,PHIS,ALMDS,PSI,ETA,V,X,WS,PSR)
C*****

```

```

IMPLICIT DOUBLE PRECISION (A-H,O-Z)
DIMENSION X(5)

```

```

C      = 1
PI     = 4.*DATAN(C)
ETS    = 1 - ETA
EMP    = M*PI
EMPS   = EMP*EMP
BMS    = PHIS*(ALMDS+EMPS)
BM     = DSQRT(BMS)
AA     = X(1)
BB     = X(2)
CC     = X(3)
DD     = X(4)

```

```

IF(ALMDS.GT.EMPS) THEN
GMS   = PHIS*(ALMDS-EMPS)
GM    = SQRT(GMS)
IF(ETA.LT.V) THEN
YS    = BB*(DSINH(BM*ETA)-(BM/GM)*DSIN(GM*ETA))
YS    = YS + AA*(DCOSH(BM*ETA)-DCOS(GM*ETA))
WS    = YS*DSIN(EMP*PSI)
ELSE
WS    = (CC*DSINH(BM*ETS)+DD*DSIN(GM*ETS))*DSIN(EMP*PSI)
ENDIF

```

```

ELSE
GMS   = PHIS*(EMPS-ALMDS)
GM    = SQRT(GMS)
IF(ETA.LT.V) THEN
YS    = AA*(DCOSH(BM*ETA)-DCOSH(GM*ETA))
YS    = YS + BB*(DSINH(BM*ETA)-BM/GM*DSINH(GM*ETA))
WS    = YS*DSIN(EMP*PSI)
ELSE
WS    = (CC*DSINH(BM*ETS)+DD*DSINH(GM*ETS))*DSIN(EMP*PSI)
ENDIF

```

```

ENDIF
RETURN
END

```

```

C*****
SUBROUTINE SSSS (M,PHIS,ALMDS,PSI,ETA,V,X,WS,PSR)
C*****

```

```

IMPLICIT DOUBLE PRECISION (A-H,O-Z)
DIMENSION X(5)

```

```

C      = 1
PI     = 4.*DATAN(C)
ETS    = 1 - ETA
EMP    = M*PI

```

```

EMPS = EMP*EMP
BMS = PHIS*(ALMDS+EMPS)
BM = DSQRT(BMS)
AA = X(1)
BB = X(2)
CC = X(3)
DD = X(4)

IF(ALMDS.GT.EMPS) THEN
GMS = PHIS*(ALMDS-EMPS)
GM = SQRT(GMS)
IF(ETA.LT.V) THEN
WS = (AA*DSINH(BM*ETA)+BB*DSIN(GM*ETA))*DSIN(EMP*PSI)
ELSE
WS = (CC*DSINH(BM*ETS)+DD*DSIN(GM*ETS))*DSIN(EMP*PSI)
ENDIF

ELSE
GMS = PHIS*(EMPS-ALMDS)
GM = SQRT(GMS)
IF(ETA.LT.V) THEN
WS = (AA*DSINH(BM*ETA)+BB*DSINH(GM*ETA))*DSIN(EMP*PSI)
ELSE
WS = (CC*DSINH(BM*ETS)+DD*DSINH(GM*ETS))*DSIN(EMP*PSI)
ENDIF

ENDIF
RETURN
END

```

```

C*****
SUBROUTINE SCSC (M,PHIS,ALMDS,PSI,ETA,V,X,WS,PSR)
C*****

```

```

IMPLICIT DOUBLE PRECISION (A-H,O-Z)
DIMENSION X(5)

```

```

C = 1
PI = 4.*DATAN(C)
ETS = 1 - ETA
EMP = M*PI
EMPS = EMP*EMP
BMS = PHIS*(ALMDS+EMPS)
BM = DSQRT(BMS)
AA = X(1)
BB = X(2)
CC = X(3)
DD = X(4)

IF(ALMDS.GT.EMPS) THEN
GMS = PHIS*(ALMDS-EMPS)
GM = SQRT(GMS)
IF(ETA.LT.V) THEN
YS = BB*(DSINH(BM*ETA)-(BM/GM)*DSIN(GM*ETA))
YS = YS + AA*(DCOSH(BM*ETA)-DCOS(GM*ETA))
WS = YS*DSIN(EMP*PSI)
ELSE
YS = DD*(DSINH(BM*ETS)-(BM/GM)*DSIN(GM*ETS))
YS = YS + CC*(DCOSH(BM*ETS)-DCOS(GM*ETS))
WS = YS*DSIN(EMP*PSI)
ENDIF

```

```

ELSE
GMS = PHIS*(EMPS-ALMDS)
GM  = SQRT(GMS)
IF(ETA.LT.V) THEN
YS  = AA*(DCOSH(BM*ETA)-DCOSH(GM*ETA))
YS  = YS + BB*(DSINH(BM*ETA)-BM/GM*DSINH(GM*ETA))
WS  = YS*DSIN(EMP*PSI)
ELSE
YS  = CC*(DCOSH(BM*ETS)-DCOSH(GM*ETS))
YS  = YS + DD*(DSINH(BM*ETS)-BM/GM*DSINH(GM*ETS))
WS  = YS*DSIN(EMP*PSI)
ENDIF

ENDIF
RETURN
END

```

```

C*****
SUBROUTINE SSSF (M,PHIS,ALMDS,PSI,ETA,V,X,WS,PSR)
C*****

```

```

IMPLICIT DOUBLE PRECISION (A-H,O-Z)
DIMENSION X(5)

```

```

C      = 1
PI     = 4.*DATAN(C)
PSRS   = 2 - PSR
ETS    = 1 - ETA
EMP    = M*PI
EMPS   = EMP*EMP
BMS    = PHIS*(ALMDS+EMPS)
BM     = DSQRT(BMS)
AA     = X(1)
BB     = X(2)
CC     = X(3)
DD     = X(4)

```

```

IF(ALMDS.GT.EMPS) THEN

```

```

GMS    = PHIS*(ALMDS-EMPS)
GM     = SQRT(GMS)
ALPH1  = BMS - PSR*PHIS*EMPS
ALPH2  = GMS + PSR*PHIS*EMPS
ALPHA  = ALPH1/ALPH2
OMEG1  = BM**3 - BM*PSRS*PHIS*EMPS
OMEG2  = GM**3 + GM*PSRS*PHIS*EMPS
OMEGA  = OMEG1/OMEG2

```

```

IF(ETA.LT.V) THEN

```

```

YS     = AA*(DCOSH(BM*ETA)+ALPHA*DCOS(GM*ETA))
YS     = YS + BB*(DSINH(BM*ETA)+OMEGA*DSIN(GM*ETA))
WS     = YS*DSIN(EMP*PSI)
ELSE
WS     = (CC*DSINH(BM*ETS)+DD*DSIN(GM*ETS))*DSIN(EMP*PSI)
ENDIF

```

```

ELSE
GMS    = PHIS*(EMPS-ALMDS)
GM     = SQRT(GMS)

```

```

ALPH1 = BMS-PSR*PHIS*EMPS
ALPH2 = GMS-PSR*PHIS*EMPS
ALPHA = ALPH1/ALPH2
OMEG1 = BM**3 - BM*PSRS*PHIS*EMPS
OMEG2 = GM**3 - GM*PSRS*PHIS*EMPS
OMEGA = OMEG1/OMEG2
IF(ETA.LT.V) THEN
YS = AA*(DCOSH(BM*ETA)-ALPHA*DCOSH(GM*ETA))
YS = YS + BB*(DSINH(BM*ETA)-OMEGA*DSINH(GM*ETA))
WS = YS*DSIN(EMP*PSI)
ELSE
WS = (CC*DSINH(BM*ETS)+DD*DSINH(GM*ETS))*DSIN(EMP*PSI)
ENDIF
ENDIF
RETURN
END

```

```

C*****
SUBROUTINE SFSF (M,PHIS,ALMDS,PSI,ETA,V,X,WS,PSR)
C*****

```

```

IMPLICIT DOUBLE PRECISION (A-H,O-Z)
DIMENSION X(5)

```

```

C = 1
PI = 4.*DATAN(C)
PSRS = 2 - PSR
ETS = 1 - ETA
EMP = M*PI
EMPS = EMP*EMP
BMS = PHIS*(ALMDS+EMPS)
BM = DSQRT(BMS)
AA = X(1)
BB = X(2)
CC = X(3)
DD = X(4)

```

```

IF(ALMDS.GT.EMPS) THEN

```

```

GMS = PHIS*(ALMDS-EMPS)
GM = SQRT(GMS)
ALPH1 = BMS - PSR*PHIS*EMPS
ALPH2 = GMS + PSR*PHIS*EMPS
ALPHA = ALPH1/ALPH2
OMEG1 = BM**3 - BM*PSRS*PHIS*EMPS
OMEG2 = GM**3 + GM*PSRS*PHIS*EMPS
OMEGA = OMEG1/OMEG2

```

```

IF(ETA.LT.V) THEN

```

```

YS = AA*(DCOSH(BM*ETA)+ALPHA*DCOS(GM*ETA))
YS = YS + BB*(DSINH(BM*ETA)+OMEGA*DSIN(GM*ETA))
WS = YS*DSIN(EMP*PSI)
ELSE
YS = CC*(DCOSH(BM*ETS)+ALPHA*DCOS(GM*ETS))
YS = YS + DD*(DSINH(BM*ETS)+OMEGA*DSIN(GM*ETS))
WS = YS*DSIN(EMP*PSI)
ENDIF

```

```

ELSE

```

```

GMS = PHIS*(EMPS-ALMDS)
GM  = SQRT(GMS)
ALPH1 = BMS-PSR*PHIS*EMPS
ALPH2 = GMS-PSR*PHIS*EMPS
ALPHA = ALPH1/ALPH2
OMEG1 = BM**3 - BM*PSRS*PHIS*EMPS
OMEG2 = GM**3 - GM*PSRS*PHIS*EMPS
OMEGA = OMEG1/OMEG2

IF(ETA.LT.V) THEN
YS = AA*(DCOSH(BM*ETA)-ALPHA*DCOSH(GM*ETA))
YS = YS + BB*(DSINH(BM*ETA)-OMEGA*DSINH(GM*ETA))
WS = YS*DSIN(EMP*PSI)
ELSE
YS = CC*(DCOSH(BM*ETS)-ALPHA*DCOSH(GM*ETS))
YS = YS + DD*(DSINH(BM*ETS)-OMEGA*DSINH(GM*ETS))
WS = YS*DSIN(EMP*PSI)
ENDIF

ENDIF
RETURN
END

```

```

C*****
SUBROUTINE SCSF (M,PHIS,ALMDS,PSI,ETA,V,X,WS,PSR)
C*****

```

```

IMPLICIT DOUBLE PRECISION (A-H,O-Z)
DIMENSION X(5)

```

```

C      = 1
PI     = 4.*DATAN(C)
PSRS   = 2 - PSR
ETS    = 1 - ETA
EMP    = M*PI
EMPS   = EMP*EMP
BMS    = PHIS*(ALMDS+EMPS)
BM     = DSQRT(BMS)
AA     = X(1)
BB     = X(2)
CC     = X(3)
DD     = X(4)

```

```

IF(ALMDS.GT.EMPS) THEN

```

```

GMS = PHIS*(ALMDS-EMPS)
GM  = SQRT(GMS)
ALPH1 = BMS - PSR*PHIS*EMPS
ALPH2 = GMS + PSR*PHIS*EMPS
ALPHA = ALPH1/ALPH2
OMEG1 = BM**3 - BM*PSRS*PHIS*EMPS
OMEG2 = GM**3 + GM*PSRS*PHIS*EMPS
OMEGA = OMEG1/OMEG2

```

```

IF(ETA.LT.V) THEN

```

```

YS = AA*(DCOSH(BM*ETA)+ALPHA*DCOS(GM*ETA))
YS = YS + BB*(DSINH(BM*ETA)+OMEGA*DSIN(GM*ETA))
WS = YS*DSIN(EMP*PSI)
ELSE
YS = DD*(DSINH(BM*ETS)-(BM/GM)*DSIN(GM*ETS))

```

```

      YS = YS + CC*(DCOSH(BM*ETS)-DCOS(GM*ETS))
      WS = YS*DSIN(EMP*PSI)
      ENDIF

      ELSE
      GMS = PHIS*(EMPS-ALMDS)
      GM = SQRT(GMS)
      ALPH1 = BMS-PSR*PHIS*EMPS
      ALPH2 = GMS-PSR*PHIS*EMPS
      ALPHA = ALPH1/ALPH2
      OMEG1 = BM**3 - BM*PSRS*PHIS*EMPS
      OMEG2 = GM**3 - GM*PSRS*PHIS*EMPS
      OMEGA = OMEG1/OMEG2

      IF(ETA.LT.V) THEN
      YS = AA*(DCOSH(BM*ETA)-ALPHA*DCOSH(GM*ETA))
      YS = YS + BB*(DSINH(BM*ETA)-OMEGA*DSINH(GM*ETA))
      WS = YS*DSIN(EMP*PSI)
      ELSE
      YS = CC*(DCOSH(BM*ETS)-DCOSH(GM*ETS))
      YS = YS + DD*(DSINH(BM*ETS)-BM/GM*DSINH(GM*ETS))
      WS = YS*DSIN(EMP*PSI)
      ENDIF

      ENDIF
      RETURN
      END

C *****
      SUBROUTINE SIMQ(A,X)
C *****

      IMPLICIT DOUBLE PRECISION(A-H,O-Z)
      DIMENSION A(4,5),X(5)
      99 FORMAT (7(E13.6,3X))
      SIGN=1.
      M = 4
      N = 5
      M=N-1
      LAST=M-1

C * * start overall loop for(N-1) pivots
      DO 7 I=1,LAST

C * * find the largest remaining term in I-TH column for pivot
      BIG=0.
      DO 2 K=I,M
      TERM=DABS(A(K,I))
      IF(TERM-BIG)2,2,1
      1 BIG=TERM
      L=K
      2 CONTINUE

C * * check whether a non-zero term has been found
      IF(BIG)3,11,3

C * * L-th row has the biggest term----is I=L

```

```

      3 IF(I-L)4,6,4
C * * if(I.NE.L) then, switch rows I and L
      4 DO 5 J=1,N
        TEMP=A(I,J)
        A(I,J)=A(L,J)
      5 A(L,J)=TEMP
C * * now start pivotal reduction
      6 PIVOT=A(I,I)
        NEXTR=I+1
C * * for each of the rows after the I-th
        DO 7 J=NEXTR,M
C * * multiplying constant for the J-th row is:
        CONST=A(J,I)/PIVOT
C * * now reduce each term of the J-th row
        DO 7 K=I,N
      7 A(J,K)=A(J,K)-CONST*A(I,K)
C * * end of pivotal reduction-- perform back substitution
        M=N-1
        DO 10 I=1,M
C * * IREV is the backward index,going from M back to 1
        IREV=M+1-I
C * * get Y(IREV) in preperation
        Y=A(IREV,N)
        IF(IREV-M)8,10,8
C      not working on last row,I is 2 or greater
      8 DO 9 J=2,I
C * * work backward for X(N),X(N-1)-----substituting previously
C * * found values
        K=N+1-J
      9 Y=Y-A(IREV,K)*X(K)
C * * finally,compute X(IREV)
     10 X(IREV)=Y/A(IREV,IREV)
        X(N)=-1
     11 RETURN
        END
C*****
      SUBROUTINE DETERM (A,N,DET)
C*****

```

```

      IMPLICIT DOUBLE PRECISION(A-H,O-Z)
      DIMENSION A(16,16)
      SIGN=1.
      LAST=N-1

C * * start overall loop for(N-1) pivots
      DO 200 I=1, LAST

C * * find the largest remaining term in I-th column for pivot
      BIG=0.
      DO 50 K=I, N
        TERM=DABS(A(K,I))
        IF (TERM-BIG)50,50,30
30     BIG=TERM
        L=K
50     CONTINUE

C * * check whether a non-zero term has been found
      IF (BIG)80,60,80

C * * L-th row has the biggest term----is I=L
      80 IF (I-L)90,120,90

C * * I NE. to L, switch rows I and L
90     SIGN=-SIGN
      DO 100 J=1, N
        TEMP=A(I, J)
        A(I, J)=A(L, J)
100    A(L, J)=TEMP

C * * now start pivotal reduction
      120 PIVOT=A(I, I)
          NEXTR=I+1

C * * for each of the rows after the I-th
      DO 200 J=NEXTR, N

C * * multiplying constant for the J-th row is
          CONST=A(J, I)/PIVOT

C * * now reduce each term of the J-th row
          DO 200 K=I, N
200    A(J, K)=A(J, K)-CONST*A(I, K)

C * * end of pivotal reduction---now compute determinant
          DET=SIGN
          DO 300 I=1, N
300    DET=DET*A(I, I)*10 .
          GO TO 61
          60 DET=0.
          61 RETURN
          END

C*****

```

```
      SUBROUTINE DETR(A,N,X)
C*****
      IMPLICIT DOUBLE PRECISION(A-H,O-Z)
      DIMENSION A(16,16),X(16)
      SIGN=1.
      M=N-1
      LAST=M-1

C * * start overall loop for (N-1) pivots
      DO 7 I=1,LAST

C * * find the largest remaining term in I-th column for pivot
      BIG=0.
      DO 2 K=I,M
      TERM=DABS(A(K,I))
      IF(TERM-BIG)2,2,1
1  BIG=TERM
      L=K
2  CONTINUE

C * * check whether a non-zero term has been found
      IF(BIG)3,11,3

C * * L-th row has the biggest term-----is I=L
      3 IF(I-L)4,6,4

C * * IF I.NE.L THEN switch rows I and L
      4 DO 5 J=1,N
      TEMP=A(I,J)
      A(I,J)=A(L,J)
      5 A(L,J)=TEMP

C * * NOW START PIVOTAL REDUCTION
      6 PIVOT=A(I,I)
      NEXTR=I+1

C * * for each of the rows after the I-th
      DO 7 J=NEXTR,M

C * * multiplying constant for the J-th row is:
      CONST=A(J,I)/PIVOT

C * * now reduce each term of the J-th row
      DO 7 K=I,N
      7 A(J,K)=A(J,K)-CONST*A(I,K)

C * * end of pivotal reduction-- perform back substitution
      M=N-1
      DO 10 I=1,M

C * * irev is the backward index,going from M back to 1
```

```
      IREV=M+1-I
C * * get Y(IREV) in preparation
      Y=A(IREV,N)
      IF(IREV-M)8,10,8
C * * not working on las. row I.GE.2
      8 DO 9 J=2,I
C * * work backward for X(N),X(N-1)-----substituting previously
C * * found values
      K=N+1-J
      9 Y=Y-A(IREV,K)*X(K)
C * * finally, compute X(IREV)
      10 X(IREV)=Y/A(IREV,IREV)
      X(N)=-1
      WRITE(6,77) X(1), X(2), X(3), X(4)
      77 FORMAT (7(E13.6,3X))
      11 RETURN
      END
```